

Posiva SKB Report 09
February 2021



The Integrated Sulfide Project – Summary report

A collaboration project 2014–2018

POSIVA OY

Olkiluoto
FI-27160 Eurajoki, Finland
Phone +358 2 8372 31
posiva.fi

SVENSK KÄRNBRÄNSLEHANTERING AB

**SWEDISH NUCLEAR FUEL
AND WASTE MANAGEMENT CO**

Box 3091, SE-169 03 Solna
Phone +46 8 459 84 00
skb.se

ISSN 2489-2742

Posiva SKB Report 09

SKB ID 1922911

Posiva ID RDOC-105019

February 2021

The Integrated Sulfide Project – Summary report

A collaboration project 2014–2018

Svensk Kärnbränslehantering AB

Posiva Oy

This report is published on www.skb.se and www.posiva.fi.

© 2021 Svensk Kärnbränslehantering AB and Posiva Oy

Preface

This document is the final report from the Integrated Sulfide Project (a collaboration between Posiva Oy and SKB AB), and it summarises the results from three different work packages (WP1: sulfide processes in the geosphere, WP2: sulfide processes in buffer and backfill and WP3: modelling of the near-field system). The work packages included several sub-projects which have been reported in detail in thirteen specific reports.

The following persons have provided text for the different chapters and sub-areas presented in the report:

Birgitta Kalinowski, Svensk Kärnbränslehantering AB

Tiina Lamminmäki, Posiva Oy

Christina Lilja, Svensk Kärnbränslehantering AB

Ann-Chatrin Nilsson, (editor) Ingenjörskontor Åke Holmqvist

Petteri Pitkänen, Posiva Oy

Ignasi Puigdomenech, Svensk Kärnbränslehantering AB

Patrik Sellin, Svensk Kärnbränslehantering AB

Susanna Maanoja, Posiva Oy

Lino Nilsson, Svensk Kärnbränslehantering AB, contributed with Figure 2-1

Abstract

The summary report from the Integrated Sulfide Project (ISP) summarises the studies performed within three different Work Packages (WP1: sulfide processes in the geosphere, WP2: sulfide processes in buffer and backfill, and WP3: modelling of the processes or fluxes of sulfide in the near field of a spent nuclear fuel repository).

WP1 includes studies regarding 1) possible release of potential nutrients from borehole installation material, 2) two different approaches to gas sampling from bedrock and 3) microbial release of iron from iron-bearing silicate minerals.

- 1) Aluminium and stainless-steel samples as well as five different polymeric materials were exposed to sterilized filtered groundwater and to natural untreated groundwater in closed vessels at oxygen-free conditions during several months. Release of hydrogen gas (H_2) due to corrosion occurred especially for the aluminium – but also for the stainless-steel samples. Several organic compounds from the different polymeric samples were found in the groundwater leachates. At non-sterile conditions, formed hydrogen gas as well as leached organic components seemed to be consumed by the bacteria present in the water.
- 2) Tests of different gas sampling conditions using a specially developed flow-through sampler showed that the flushing prior to sampling and also the counter pressure have impacts on the gas contents and especially on the H_2 and He concentrations in the groundwater samples.

An *in situ* gas monitoring experiment measured the amounts of gas that diffuses from the bedrock into a dry borehole at repository depth. Besides N_2 , the diffused gas from the bedrock contained CH_4 , He and H_2 as well as Ar, CO_2 and ethane in lower concentration. Drill core samples from the experiment borehole revealed significantly higher dissolved hydrogen concentrations in the matrix pore-water than that found in fracture groundwater.

- 3) Microbial release of Fe(II) from biotite and garnet was studied using serum bottles filled with groundwater (including microbes in the groundwaters) and supplied with varying electron donors. These tests were followed by two field experiments in pressure cells where the minerals biotite, garnet and chlorite were exposed to non-sterile sulfate-rich and sulfate-poor borehole groundwater, respectively. Finally, the effect of solely dissolved sulfide on iron release from the minerals was studied in the laboratory. The pressure cells with added H_2 showed bacterial iron reduction. It is also possible that some bacterial iron reduction together with methane oxidation occurred in the case of the sulfate-poor groundwater. In addition to the production of dissolved Fe^{2+} which can react with sulfide and form FeS, sulfide in Olkiluoto groundwater can also be immobilised by direct reaction with Fe(III) bearing minerals (i.e. mostly iron silicates, though some iron(III)oxides have been found in mineral separations, see Johansson et al. 2019).

WP2 covers 1) determinations of the solubility of sulfur minerals naturally present in bentonites and their equilibrium concentrations. From the solubility tests it was found that the concentration of sulfide in the water after contact with bentonite was below the limit of detection. This was true also after minor additions of sulfide to the bentonite. This indicates that bentonite lowers the sulfide concentration in solution. Furthermore, 2) the microbial sulfide producing activity in five different clays was studied as a function of total density at full water saturation to find the threshold buffer density. The studies demonstrate that there is a material-specific threshold of saturated density for most of the tested bentonite clays above which microbial sulfide-producing activity is insignificant even if the other conditions are favourable for growth of SRB. This proves that sulfide-producing activity can be prevented by setting requirements on the bentonite density which is important information regarding the bentonite buffer in the repository case. Lastly, 3) the microbial utilisation of organic matter dissolving from compacted bentonite was studied and the results showed that the organic matter of all the studied bentonites have a potential for sustaining activity of SRB and other microbes.

WP3 implies modelling tool inter-comparison and partial verification. Three teams of modellers worked independently to develop *reactive transport modelling tools* that are able to describe and simulate the sulfide fluxes and evolution (sources and sinks) in the different parts of the near field of a KBS-3 repository (canister, buffer, backfill, rock-backfill interface and rock bolts). A Base Case where

sulfate reduction takes place only in the rock-bentonite interfaces through bacterial activity was defined to be used in a modelling tool inter-comparison and partial verification. Furthermore, a series of Variant Cases were established to test the capabilities of the different modelling strategies implemented in the developed modelling tools. The agreement between the results from the teams was reasonable when considering the profound differences between the modelling tools. Therefore, the expectations to develop tools that can provide future safety analyses with integrated models that include both the formation and evolution of sulfide and sulfide corrosion and that can replace the uncoupled or loosely coupled models used until now, may be considered at least partly fulfilled.

Sammanfattning

Sammanfattningsrapporten från det Integrerade Sulfidprojektet (ISP) sammanfattar studier som utförts inom tre olika arbetspaket (WP1: sulfidprocesser i geosfären, WP2: sulfidprocesser i buffert och återfyllnad, och WP3: modellering av processer eller flöden av sulfid i närområdet för ett använt kärnbränsleförvar).

WP1 inkluderar studier avseende 1) möjlig mobilisering av potentiella näringsämnen från material i borrhålsinstallationer, 2) två olika metoder för gasprovtagning och 3) mikrobiell mobilisering av järn från järninnehållande mineral.

- 1) Prov av aluminium och rostfritt stål samt fem olika polymera material exponerades för steriliserat filtrerat grundvatten och för naturligt obehandlat grundvatten i slutna kärl vid syrefria förhållanden under flera månader. Avgivning av vätgas på grund av korrosion inträffade särskilt för aluminium – men också för de rostfria proverna. Flera organiska föreningar från de olika polymerproven hittades i lakvattnen. Vid icke-sterila förhållanden verkade bildad vätgas samt lakade organiska komponenter konsumeras av bakterierna i vattnet.
- 2) Test av olika provtagningsförhållanden med en speciellt utvecklad genomströmnings-provtagare visade att spolvolym före provtagningen liksom pålagt mottryck har påverkan på gasinnehållet och i synnerhet H₂- och He-koncentrationerna i grundvattenproverna. Ett gasövervakningsexperiment in situ mätte mängderna gas som diffunderar från berggrunden till ett torrt borrhål på försvarsdjup. Förutom N₂ innehöll den diffunderade gasen från berggrunden CH₄, He och H₂ samt Ar, CO₂ och etan i lägre koncentrationer. Borrkärneprov från experimentets borrhål avslöjade signifikant högre vätgaskoncentrationer i matrisporvattnet än vad som tidigare har observerats i grundvattnet i vattenförande sprickor i berget.
- 3) Mikrobiell mobilisering av Fe(II) från biotit och granat undersöktes i serumflaskor innehållande grundvatten med tillsatser av olika elektrondonatorer. Dessa ympades med mikrober från olika grundvatten. Laboratorietesterna följdes av två fältförsök i tryckceller där mineralen biotit, granat och klorit utsattes för icke sterilt sulfatrikt respektive sulfatfattigt grundvatten från två olika borrhål. Slutligen gjordes en laboratoriestudie för att se effekten av enbart upplöst sulfid på järnmobilisering från mineralen. Mikrobiell järnreduktion kunde påvisas i tryckcellerna med H₂. Det är också möjligt att viss bakteriell järnreduktion förekom tillsammans med metanoxidation i det sulfatfattiga grundvattnet. Förutom produktionen av upplöst Fe²⁺ som kan reagera med sulfid och bilda FeS, kan sulfidkoncentrationer i Olkiluotos grundvatten också immobiliseras genom direkt reaktion med Fe(III)-bärande mineraler.

WP2 omfattar 1) bestämningar av lösligheten hos svavelinnehållande mineral som förekommer naturligt i bentoniter samt deras jämviktskoncentrationer. Från löslighetstesterna konstaterades att koncentrationen av sulfid i vattnet efter kontakt med bentonit var under detektionsgränsen. Detta gällde även efter mindre tillsatser av sulfid till bentoniten, vilket indikerar att bentonit sänker sulfidkoncentrationen i lösningen. Vidare studerades 2) mikrobiell aktivitet med avseende på sulfidproduktion i de olika lerorna som en funktion av total densitet vid full vattenmättnad för att hitta tröskelbuffertdensiteten. Studierna visar att det finns ett materialspecifikt tröskelvärde på densiteten vid mättad för de flesta av de testade bentonitlerorna över vilken mikrobiell sulfid-producerande aktivitet är obetydlig även om de andra förhållandena är gynnsamma för tillväxt av SRB. Detta bevisar att sulfidproducerande aktivitet kan förhindras genom att ställa krav på bentonitens densitet vilket är viktig information när det gäller bentonitbuffert och slutförvar. Slutligen studerades 3) den mikrobiella tillgängligheten hos lösligt organiskt material från kompakterad bentonit. Det organiska materialet från samtliga studerade leror visade potential för att upprätthålla aktivitet för såväl SRB som andra mikrober.

WP3 innebär en jämförelse och delvis verifiering av modelleringsverktyg. Tre modelleringssteam arbetade oberoende av varandra för att utveckla reaktiva transport-modelleringsverktyg som kan beskriva och simulera sulfidflödena och utvecklingen (källor och sänkor) i olika delar i närzonen till ett KBS-3-förvar (kapsel, buffert, återfyllning, berg-backfill-gränssnitt och berg-bultar). Ett basfall som innebär att bakteriell sulfatreduktion endast äger rum i berg-bentonitgränssnitten definierades för att användas i en jämförelse mellan olika modelleringsverktyg och för partiell verifiering av verktygen.

Dessutom upprättades en serie variantfall för att testa kapaciteten hos de olika modellstrategierna implementerade i de utvecklade modelleringsverktygen. Samstämmigheten mellan resultaten från teamen var acceptabel när man beaktar de stora skillnaderna mellan modelleringsverktygen. Syftet att utveckla verktyg som kan förse framtida säkerhetsanalyser med integrerade modeller som inkluderar både bildning och utveckling av sulfid och sulfidkorrosion och som kan ersätta de okopplade eller löst kopplade modeller som hittills har använts får anses vara i varje fall delvis uppnått.

Tiivistelmä

Integroidun sulfidiprojektin (Integrated Sulfide Project, ISP) yhteenvetoraportti esittää lyhyesti kaikki projektissa tehdyt tutkimukset, jotka olivat jaettu kolmeen työpakettiin (Work Package WP): WP1 sulfidiprosessit geosfäärissä, WP2 sulfidiprosessit puskurissa ja täytössä sekä WP3 sulfidivuon mallinnus käytetyn ydinpolttoaineen loppusijoituslaitoksen lähialueella.

Työpaketti WP1:ssä tutkittiin 1) mikrobeille otollisten ravintoaineiden mahdollista vapautumista kairareissä olevista laitteistoista, 2) kahta eri kallioperän kaasunäytteenottoon soveltuvaa tutkimusmenetelmää ja 3) raudan mikrobiologista vapautumista rautaa sisältävistä silikaattimineraaleista.

- 1) Näytteet, jotka koostuivat alumiinista ja ruostumattomasta teräksestä sekä viidestä erilaisesta polymeerimateriaaliasta, asetettiin sekä steriloituun suodatettuun pohjaveteen että käsittelemättömään pohjaveteen hapettomissa olosuhteissa usean kuukauden ajaksi. Korroosiossa muodostuvan vedyn vapautumista havaittiin erityisesti alumiininäytteen kohdalla, mutta myös ruostumattoman teräksen tapauksessa. Eri polymeerinäytteiden uutevesistä havaittiin useita orgaanisia yhdisteitä. Steriloimattomissa näytteissä sekä muodostunut vety että uuttuneet orgaaniset yhdisteet kulutettiin todennäköisesti pohjavedessä luonnollisesti olevien mikrobien toimesta.
- 2) Erilaisten kallioperän kaasunäytteenotto-olosuhteiden testaaminen siihen suunnitellulla läpivirtaukseen perustuvalla näytteenottimella osoitti, että ennen näytteenottoa tehtävällä valuttamisella sekä käytetyllä vastapaineella oli vaikutus määritettyihin kaasupitoisuuksiin. Vaikutus nähtiin erityisesti pohjaveden vety- ja heliumpitoisuuksissa.

In situ kokeessa mitattiin kallioperästä diffuntoituvia kaasumääriä mahdollisimman kuivaan kairareikään loppusijoituslaitoksen syvyydellä. N₂ lisäksi määritettiin isompia pitoisuuksia CH₄, He ja H₂ ja pienempiä pitoisuuksia Ar, CO₂ ja C₂H₆. Kairasydännäytteiden perusteella havaittiin, että matriksin huokosvesi sisälsi huomattavasti korkeampia vety- ja heliumpitoisuuksia kuin rakovesi.

- 3) Biotiitista ja granaatista mikrobiologisesti vapautuvaa Fe(II) tutkittiin ensin pullokoikeissa, jossa pullo täytettiin Olkiluodon pohjavedellä (sisältäen pohjavedessä olevat mikrobit) ja niihin lisättiin erilaisia elektronien luovuttajia. Pullostien perusteella suoritettiin kaksi kenttäkoetta painekennoja käyttäen. Mineraaleina kenttäkoikeissa olivat biotiitti, granaatti ja kloriitti, jotka altistettiin sekä sulfaattirikkaalle että -köyhälle steriloiduille pohjavesille. Viimeiseksi tutkittiin liuennon sulfidin reaktioita kyseisten rautapitoisten mineraalien kanssa. Mikrobiologinen raudanpelkistys havaittiin erityisesti painekennoissa, joihin lisättiin vetyä. Joitakin havaintoja saatiin myös mahdollisesta metaanin hapettumiseen liittyvästä raudanpelkistyksestä sulfaattiköyhässä pohjavedessä. Lisäksi havaittiin, että liuennut sulfidi pystyi reagoimaan suoraan mineraalissa olevan Fe(III) kanssa (pääsääntöisesti rautasilikaattien, mutta vähäisiä määriä rauta(III)oksidaa) löydettiin myös mineraaliparaateista, Johansson et al. 2019) saostuen rautasulfidina.

Työpaketissa WP2 1) määritettiin bentoniitin sisältämien rikkimineraalien liukoisuudet ja niiden tasapainokonsentraatiot. Liukoisuustestien tuloksena havaittiin, että bentoniitin kanssa kontaktissa olevassa vedessä sulfidipitoisuus oli alle määrittämiskokona. Vastaava tulos saatiin myös, kun bentoniittiin lisättiin pieniä määriä sulfidia. Tulokset viittaavat siihen, että bentoniitti alentaa vedessä olevaa sulfidipitoisuutta. Lisäksi 2) tutkittiin viiden eri saturoituneen bentoniitin tiheyden vaikutusta mikrobiologiseen aktiivisuuteen tuottaen sulfidia. Tavoitteena oli löytää kynnystiheys mikrobiaktiivisuuden suhteen. Kokeet osoittivat, että testatuilla bentoniiteilla oli materiaalista riippuva kynnystiheys, jota korkeammilla tiheyksillä mikrobiologinen sulfidintuotanto oli merkityksettömän vähäistä, vaikka muut olosuhteet olivat otolliset sulfaatinpelkistäjäbakteerien toiminnalle. Tämä todistaa, että sulfidin tuotantoaktiivisuutta voidaan estää asettamalla vaatimus bentoniitin tiheydelle, mikä on tärkeä tieto loppusijoituskonseptissa käytettävälle bentoniittipuskurille. 3) Tutkittiin mikrobien kykyä hyödyntää kompaktoidusta bentoniitista liukenevaa orgaanista ainetta. Tulokset osoittivat, että kaikista tutkituista bentoniittimateriaaleista uuttuva orgaaninen aine pystyy ylläpitämään sulfaatinpelkistäjäbakteerien ja muiden mikrobien aktiivisuutta.

WP3 käsitti työpaketissa sovellettujen mallinnustyökalujen keskinäisen vertailun ja osittaisen verifiointin. Kolme mallinnusryhmää kehitti toisistaan riippumattomasti reaktiivisen kulkeutumismallinnuksen työkaluja, joiden päämääränä on pystyä kuvaamaan ja simuloimaan sulfidivuota ja -evolu-

tiota (lähteet ja nielut) KBS-3 konseptin lähialueen eri osissa (huomioiden kapselin, puskurin, täytön, kivi-täyttö rajapinnan ja lujituspultit). Perustapaus (Base Case), jossa sulfaatin pelkistys tapahtui mikrobiaktiivisuuden vaikutuksesta ainoastaan kallio-bentoniitti-rajapinnassa, valittiin käytettäväksi mallien väliseen vertailuun ja osittaiseen verifiointiin. Lisäksi testattiin kehitetyillä työkaluilla toteutettujen eri mallinnusstrategioiden kykyä mallintaa valittuja erillistapauksia (Variant Cases). Eri ryhmien mallinnustulokset vastasivat toisiaan kohtuullisesti huomioiden merkittävät erot mallinnusten lähestymistavoissa. Voidaankin sanoa, että tavoite kehittää tulevien turvallisuusanalyysien tarpeisiin rikin kiertoa ja sulfidin aiheuttamaa kapselikorroosiota koskevat kytketyt mallinnusmenetelmät, joilla voidaan korvata aiemmin käytetyt erilliset tai löyhästi kytketyt mallit, täyttyi ainakin osittain.

Contents

1	Introduction	13
1.1	Background	13
1.2	Objectives	13
1.3	Reporting	14
1.4	Abbreviations	15
2	WP1 – Sulfide concentrations and processes in the geosphere	17
2.1	Background	17
2.1.1	Sulfide concentrations in groundwater samples from Forsmark	17
2.1.2	Sulfide concentrations in groundwater samples from Olkiluoto	18
2.1.3	The sulfate reduction process	19
2.1.4	Investigations and objectives	20
2.2	Leaching of potential nutrients from borehole installation material	20
2.2.1	Performance	21
2.2.2	Results	22
2.2.3	Conclusions	23
2.3	Development of gas sampling equipment and tests of sampling conditions	24
2.3.1	Performance	24
2.3.2	Results	25
2.3.3	Conclusions	27
2.4	The Gas Monitoring Experiment in ONKALO – GAME	27
2.4.1	Performance	27
2.4.2	Results	31
2.4.3	Conclusions	35
2.5	Microbial release of Fe from iron-bearing minerals – FRED	35
2.5.1	Performance	36
2.5.2	Results	39
2.5.3	Conclusions	42
3	WP2 – Sulfide processes in the buffer and backfill	43
3.1	Background	43
3.2	Solubility of sulfide minerals originally present in the buffer	44
3.2.1	Description	44
3.2.2	Results	46
3.2.3	Conclusions	49
3.3	Threshold buffer density	50
3.3.1	Description	50
3.3.2	Results	52
3.3.3	Conclusions	55
3.4	FaTSu – Microbial utilization of bentonite organic matter	56
3.4.1	Description	56
3.4.2	Results	57
3.4.3	Conclusions	57
4	WP3 – Integration for the safety case – modelling	59
4.1	Background	59
4.2	The conceptual model	60
4.3	The models used by the teams	61
4.4	Results	63
4.4.1	Progress in development	63
4.4.2	Inter-model comparison for the Base Case	63
4.4.3	Results for the Variant Cases	65
4.5	WP3 – Achievements and implications for the KBS-3 safety case	67
5	Overall conclusions	69
	References	71
	Appendix Simulation cases for WP3	75

1 Introduction

1.1 Background

The sulfide concentration in groundwaters and in porewaters in the buffer and backfill is important for the safety assessment of a KBS-3 repository for nuclear waste. Sulfide reacts with copper, causing corrosion of the waste canisters in an anaerobic environment. This failure mechanism in the safety assessment is treated in SR-Site (SKB 2011) and Posiva's Performance Assessment 2012 e.g. Posiva (2013a).

Earlier studies (e.g. Tullborg et al. 2010) have shown that further knowledge about different sulfide issues are needed. Such issues are for example the sulfide production by SRB (sulfate reducing bacteria), sources and sinks for the sulfide as well as its limiting processes. Reliable and representative data are important for the interpretations and especially the data on dissolved organic components and gases have been questioned. An especially critical step is the sampling of groundwater for determinations of dissolved gases. As an example, H₂ which is especially important in the microbial sulfide generation context, may easily escape during sampling and sample handling. Therefore, there is a need for tests of different sampling conditions as well as different sampling methods to interpret and understand the representativity of the gas data and the size of the spread.

Furthermore, there are different possible sulfide modelling approaches with different focus on transport, chemistry, and electrochemical details (King 2008). The update in detail and the tests of robustness between these approaches are steps in the development of tools for the integrated modelling of sulfide corrosion.

1.2 Objectives

The general aim with the Integrated Sulfide Project (ISP) was to assemble data and increase the knowledge on sulfide formation and attenuation processes that affect the sulfide concentration and/or the sulfide production rate in groundwater as well as in bentonite.

The purpose of the joint project was to conduct several studies and investigations at Posiva as well as SKB to gain knowledge on sulfide formation and attenuation processes. The intention was also to collect more sulfide data from groundwater and to compare the experiences from the two different groundwater systems in Finland and Sweden, respectively, to increase the understanding. The project covered both the geosphere and the buffer-backfill systems. Furthermore, development work for the overall modelling of sulfide in the near field (i.e. the canister, the buffer-backfill system and adjacent rock) was included in the project.

The project was divided into three work packages (WP) with their respective leaders:

- WP1 – Sulfide concentrations and processes in the geosphere.
- WP2 – Sulfide concentrations and processes in bentonite.
- WP3 – Integration with the safety case.

The aims of WP1 were to better understand: i) the processes or factors controlling sulfide production in deep groundwaters, ii) the amount and transport of the gases that can be used by SRB (sulfate reducing bacteria) and iii) the extent of microbial release of iron from iron-bearing minerals that limits the availability of sulfide by precipitation of FeS.

WP2 concerned characterisation of all processes that may produce sulfide in the buffer and backfill: i) dissolution of sulfide accessory minerals in the bentonite and ii) microbial sulfate reduction. The task was also to define bentonite threshold densities for sulfide formation and transport in the near field and to evaluate the role of bentonite organic matter in sustaining microbial sulfate reduction.

WP3 focused on development of a conceptual model as well as reactive transport modelling tools. The conceptual model implies identification of potential sulfide sources and sinks as well as processes and reactions which affect sulfide concentrations and transport in different parts of a repository, including canister corrosion. The modelling tools should be possible to use for description and simulation of the evolution of dissolved sulfide concentrations and fluxes in different parts of the repository: i) near geosphere with EDZ (excavated damaged zone) and rock bolts, ii) deposition tunnel with backfill and iii) deposition hole with buffer and canister.

1.3 Reporting

The results of all the work packages are summarised in this report while details of the different studies are presented in separate SKB reports or Posiva working reports (Table 1-1). In the FaTSu project the parts that were included in the ISP were reported in one internal memo and as a research paper (Table 1-1). Another emphasis of this report is to consider the suitability of the new information in the safety cases for both parties (SKB and Posiva) as well as to evaluate the different modelling approaches and their pros and cons. Finally, identification of possible need for further development work is also of concern.

Table 1-1. List of the Sub-reports.

Title	Report no/	Reference in the text
Release of H ₂ and organic compounds from metallic and polymeric materials used to construct stationary borehole equipment	R-16-01	Chukharkina et al. 2016
Microbial sulfide production during consumption of H ₂ and organic compounds released from stationary borehole equipment	R-16-17	Chukharkina et al. 2017
Development and testing of gas samplers in tunnel environments	R-16-16	Nilsson et al. 2017
The Gas Monitoring Experiment in Olkiluoto underground drillhole ONK-KR17: Extracting gases from crystalline rock matrix.	WR 2021-01	Lamminmäki et al. 2021
Microbial release of iron from Olkiluoto rock minerals	WR 2018-30	Johansson et al. 2019
Experiments with bentonite and sulfide – results from experiments 2013–2016	P-18-31	Svensson et al. 2018
Microbial sulfide-producing activity in MX-80 bentonite at 1750 and 2000 kg m ⁻³ wet density	R-15-05	Bengtsson et al. 2015
Microbial sulfide producing activity in water saturated MX-80, Asha and Calcigel bentonite at wet densities from 1500 to 2000 kg m ⁻³	TR-16-09	Bengtsson et al. 2017a
Bacterial sulfide-producing activity in water saturated iron-rich Røkle and iron-poor Gaomiaozi bentonite at wet densities from 1750 to 1950 kg m ⁻³	TR-17-05	Bengtsson et al. 2017b
Verification of microbial sulfide-producing activity in calcigel bentonite at wet densities of 1750 and 1900 kg m ⁻³	P-19-07	Haynes et al. 2019
Compacted bentonite as a source of substrates for sulfate-reducing microorganisms in a simulated excavation-damaged zone of a spent nuclear fuel repository	Applied Clay Science	Maanoja et al. 2020a
Simulating the dissolution of organic compounds and sulfate from compacted clay and growth of sulfate-reducing bacteria in an excavation-damaged zone (FaTSu theme 3)	Internal memorandum POS-029982	Maanoja et al. 2020b
3D and 1D Dual-Porosity Reactive Transport Simulations – Model Improvements, Sensitivity Analyses, and Results from the Integrated Sulfide Project Inter-Model Comparison Exercise	WR 2018-31	Pekala et al. 2019
Reactive transport modelling considering transport in interlayer water – New model, Sensitivity Analyses, and Results from the Integrated Sulfide Project Inter-Model Comparison Exercise	TR-18-07	Idiart et al. 2019
Copper Sulfide Model (CSM). Model Improvements, Sensitivity Analyses, and Results from the Integrated Sulfide Project Inter-Model Comparison Exercise	TR-18-08	King and Kolář 2019

1.4 Abbreviations

Table 1-2. The abbreviations and acronyms used in this report are explained below.

AM	Autotrophic methanogens
AGW	Anaerobic Ground Water
ATP	Adenosine triphosphate
BFZ	Brittle fracture zone
CCC	Complete Chemical Characterization (an investigation method used by SKB)
DGN	Diatexitic Gneiss
DOC	Dissolved organic carbon
EDZ	Excavation damage zone
FaTSu	Formation and Transport of Sulfide in buffer and backfill project (in WP2)
FRED	Microbial iron reduction (Fe-REDuction) experiment (in WP1)
GAME	GAs Monitoring Experiment in ONKALO® (in WP1)
HZ	Hydrological zone
ISP	Integrated Sulfide Project
MFGN	Mafic Gneiss
ONKALO®	The underground rock characterisation facility. ONKALO® is a registered trademark of Posiva Oy
PA	Polyamide
PEHD	Polyethylene high density
PGR	Granitic Pegmatoid
PU	Polyurethane
PVC	Polyvinylchloride
PEEK	Polyether ether ketone
SRB	Sulfate reducing bacteria
SR-Site	Safety assessment (SKB 2011)
VGN	Veined Gneiss
WP	Work package
Äspö HRL	Äspö Hard Rock Laboratory

2 WP1 – Sulfide concentrations and processes in the geosphere

2.1 Background

This chapter treats the experiments performed within the collaboration project to further understand the sulfide processes in the geosphere. High sulfide concentrations in the order of several milligrams per litre have been observed both in the Swedish and the Finnish groundwaters during the hydrogeochemical investigations. However, the circumstances and the sampling conditions have been somewhat different. Information such as observations of high sulfide concentrations reported by SKB and Posiva and some previous studies within this topic are summarised in this background section. Furthermore, a short discussion about sulfate reduction is included as well as a list of the studies performed within the geosphere work package and their objectives.

2.1.1 Sulfide concentrations in groundwater samples from Forsmark

A significant increase in the sulfide concentrations have been observed in Forsmark and to some extent also at Äspö and Laxemar, when comparing the first investigations in a borehole with later regular monitoring at corresponding depths. This initial extensive investigation in each borehole (Complete Chemical Characterisation or CCC) is performed by using packers that are moved along the borehole and stay for a few weeks in the same position. The sampling within the monitoring programme, on the other hand, is conducted in borehole sections isolated by fixed packer installations that stay in the borehole for several years. Due to the observed sulfide increase, more efforts were put in the hydrogeochemical monitoring in the Forsmark boreholes to find explanations. It was found that the sulfide concentrations decreased with the increase in exchanged groundwater volume prior to collection of each sample in a sample series and that unintended pump stops made a break in these decreasing sulfide trends. This systematic decrease is illustrated in Figure 2-1 using sulfide data from the hydrochemical monitoring of isolated borehole sections in Forsmark between 2010 and 2018.

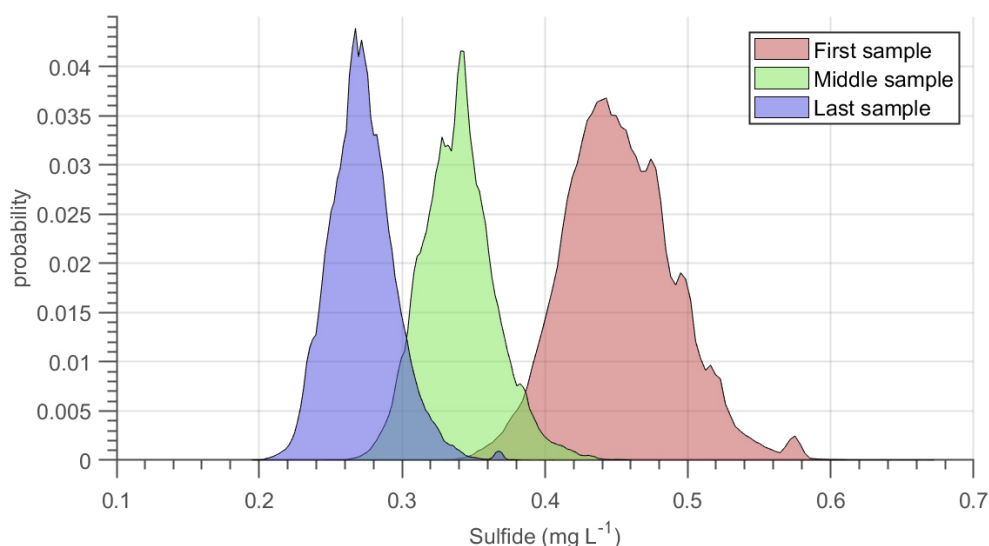


Figure 2-1. Discrete probability density function for the sulfide concentrations in consecutive samples taken in sample series. Statistically significant distributions of sulfide concentrations showing the difference between the first, second and third sample in all sample series. Data obtained between 2010 and 2018 are included and they represent the monitored borehole sections in the core boreholes in Forsmark.

Due to the systematic difference, individual plug flow calculations were done for each monitored borehole section, considering the number, location and hydraulic transmissivity of the water yielding fractures in each borehole section. This in order to estimate the volume to be exchanged to obtain a sample with water directly from the bedrock formation, i.e. with as little contribution as possible to the sample from the water standing in the borehole section prior to flushing and sampling. The difference between the required volume to be exchanged and the actual exchanged volume seemed to have an impact on the sulfide concentration measured in the sample. The conclusion was that the high sulfide concentrations were present in this initial water standing in the borehole sections and not in the groundwater taken directly from the fracture system (Tullborg et al. 2010).

The findings in Forsmark led to more thorough investigations concerning high sulfide concentrations and their causes. Three core drilled boreholes from the surface in Äspö and Laxemar were studied and they confirmed the findings from Forsmark (Rosdahl et al. 2011).

As a second step, studies were performed in three boreholes in the Äspö Hard Rock Laboratory (Äspö HRL) to investigate whether different plastic material and metals used in borehole installations could promote sulfide production in the water standing in the borehole sections (Drake et al. 2014). The leaching and corrosion experiments as described in Section 2.2 imply more studies on the same theme.

Furthermore, a field study of microbial coating on different materials was conducted *in situ* in borehole KFM03A in Forsmark (Bengtsson et al. 2019). It was observed from ATP determinations that on-site growth of biofilms on the PEHD and PU samples contained more ATP than the other samples (Table 2-1) which imply larger and more active cells.

Table 2-1. ATP determinations for the microbial coating on different materials in the flow cell installation in KFM03A.

Sample	ATP (amol mL ⁻¹)	
	Sub sample 1	Sub sample 2
PA	53 900	46 400
PVC	85 400	267 000
PEHD	366 000	307 000
PU Slitan 90A-05	392 000	354 000
PU Slitan 80A-71	142 000	115 000
Al	30 700	34 800
Fe	37 100	47 400

2.1.2 Sulfide concentrations in groundwater samples from Olkiluoto

The presence of the ONKALO underground facility has changed the groundwater flow pathways compared to the natural situation without this tunnel system. If deep boreholes are kept open, the created head differences allow groundwater flow along them due to the drawdown towards the tunnel system (Posiva 2012a, Section 7.3.6). This is especially notable in boreholes which intersect both the higher head feature HZ19 and the lower head feature HZ20 in the middle of the Olkiluoto island including the ONKALO site. Less saline groundwater from HZ19 flowing through the open pathway towards a zone of lower pressure has caused dilution of the groundwater particularly in the HZ20A intersections – this has been observed in several boreholes. Therefore, the boreholes have been closed with multi-packer systems to isolate all hydrological zones from each other. During the open borehole phase after drilling, prior to the installation of the multipacker system, the hydraulic conditions in OL-KR13 resulted in elevated dissolved sulfide concentrations (12 mg L⁻¹) in the low head intersection of feature HZ001 in 2001 (Posiva 2012a, Wersin et al. 2014). It was concluded that the drawdown of sulfate-rich groundwater and the mixing with hydrocarbon-rich brackish Cl type groundwater in this fracture zone had activated sulfate reducing bacteria (SRB). These groundwaters showed a different oxidation-reduction potential (redox state), prior to the mixing. Elevated sulfide concentrations have also been observed at several other sampling locations with similar hydraulic conditions. The highest sulfide concentration observed is 49 mg L⁻¹. This sample was collected from borehole OL-KR46 at a depth of approximately 530 m (Bell et al. 2020). The borehole intersects the fracture zone HZ056 as well as the ONKALO-

tunnel system and this causes a constant drawdown. Which electron donor (energy source) that enables the SO_4 reduction process in brackish Cl and saline type groundwaters is a complex question. There are minor indications of anaerobic CH_4 or other hydrocarbon oxidation (Posiva 2012a, Section 7.4) and oxidation of DOC is evident in shallow depths. However, hydrogen in hydrocarbon-rich groundwaters has been considered the most potential electron donor, which is easily usable by SRB. Recently, this subject of sulfide formation has been studied, and DOC and H_2 have been found to fuel sulfate reduction at different depth intervals and hydrological conditions in Olkiluoto (see details in Bell et al. 2020).

The high hydraulic gradient created by the underground spaces and excavations in the final disposal facility may intensify chemical effects in open boreholes as compared to a situation with natural head distribution (Penttinen et al. 2019). Most of the boreholes have now been plugged with multi-packer systems. The plugging has been prioritised in the boreholes near the underground tunnels and facilities. This in order to avoid open borehole conditions. However, occasional malfunctions in multipacker systems (e.g., pressure loss from plugs) may still result in drawdown of shallower groundwater types to deep fractures. Although these cases, caused by open borehole conditions, represents artificial mixing of groundwater and subsequent sulfide formation, the changes in groundwater chemistry can be significant. Furthermore, the recovery can take several years or tens of years and some of the effects may persist and never return to the baseline situation. Therefore, these samples can be considered to represent the site hydrogeochemistry during the construction and operational phase of a repository.

Most importantly, the above discussed phenomenon is also observed within water conductive fractures or fracture zones, when they are intersected by underground tunnels causing groundwater flow towards the tunnels. This results in mixing of different water types (e.g. SO_4 -rich water from the upper part of the bedrock is mixed with more saline deep groundwater with higher CH_4 and H_2 concentrations), and possibly sulfide formation.

2.1.3 The sulfate reduction process

Sulfate reduction has been associated with transient hydrological conditions where SO_4 -rich waters are mixed with saline groundwaters with abundant CH_4 and other hydrocarbon gases. However, recent monitoring and experimental data from Olkiluoto (Edlund et al. 2016) indicate that the major electron donor is probably neither CH_4 nor DOC. At these hydrogeochemical conditions it is rather H_2 that fills this need. Hydrogen formation is possible by water-mineral interaction at the elevated temperatures prevailing at depth in the bedrock, e.g. by the processes described by Mayhew et al. (2013). Throughout the geological history, H_2 may have migrated upwards and accumulated in groundwater and matrix pore water. Hydrogen is the favoured energy source for many lithotrophic microorganisms such as SRB and autotrophic methanogens (AM) and acetogens (AA). Observations of high H_2 contents (millimolar level) are however few in the groundwater samples from Olkiluoto and Forsmark (Appendix 1 in Pitkänen and Partamies 2007, Hallbeck and Pedersen 2008a). The reasons may be loss of H_2 during pumping or sample handling, and/or H_2 consumption by the microbes in the fracture groundwater. The concentrations are nevertheless somewhat enriched and frequently above the threshold $1 \mu\text{M}$ at which sulfate reduction ceases (Pedersen 2012b). In the presence of SO_4^{2-} , SRB outcompetes AM since the hydrogen threshold concentration of AM is much higher (Kristjansson et al. 1982, Stams et al. 2003). Although H_2 is easily degassed and lost from the groundwater due to the pressure decrease during pumping, it may still be conserved in the matrix pores. Reliable information on available H_2 concentrations is therefore important to confirm the energy and electron source for microbial sulfate reduction. The overall concerns regarding H_2 are the effect of sampling and the lack of information about H_2 in the rock matrix and its migration from great depths.

The sulfate reduction is an ongoing process also at baseline steady state conditions, when SO_4 and a suitable electron donor is available. However, most of the observed sulfide concentrations in fracture groundwater have generally been only slightly over the detection limit. The high values in Forsmark and Olkiluoto are explained in Sections 2.1.1 and 2.1.2 above. From time to time, during past paleohydrogeological changes SO_4 has been provided into the deeper part of the bedrock (cf. Littorina Sea stage). At present, sulfate rich water reaches deeper levels due to drawdown caused by the presence of boreholes or construction of underground tunnels. This intrusion of sulfate rich water, in turn, causes enhanced sulfide formation. However, monitoring and modelling results indicate that elevated sulfide concentrations are unstable and tend to disappear within a few years when the hydrogeological conditions have been stabilised (Wersin et al. 2014). The reason may be depletion of energy sources (e.g. H_2 /DOC) or

precipitation of insoluble iron sulfides. Fine grained, black iron sulfide precipitates as well as minor recent pyrite precipitates have been observed during sampling of sulfide rich groundwaters in Olkiluoto (Seitsamo-Ryynänen and Karhu 2020). The concentrations of dissolved iron in the groundwater is generally low and rock types or fracture infillings in Olkiluoto do not contain any iron oxyhydroxides which can be easily usable for iron reducers to precipitate sulfide. Iron oxyhydroxides as fracture filling has only been found at very shallow depths. Therefore, the hypothesis was that iron could be released from silicate minerals such as biotite, chlorite, garnet, or epidote. These silicates contain mainly ferrous iron but can also include low amounts of ferric iron. However, iron minerals display a wide variability in terms of reactivity towards dissolved sulfide, ranging from reactive Fe(III)-oxyhydroxides with very fast kinetics to Fe-silicates with very slow kinetics (Gimeno et al. 2008).

2.1.4 Investigations and objectives

The outlines of investigations related to the sulfide processes in the geosphere and their objectives are summarised below.

1. Two measures were taken to increase the understanding of the controlling processes related to sulfide production in deep groundwaters:
 - a. Experiments to find out if any material from borehole instrumentations may provide energy sources for SRB, for example by releasing organic components to the groundwater in the borehole section. The possible release of hydrogen from metal parts of the borehole installations (packers) was also studied since galvanic metal corrosion may produce hydrogen as well as acting as a source of metal ions in the water (Section 2.2).
 - b. Sharing of data from the hydrochemical monitoring performed in the two countries, see Sections 2.1.1 and 2.1.2. to benefit from the investigations and findings regarding the different groundwater conditions in Forsmark and Olkiluoto.
2. The following actions were taken to increase the understanding of transport processes that involve hydrogen and other gases that can be used by SRB:
 - a. Development of sampling techniques and equipment for analyses of gases including stable isotopes (Section 2.3).
 - b. Analyses of the gas concentration in the bedrock and studies of its diffusion using a new technique, called Gas Monitoring Experiment (GAME) in ONKALO. A new borehole was drilled, packed off and filled with nitrogen gas. The gas concentration was then monitored on a regular basis from December 2015 to June 2017 (Section 2.4).
3. The microbiological iron reduction of iron silicates was studied in the subproject FRED (Section 2.5) to understand if microbes are able to release dissolved Fe(II) from fracture infillings and serve as a source to limit the sulfide concentration in the groundwater.

2.2 Leaching of potential nutrients from borehole installation material

The leaching experiments are reported in Chukharkina et al. (2016, 2017). A short summary is given below.

The only possible process for production of sulfide in groundwater is the reduction of sulfate by sulfate reducing bacteria (SRB) using available sources of electron donors and carbon sources. This study was initiated to investigate if the materials used in borehole equipment could provide electron donors for SRB, in the form of H₂ or organic compounds. The extraction and leaching experiments described in this section were performed in order to reveal if material in stationary borehole equipment may release such compounds to the groundwater.

While the presence, numbers, and diversity of SRB in deep groundwater have been well documented, their activity is less well studied. In Posiva SKB (2017) an upper limit of 3 mg L⁻¹ (≈ 0.094 mM) as a performance target for sulfide concentrations in the groundwater is given. Sulfide concentrations of around 4 mg L⁻¹ (0.12 mM) have been observed in groundwater from boreholes with stationary equipment for isolation of borehole sections in Forsmark (Tullborg et al. 2010). Extreme values of

3 mM (96 mg L⁻¹) sulfide were observed in boreholes at the Äspö Hard Rock laboratory (Äspö HRL) (Rosdahl et al. 2011) and the underlying reasons for this accumulation have not been fully understood (Drake et al. 2014).

Hence, a remaining key issue for the safety case was to identify the factors controlling the rate of sulfide production in the geosphere, including man-made artefacts. The extremely high sulfide concentrations in Sweden have always been observed in boreholes with packer installations where borehole sections have been left unattended without any sampling for several months or years (Tullborg et al. 2010, Rosdahl et al. 2011).

2.2.1 Performance

In Forsmark, the metallic material used in equipment for core drilled boreholes is generally stainless steel, however, percussion boreholes were initially equipped with aluminium parts. These have now been replaced with stainless-steel equipment. The borehole equipment at Äspö HRL are generally made of aluminium and only some boreholes designed for special experiments or new boreholes drilled after 2011 have equipment made of stainless steel.

Aluminium and stainless-steel samples were exposed to sterilized filtered groundwater at 30 °C and 70 °C and to natural groundwater at 30 °C. The experiments were carried out in closed vessels at oxygen-free conditions during several months (Figure 2-2). Samples for gas analyses were collected regularly from the top of each vessel during this period.

Five different polymeric materials often used in borehole equipment were selected (Figure 2-3) for the study of organic release from equipment. A first step was extraction by hexane to get a comprehensive knowledge about possible compounds that can be released to groundwater.

The next step implied leaching of the different materials in sterile-filtered groundwater and in natural untreated groundwater at oxygen-free conditions for six months. The released compounds were determined by Solid-Phase Extraction (SPE) followed by gas chromatography with mass spectroscopic (GC-MS) detection.

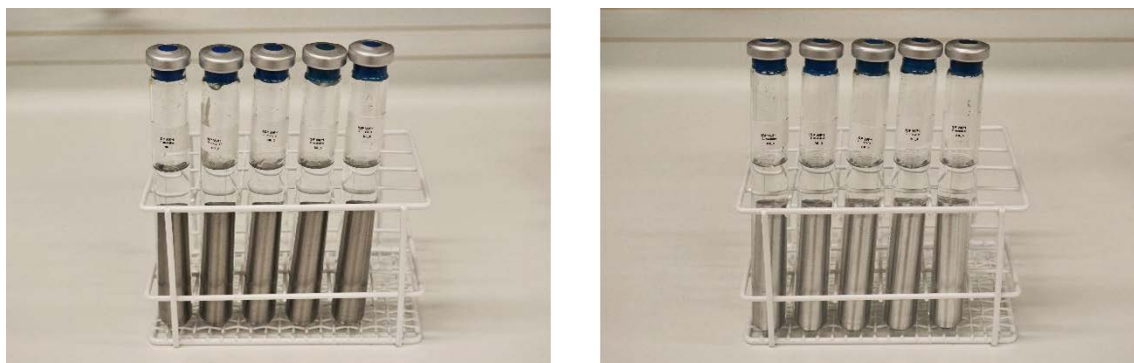


Figure 2-2. Metallic rods contained in glass vessel with O₂-free sterile filtered groundwater. Left, stainless steel and right aluminium (Chukharkina et al. 2016).

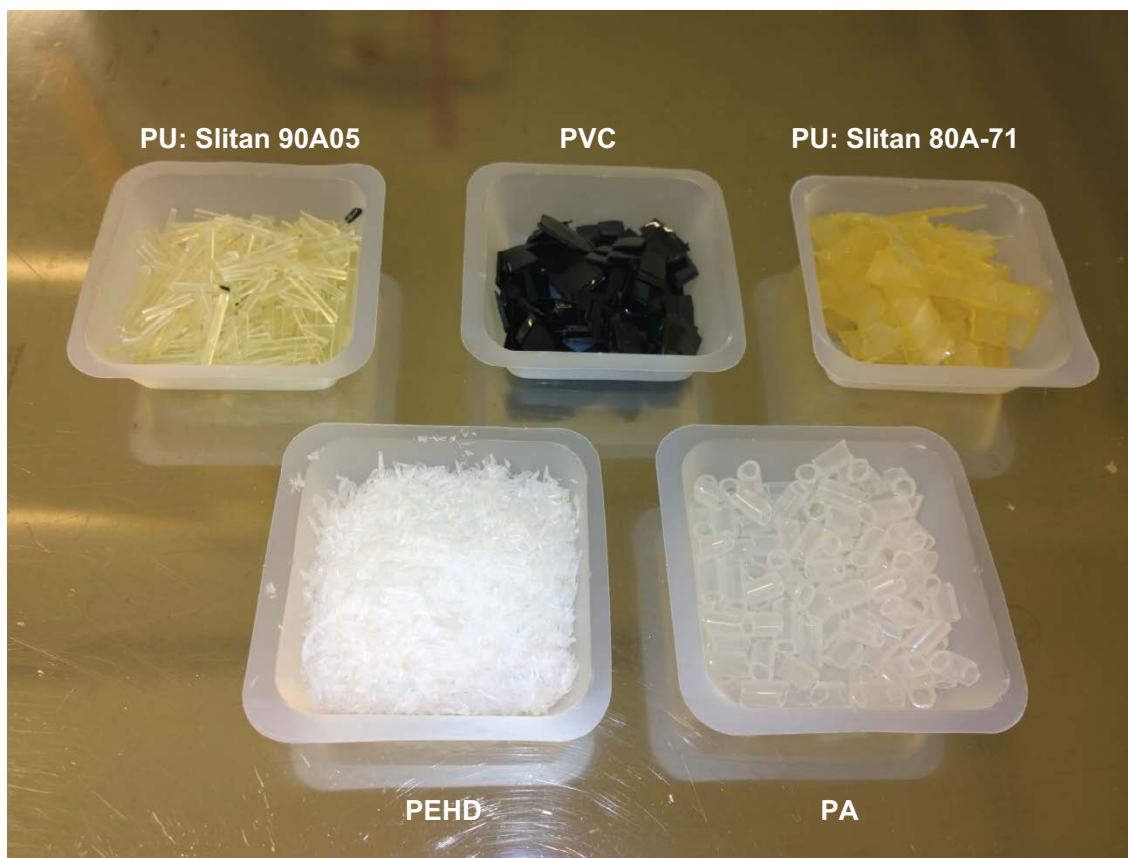


Figure 2-3. Polymeric materials used in the leaching experiments: PU, polyurethane; PVC, polyvinylchloride; PEHD, polyethylene high density; PA, polyamide (Chukharkina et al. 2016, 2017).

2.2.2 Results

Release of hydrogen gas occurred in both types of vessels containing stainless steel and aluminium rods, respectively. However, higher release rates were observed for the aluminium samples compared to the steel samples. At sterile conditions, the release continued during the entire experiment period. With untreated groundwater, the concentrations of H₂ levelled out after a few weeks of leaching. This showed that hydrogen gas may be consumed by the bacteria present in this water (Figure 2-4).

Several of the compounds that were found in the hexane extracts of the polymeric material were also found in the SPE extracts of the groundwater leachates. The concentrations of the compounds increased with time at sterile conditions, and they generally decreased at natural conditions (using untreated groundwater). Microbiological analyses showed high levels of cells including SRB in the latter water samples.

Combined results of microbiological and chemical analyses showed that PVC and PU Slitan 90A-05 were more favourable for sulfide production than the other organic materials (Chukharkina et al. 2017). However, growth of SRB were more extensive in presence of PU Slitan 80A-71 and PU Slitan 90A-05 than with the other polymers (Table 2-2).

The results can be compared with the data from the microbial coating experiment in Table 2-1. Here the ATP determinations showed that there was more microbial coating on the PEHD and the PU samples than on the other materials.

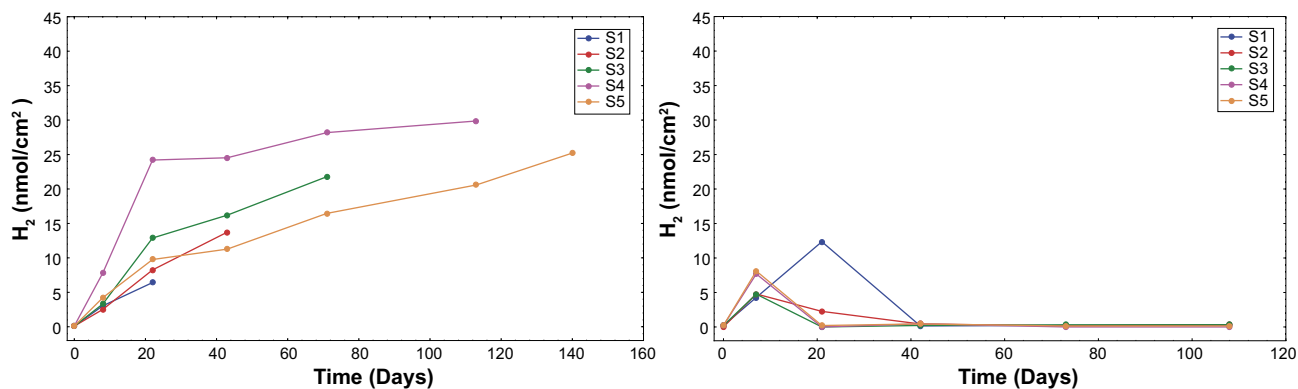


Figure 2-4. H_2 leaching under sterile conditions (left) compared with natural conditions (right) (Chukharkina et al. 2016, 2017). S1–S5 represent discrete samples containing stainless steel. For details see Table 2-1 in Chukharkina et al., (2017).

Table 2-2. Results from the leaching experiments showing SRB data for the different polymeric materials under natural conditions i.e. using not sterile-filtered groundwater for leaching.

Sample	SRB (cell mL ⁻¹) (low and upper limits for 95 % confidence interval)					
	98 days			186 days		
	MPN index	Lower	Upper	MPN index	Lower	Upper
Control	≥ 16 000	-	-	8.0	3.0	25.0
PA	≥ 1 600	-	-	70 000	30 000	210 000
PVC	90 000	30 000	290 000	17 000	7 000	48 000
PEHD	≥ 1 600	-	-	11.0	4.0	29.0
PU 90A-05	≥ 16 000	-	-	300 000	100 000	1 300 000
PU 80A-71	1.7	0.7	4.0	160 000	60 000	530 000

2.2.3 Conclusions

The experiments showed that both metallic and organic materials in the borehole equipment can provide electron donors to stimulate sulfide production by SRB. Furthermore, the leaching experiments of polymeric materials indicated that bacteria present in groundwater will trigger processes causing sulfide and sulfur production. These types of instrumentation materials will not be present after the closure of a repository. Therefore, sulfide production favoured by these materials will be of no relevance for the safety assessment. On the other hand, the possibility of artificially high sulfide values may appear and need to be considered during the construction of the repository due to the different materials used in equipment and installations during this phase.

2.3 Development of gas sampling equipment and tests of sampling conditions

The development of sampling equipment and the tests performed are reported in detail in Nilsson et al. (2017). The text below gives a short summary.

Since SRB can use hydrogen and methane gas in groundwater as electron donors, reliable gas data are important for the understanding of sulfide production processes. The data from the gas sampling conducted during the previous site investigation in Forsmark are rather few (Hallbeck and Pedersen 2008a) and there are only a small number of replicate samples. Although the data seem consistent and repeatable it is a possibility that they are biased by systematic errors due to the sampling method used. A sampling technique issue arose due to these doubts. Furthermore, there is a need to develop a new type of sampling equipment and method to be used in horizontal and sub-horizontal boreholes during the coming Detailed Investigations in Forsmark for the construction phase of the repository. The main part of the new boreholes will be drilled from tunnels and not from the ground surface. Therefore, the existing equipment is unsuitable.

2.3.1 Performance

Two sampling methods for gas analyses and isotope determinations, respectively, were tested in selected boreholes and borehole sections at the Äspö Hard Rock Laboratory (Äspö HRL).

- Sampling of groundwater for determination of dissolved gases (H_2 , He, Ar, O_2 , N_2 , CO_2 , CO, CH_4 and other hydrocarbon gases).
- Sampling of released gas in order to determine stable isotope ratios in gases (deuterium in H_2 and CH_4 , $\delta^{18}O$ in CO_2 as well as $\delta^{13}C$ in CO_2 and CH_4).

The use of boreholes drilled from a tunnel system facilitated the sampling since no pumping was needed due to the pressure gradient out from the boreholes. The sampling of released gas (b) using the so-called gas-trap principle proved to be less useful since the filling of the sample containers with gas was very time consuming. Therefore, the following description concentrates on the determination of dissolved gases (a) which is also the most relevant topic for the sulfide issue.

Groundwater sampling for analyses of dissolved gas was performed by using a flow through sampler, see Figure 2-5. Several series of samples were collected and the exchanged water volumes from the sampled borehole section prior to sampling as well as the pressure drops (counter pressure) were varied. The purpose was to study if these conditions can affect the amount of dissolved gas in the samples. The gas transfer to the appropriate sample vessels and the compression of the gas was conducted in the laboratory.

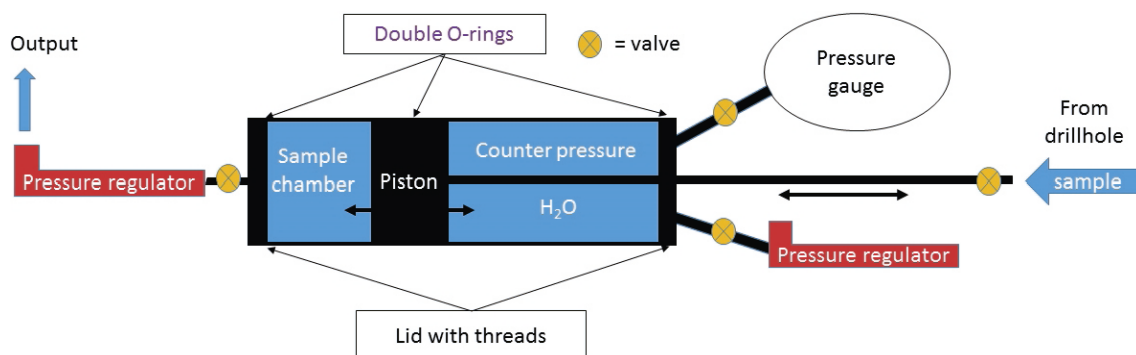


Figure 2-5. Schematic outline of the sampler for dissolved gas (Nilsson et al. 2017).

2.3.2 Results

- The samples of gas extracted from the water standing in the borehole were overrepresented with N_2 in all targets and also with O_2 and CO_2 in the case where the sampled borehole section is located close to the tunnel, see Figure 2-6.
- The gas samplers performed well, and reproduced volumes of extracted gas were obtained after approximately a volume twice the individual plug flow volume of each borehole section was flushed out.
- The gases Ar, CH_4 , CO_2 and He all reproduced well over 4 discrete sampling occasions representing borehole section water and water obtained after flushing 2, 3 and 5 times the plug flow volumes of each sampled borehole section.

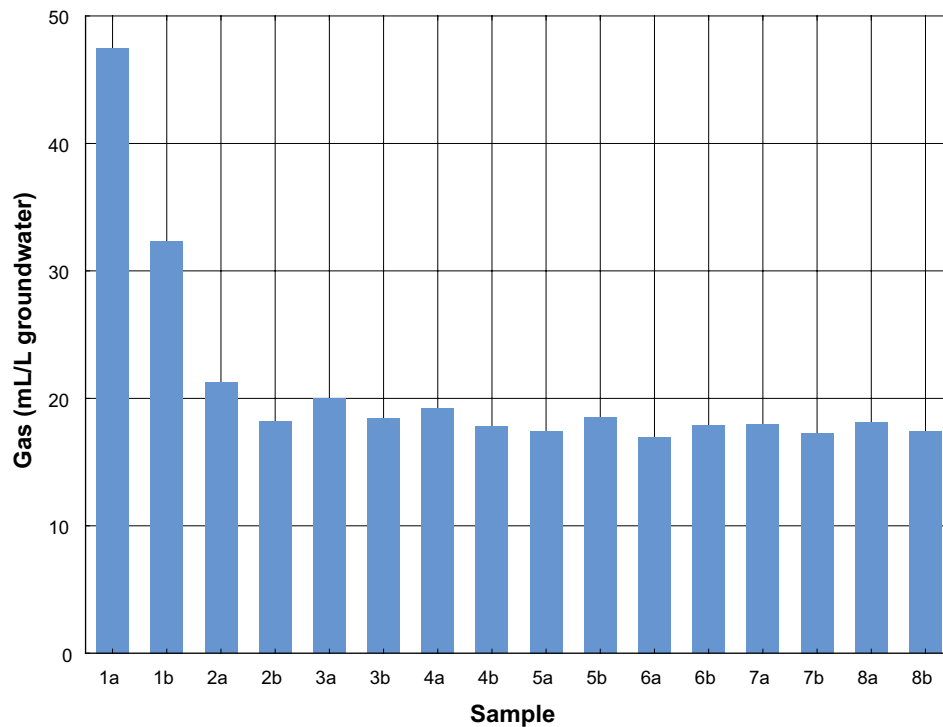


Figure 2-6. Total amount of extracted gas in the series of samples from borehole KA2563A:1 calculated as mL of gas per L of groundwater. The samples a and b are collected in two different containers and the filling is made with a minimum of flushing and time in between them. The larger gas concentrations in the first two samples reflect the enhanced gas content in the groundwater initially present in the borehole section compared to the concentration in the formation groundwater. The higher concentrations of dissolved gas in these samples were mainly due to more N_2 (Nilsson et al. 2017).

- The analysis of H₂ was performed on pairwise samples and each pair generally reproduced very well which attests the precision in sampling, extraction, and analysis of the applied methods. However, H₂ was the gas that varied most in concentration when pressure and sample flow rate were altered, see Figure 2-7. The larger the flow rate, the less H₂ was detected. It appeared important to have a slow flow rate and as small pressure drop as possible prior to and during the sampling to obtain relevant concentrations since H₂ is easily degassing. Furthermore, the borehole sections may contain enhanced H₂ concentrations due to corrosion processes if the equipment contains parts made of aluminium. Therefore, to exchange sufficient but not too large water volumes prior to sampling is important to ensure samples representing groundwater from the bedrock fractures.
- H₂ and He were the two gases that differed most in concentrations between the targets. Both the H₂ and He contents are usually related to the residence times of the groundwaters. However, the H₂ contents of these sampled boreholes are more significantly affected by the material in the equipment and boreholes equipped with pull rods made of aluminium show 10 to 100 times higher H₂ concentrations in the groundwater. If the two borehole sections (KA205A01:5 and KA205A01:9) from a borehole equipped with acid resistant steel parts are compared the totally 8 + 2 samples vary within 0.96 to 4.08 µL L⁻¹ (both extreme values are from KA205A01:9). This may also be values that are impacted by the discharge of water prior to sampling and it may be the case that they are too low.
- The diverging gas concentrations obtained by small variations in the sampling procedure indicate that the sampling performance has a significant impact on the results (especially for H₂ and He). It cannot be excluded that some of the previous results indicating large differences in the amount and composition of dissolved gases between the Äspö groundwaters may be due to inadequate control of the sampling procedures. The results generally show that the first samples in the series diverges the most from the others which may be expected since these samples represent the groundwater present in the borehole sections.

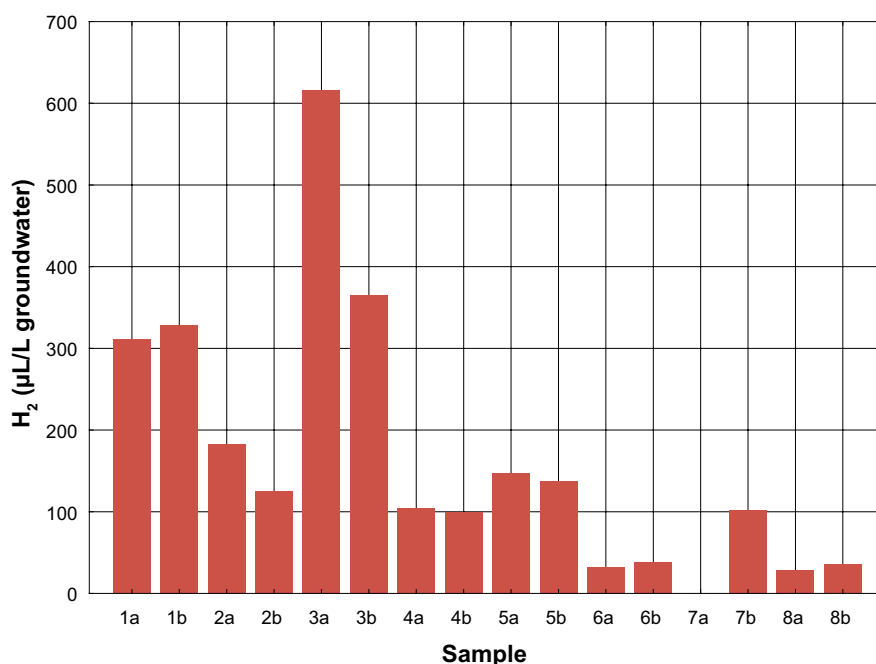


Figure 2-7. The concentrations of dissolved H₂ in sampled groundwater from borehole KA2563A:1 (the same samples as in Figure 2-6). The H₂ concentration was relatively high in the samples from this borehole section (aluminium rods) compared to some of the other sampled sections and it was highest after periods without withdrawal of water. The concentration decreased significantly when the borehole was drained but increased after interruption in the draining (samples 3a and 3b). A faster flow rate was used during the second day of sampling (starting with samples 5a and 5b) which further lowered the concentrations of H₂. The results from the two samplers representing each sampling occasion and flow-pressure combination generally reproduced as well as could be expected (Nilsson et al. 2017).

2.3.3 Conclusions

The most important achievement from this gas study is the improved understanding of the importance of the sampling conditions and how they affect the samples, especially the N₂, H₂ and He concentrations.

Collection of sample series during continuous discharge of water revealed that the amount of dissolved gas in the groundwater initially present in the borehole sections (the first samples in the series) may be larger than the amount in the groundwater directly from the bedrock formation (the latter samples in the series). Furthermore, the size of the pressure drops (back pressure) was found to be important, especially for dissolved hydrogen. Generally, the results stress the importance of a proper and well tested sampling procedure when investigating dissolved gas concentrations in groundwater.

Another factor that affects primarily the amount of dissolved hydrogen but may also affect gases like carbon dioxide and/or methane is corrosion of equipment parts in the borehole.

The aluminium rods reacted with water and produced much higher H₂ concentrations than was observed from the stainless-steel equipped boreholes.

Finally, it is a general impression that the handling of this sampling equipment and the method for dissolved gas is somewhat too complicated for routine sampling. Ongoing tests of simpler equipment in cooperation with the laboratory making gas analyses have shown promising results.

2.4 The Gas Monitoring Experiment in ONKALO – GAME

This experiment is documented in detail in Lamminmäki et al. (2021). The text below presents a short summary.

There are indications, from observations in Olkiluoto, that H₂ may be the major electron donor in the microbial sulfate reduction process rather than CH₄ and other hydrocarbon gases. The experiment was initiated to obtain more gas data and to verify or reject this indication. This since there is only a few observations of high contents of dissolved H₂ (1 mM level) in the groundwater samples from Olkiluoto (as well as from Forsmark) and the data may be somewhat uncertain. Furthermore, it has been shown that the porewater in the connected inter- and intragranular pore space of the bedrock in Olkiluoto contains dissolved gases. The porewater reservoir exchanges gases with the adjacent groundwaters through diffusion, as driven by the concentration gradient between the respective reservoirs. During the raise bore drilling of shafts and excavation of tunnels as well as the heating-up of the bedrock adjacent to the technical barrier during the operational phase of a repository, the physical parameters, pressure, and temperature, will change, leading to a change in the solubility of different gas species and thereby to their possible degassing.

2.4.1 Performance

A ~70 m long borehole (ONK-KR17) drilled from the ONKALO tunnel was used for the gas monitoring experiment, which aimed to obtain data on gas concentrations and diffusive fluxes from the bedrock at repository depth in Olkiluoto. The borehole is inclined slightly upwards and the vertical depth is -446 m a.s.l. and was selected to provide as dry conditions as possible. The borehole was closed with gas tight packers as soon as possible after the drilling and flow measurement (i.e., five days after the drilling was completed) to avoid gas loss into the tunnel via the borehole. Special care was taken to prevent gases (especially light gases like hydrogen) from being lost during gas sampling from the borehole or during sample transportation to the laboratory. Due to the chemical and biological reactivity of certain gases, the volume of gases dissolved in porewater and their origin and genesis were also evaluated. Altogether, the experiment included continuous pressure monitoring in the borehole, as well as gas, water, and drill core sampling. In addition, five drill core samples were taken for method development purposes of porewater gas analysis.

Matrix pore water analyses

Drill core samples were taken from between 50 and 66 m lengths along the borehole. The gases were extracted using the improved methods developed and applied during previous studies of the Olkiluoto bedrock (Eichinger et al. 2013, 2018). All analyses were performed at Hydroisotop GmbH. Gases in porewater were allowed to outgas into the void volume (514–597 mL) of the gas-tight cylinder over a period of 365 days at room temperature. The measured gases include gases such as oxygen, nitrogen, hydrogen, carbon dioxide and argon, as well as saturated and unsaturated hydrocarbons. The analytical protocol is summarised in Table 2-3.

Table 2-3. Analytical programme conducted for the drill core samples and extracted gases. C_xH_x refers to higher hydrocarbons.

Sample		Quantification of gases by GC-FID and WLD			Isotope analyses	Rock properties	
		CH ₄ , C _x H _x	He, Ar, O ₂ , CO ₂ , N ₂	H ₂		Water content	WL-porosity
KR 17-6B	50.28–50.49 m	KR17-6B	X	X	X	X	X
KR 17-7A	53.01–53.22 m	KR17-7A	X	X	X	n.a.	X
KR 17-7B	53.22–53.45 m	KR17-7B	X	X	X	X	X
KR 17-8A	58.58–58.74 m	KR17-8A	X	X	X	n.a.	X
KR 17-8B	58.74–58.98 m	KR17-8B	X	X	X	X	X
KR 17-9A	61.90–62.12 m	KR17-9A	X	X	X	n.a.	X
KR 17-9B	62.12–62.34 m	KR17-9B	X	X	X	X	X
KR 17-10A	65.8–66.14 m	KR17-10A	X	X	X	n.a.	X
KR 17-10B	66.14–66.38 m	KR17-10B	X	X	X	X	X

GC-FID = Gas chromatography – Flame ionisation detector.

GC-TCD = Gas chromatography – Thermal conductivity detector.

WL-porosity = Water-loss porosity.

n.a. = not analysed.

Method development by Micans

Samples were also collected for the purpose of developing and testing another method for analysing porewater gas concentrations. The parts of this study were included in the EU-project MIND (Microbiology In Nuclear waste Disposal), Grant Agreement: 661880 (Kietäväinen et al. 2017). The sample vessels and analyses were provided by Microbial Analytics Sweden AB (Micans).

Five drill core samples were collected from the borehole ONK-KR17 (Table 2-4) and placed directly in gas-tight brass tubes. The gases released from the drill cores were withdrawn at different length intervals and analysed for H₂, CH₄, C₂H₆ and Ar content by gas chromatography. The drill cores were incubated for 160 days, the emitted gas was withdrawn, and the sum of each gas amount was calculated when no more gases were released from the cores (Kietäväinen et al. 2017).

Table 2-4 Drill core samples, drill core intervals and rock types. The vertical depth is approximately 446 m.

Drill core (number)	Length along the borehole (m)	Rock type
1	36.65–37.11	DGN*
2	38.46–38.93	PGR
3	40.01–40.46	DGN
4	41.23–41.66	DGN/VGN
5	42.93–43.36	MFGN/DGN
Average		

* with 80 % leucosome.

DGN = Diatexitic Gneiss

PGR = Granitic Pegmatoid

VGN = Veined Gneiss

MFGN = Mafic Gneiss

The in situ system in the borehole

The gas sampling system was designed for a borehole up to 70 meters long with a nominal diameter of 76 mm. The borehole was drilled with an upwards inclination of 9.9 degrees. All parts of the system were designed for a pressure 4 500 kPa in the rock formation. The use of metal in the system was minimised to avoid corrosion-induced hydrogen production. The *in situ* borehole system, including the material composition of its parts, is illustrated in Figure 2-8.

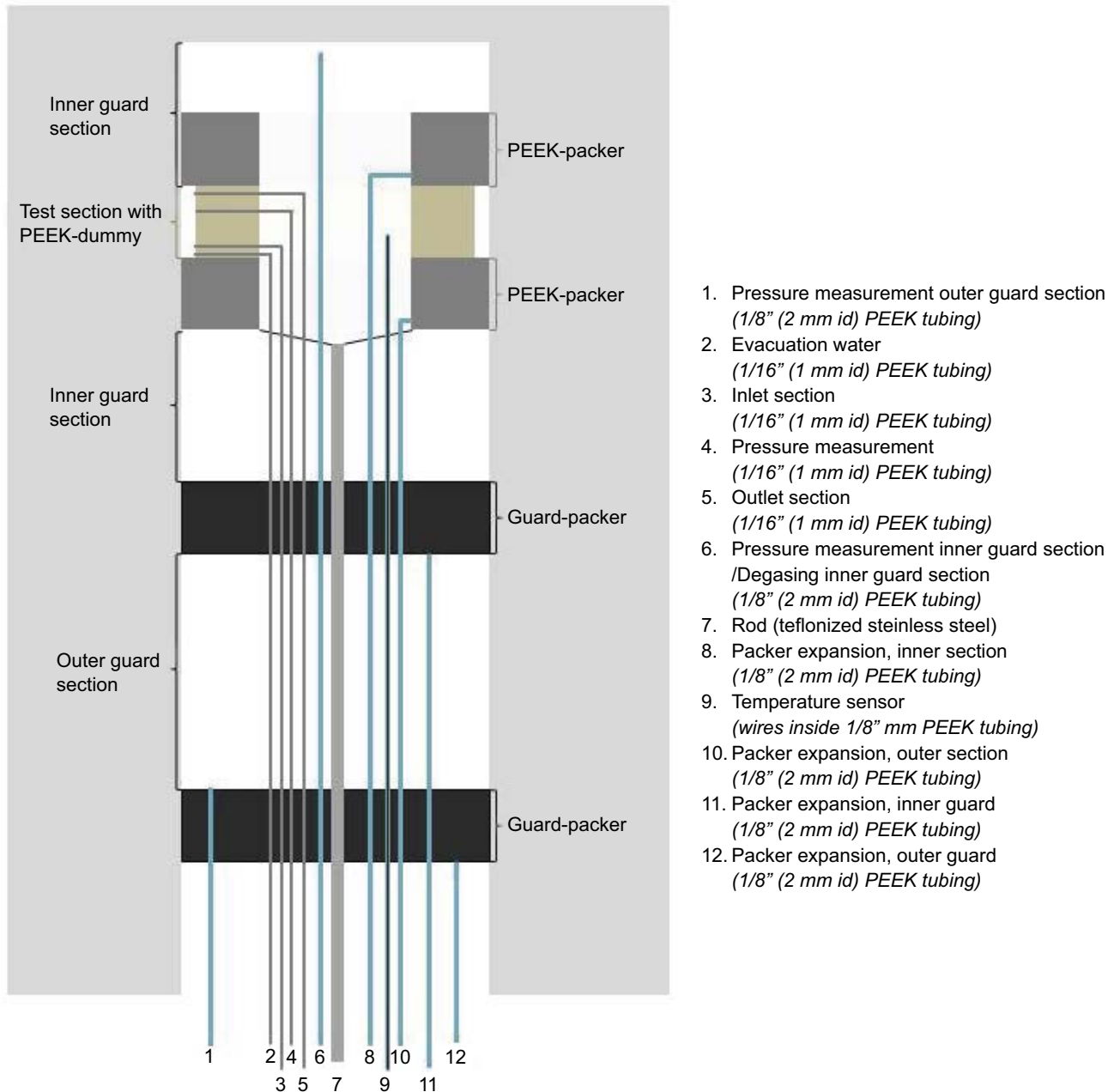


Figure 2-8. Schematic diagram of the equipment in the borehole (Lamminmäki et al. 2021). The different parts of the equipment and the material they are made of are presented in the legend.

In principle, the monitoring section was assumed to be dry, and therefore the collected sample (from the uppermost part of the monitoring section) would have been in the gas phase. However, the section slowly filled with groundwater, and no gas phase remained in the monitoring section. Consequently, diffusing gases from rock matrix dissolved into the groundwater. Therefore, at the beginning of each sampling occasion, a small amount of groundwater was drained from the bottom of the monitored section (Figure 2-9a). The draining of water (from 20 mL to several tens of mL) reduced the pressure, resulting in the degassing of dissolved gases from the groundwater into the gas phase, and enabled the direct sampling of the gas phase formed at the upper part of the monitored section (Figure 2-9b). After a half-year of monitoring, the packer system was re-positioned outward from the first monitored section at 51.5–56.5 m borehole length to another 5 m long section at 45.0–50.0 m.

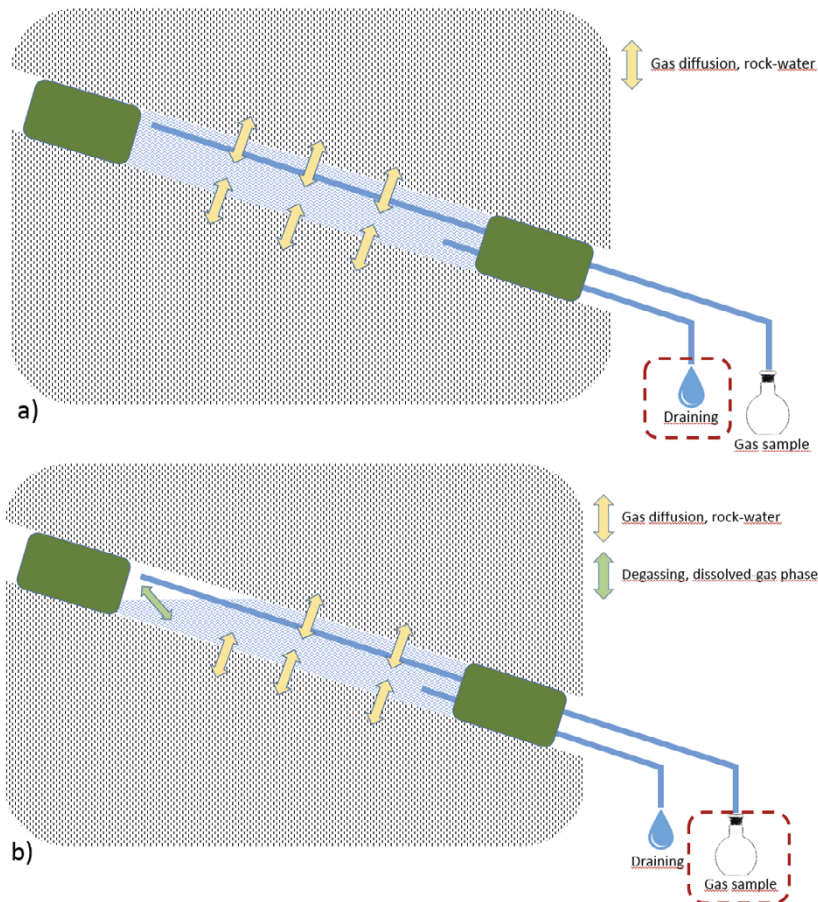


Figure 2-9. Schematic diagram of the sampling procedure. The groundwater seeped into the monitoring section, filling it in a few days after each sampling, and diffused gases from the rock matrix dissolved into the groundwater standing in the monitoring section. Therefore, a small volume was first drained from the monitoring section (a). The decrease in pressure due to the draining caused degassing from the groundwater, forming the gas phase in the upper part of the monitoring section, which was sampled (b) (Lamminmäki et al. 2021).

2.4.2 Results

Gases in matrix pore-water analysed from drill core samples

Gases dissolved in porewater were extracted using out-gassing experiments (see Lamminmäki et al. 2021, Section 3.1.2) and back-calculated to the concentration dissolved in porewater using the water content of the naturally saturated core samples. Two adjacent core pieces (replicate samples) were used in this calculation. The calculated porewater gas concentrations were normalised to 273 K (0 °C) and 1 bar (STP = Standard Temperature and Pressure) and are given in the unit NmL L⁻¹ (mL of gas in L of pore water) in the following text.

Large variations in the total gas concentrations in the porewater of the individual core samples (corrected for air contamination by oxygen), from 1 150 to 4 140 NmL L⁻¹, were observed (Table 2-5). The individual core samples taken next to each other (replicate samples) showed partly high variations in the porewater gas concentrations (Table 2-5).

Table 2-5. Gas concentrations in porewater from the drill core of borehole ONK-KR17. The values are corrected for air contamination by using the oxygen concentration; The mean concentration of the two sub-samples is denoted Mean, and std is the standard deviation.

Sample		KF17-6 Mean	std	KF17-7 Mean	std	KF17-8 Mean	std	KF17-9 Mean	std	KF17-10 Mean	std
Depth	m a.b.	50.3		53.2		58.8		62.1		66.1	
Lithology		VGN/ PGR		MGN		PGR		VGN/ PGR		VGN/ PGR	
Methane	NmL/L	155	36.5	54.1	49.2	173	40.7	162	73	18.4	55
Ethane	NmL/L	1.6	0.1	0.39	0.40	4.2	1.4	1.7	1.1	3.7	2.4
Propane	NmL/L	0.12	0.02	0.017	0.013	0.36	0.13	0.19	0.08	0.35	0.21
i-Butane	NmL/L	0.012	0.006	< 0.001	< 0.001	0.065	0.046	0.031	0.010	0.030	0.005
n-Butane	NmL/L	0.029	0.034	0.027	0.001	0.128	0.039	0.158	0.026	0.185	0.104
i-Pentane	NmL/L	0.012	0.004	0.007	0.005	0.037	0.010	0.061	0.005	0.074	0.031
n-Pentane	NmL/L	0.011	0.002	0.004	0.006	0.015	0.002	0.086	0.005	0.035	0.016
Ethene	NmL/L	0.004	0.003	0.010	0.008	0.007	0.007	0.004	0.002	0.005	0.00004
Propene	NmL/L	0.005	0.002	0.010	0.003	0.005	0.003	0.003	0.001	0.005	0.00004
1-Butene	NmL/L	0.002	0.003	0.017	0.013	0.010	0.006	0.007	0.002	0.007	0.00006
Argon	NmL/L	42.6	14.1	52.4	20.0	27.5	11.7	46.0	0.0	40.9	2.1
Nitrogen	NmL/L	1892	307	2244	876	1 113	366	1952	40	1 616	288
Carbondioxide	NmL/L	10.8	6.7	2.0	2.2	3.5	1.7	1.2	1.6	3.9	3.5
Hydrogen	NmL/L	462	31	800	451	167	52	190	61	86	8
C1/(C2 + C3) ¹		89	26	132	28	38	4	85	15	46	20

m a.b. = meters along borehole.

¹ Ratio of methane (C1) and higher hydrocarbons (C2 + C3).

The average porewater hydrogen concentrations (H_2) of the core samples varied widely from 86 NmL L^{-1} to 800 NmL L^{-1} (Table 2-5, Figure 2-10). Maximum porewater H_2 concentrations were detected in the mica gneiss samples and the veined gneiss/granitic pegmatoid samples (Table 2-5, Figure 2-10).

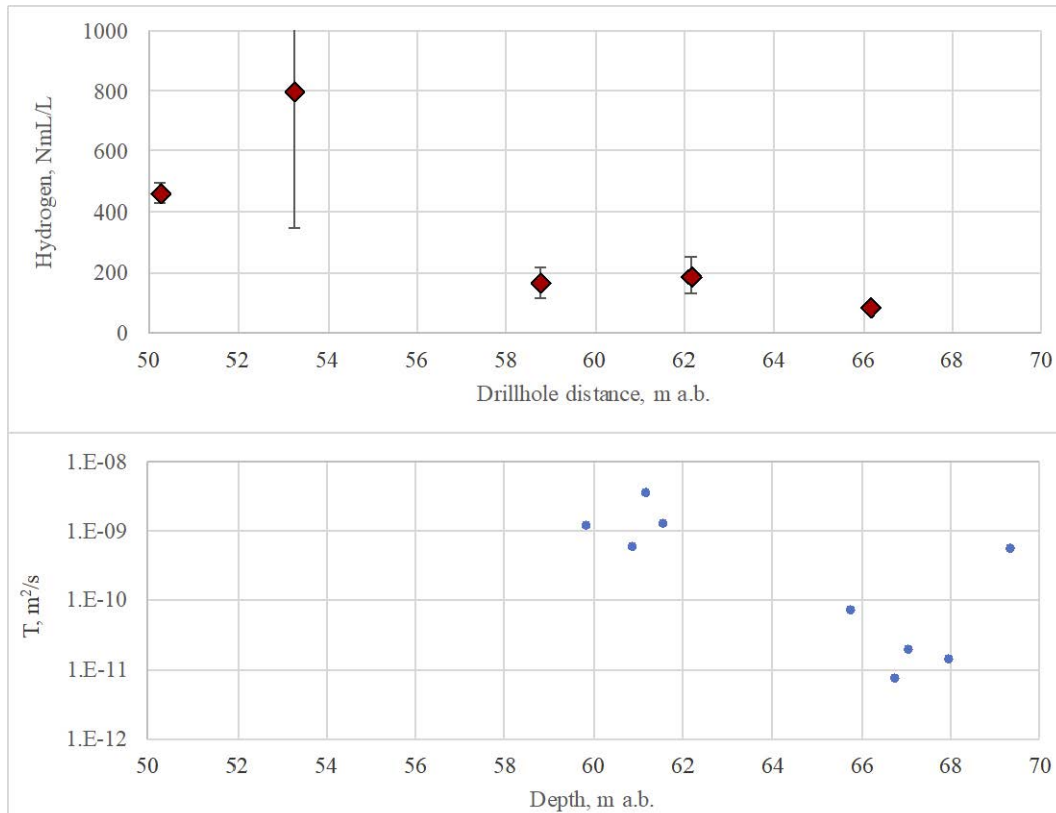


Figure 2-10. Hydrogen concentrations dissolved in the porewater of the core samples from the drillhole ONK-KR17 (top); the bottom diagram shows the water-conducting fractures and their transmissivities detected in the drillhole. (Lamminmäki et al. 2021).

Method development by Micans

The five samples collected by this alternative method showed decreasing gas concentrations in the order argon, methane, hydrogen, and ethane (Table 2-6). The gas concentrations were calculated as mL gas per L of pore water, assuming a pore-water volume (porosity of rock) of 0.5 %.

Table 2-6. Gas concentrations in the porewater of the drill cores collected for method development by Micans (borehole ONK-KR17).

Drill core (number)	Length (m)	Rock type	H ₂ (mL/L)	CH ₄ (mL/L)	Ar (mL/L)	C ₂ H ₆ (mL/L)
1	36.65–37.11	DGN*	32	37	72	0.44
2	38.46–38.93	PGR	2.9	34	87	0.42
3	40.01–40.46	DGN	31	49	99	0.87
4	41.23–41.66	DGN/VGN	12	18	77	< 0.024
5	42.93–43.36	MFGN/DGN	13	15	84	< 0.024
Average			18	31	84	0.57 ⁽¹⁾

* With 80 % leucosome.

⁽¹⁾ = Mean value including the concentrations above the detection limit.

Overall, the gas concentrations were roughly one order of magnitude lower than the ones obtained with the advanced method by Hydroisotop described above, except for the argon concentration, which was higher. However, a few uncertainties were recognised. First, it is possible that some of the gases were already released during sampling, as the drill cores were exposed to air after the drilling before closing the vessels, though this uncertainty also applies to the other method. Second, the measurement period of 106 days may be too short to achieve equilibrium. And, third, the drill core samples were collected from 36 to 44 m along the drillhole, where the close proximity to the excavated tunnel leads to decreased hydrostatic pressure and, potentially, degassing of the dissolved gases from the rock matrix. It is known from the pressure monitoring that the hydrostatic pressure in the bedrock volume around the tunnel is lowered to about 50 m (Vaittinen et al. 2019) from the tunnel wall.

Gas data from *in situ* measurements

Five to ten parallel samples were collected at each sampling occasion. The representativity of gas phase samples was estimated from the oxygen contamination levels, and below 1 % O₂ was considered acceptable. Nitrogen was the main gas in all samples, but since the sampling lines were flushed and the section pressurised by using pure nitrogen, the results do not represent natural concentration *in situ*. Therefore, the nitrogen data are not further discussed. The results of the gas sampling are presented in Figure 2-11.

To evaluate the accumulation and depletion of gas concentration, estimates of the amounts of dissolved gases in the groundwater within the monitored section were made (see calculations and equations in detail in Lamminmäki et al. 2021, Section 5.4.3). Henry's law was used to calculate the remaining dissolved gas amount in the groundwater in the section. The results are only a rough estimation, as the sample was taken immediately after the decrease of pressure and thus dissolved gases in groundwater did not have time to reach equilibrium with the gas phase. Therefore, the use of Henry's constants is not fully applicable (see details in Lamminmäki et al. 2021). When the samples were collected, the groundwater was probably still over-saturated with gas in respect of Henry's law, so the calculated values maybe somewhat lower than the true values. The gas concentration was calculated in STP conditions (T = 273.15 K and P = 1 bar) according to the Ideal Gas Law. In addition, one groundwater sample was collected for analysis of dissolved gases (red circles in Figure 2-11).

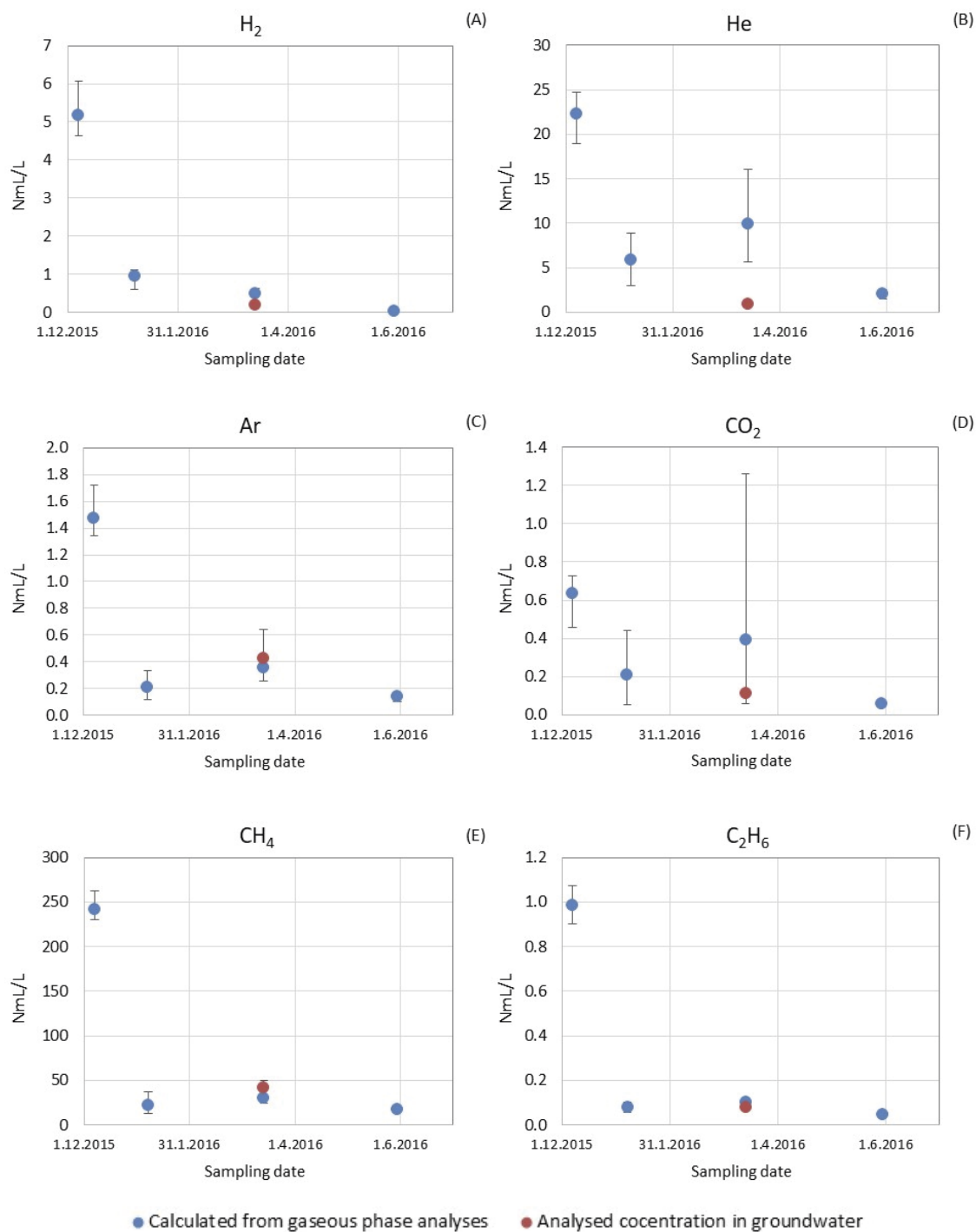


Figure 2-11. (A) Hydrogen, (B) helium, (C) argon, (D) carbon dioxide, (E) methane and (F) ethane concentrations in ONK-KR17/51.5–56.5 m calculated from the mean value of the results on each sampling occasion. Whiskers indicate the maximum and minimum result of parallel samples of each sampling occasion (only for gaseous phase analyses).

2.4.3 Conclusions

The porewater H₂ concentration was clearly higher in the mica gneiss sample (MGN; drill core sample at 53.2 m along the drillhole), whereas the methane and ethane concentrations were lower in this sample. The argon and nitrogen concentrations were also higher in MGN compared to the other drill core samples. However, Ar and N₂ results are uncertain, namely due to exceptionally high contents in all samples and observed air contamination (Lamminmäki et al. 2021, Section 5.1.3.3). The distinct gas composition signature of the MGN core sample may relate to the mineralogy of the host rock (mica gneiss is rich in biotite and chlorite), to distance to water-conductive fractures, or to a combination of these factors. However, since the Olkiluoto bedrock is estimated to contain only ~7 % MGN, the results are not considered to represent the entire bedrock volume at this depth; notable variation in gas concentrations may occur. If the porewater H₂ concentration depends on the rock type (mica content, in particular) and on the distance to conductive fractures, then the H₂ distribution is notably heterogeneous in the bedrock. Average values might be rather closer to 200 mL/L than 800 mL/L, especially as the dominant gneiss types contain significant fractions of granitic veins and dyke networks. Observations of abundant microbial sulfate reduction and/or acetogenesis are also sporadic (Tuomi et al. 2020), which likewise indicates that the H₂ distribution and availability to microbes is heterogeneous.

Finally, it is concluded that the matrix porewater is an evident storage of gases. When intact bedrock is disturbed by drilling, as was the case in this reported experiment, or by excavation of a repository, gas is released almost instantaneously. Microbes might take advantage of this gas release, resulting in enhanced microbial metabolism in the disturbed locations. After rapid release of matrix porewater gases into the groundwater, gas transport is probably limited by diffusion rates in the rock matrix, and the dissolved concentrations in groundwater reach certain gas-specific levels depending on the prevailing conditions, e.g., hydrostatic pressure and salinity as well as the availability/consumption of electron donors/acceptors for microbial metabolism.

2.5 Microbial release of Fe from iron-bearing minerals – FRED

The sub-project is presented in detail in a Posiva working report (Johansson et al. 2019). A short summary is given below.

Dissolved ferrous iron (Fe²⁺)¹ and dissolved sulfide (H₂S/HS⁻/S²⁻) concentrations in the groundwater samples from Olkiluoto show an inverse relationship (Posiva 2012). This supports the theory that iron sulfide precipitation is limiting the concurrent presence of these dissolved species. The relationship is clear for both baseline data and monitoring data regardless of sulfide concentration. This suggests an active role of solid iron sulfide phases in controlling the concentration of dissolved sulfide (Wersin et al. 2014). If no release of Fe²⁺ in solution occurs, the dissolved sulfide concentration will primarily depend on microbial production of sulfide which, in turn, depends on the availability of electron donors and acceptors. Iron-reducing bacteria produce Fe²⁺ from ferric iron (Fe(III)), and Fe²⁺ reacts readily with sulfide, forming iron sulfide that precipitates out of the solution. In addition, it is possible that sulfide reacts directly with Fe(III) in iron minerals and oxides resulting in the formation of Fe²⁺, iron sulfide, and elemental sulfur, as have been shown for clay minerals (Pedersen et al. 2017). The objective of this study was to investigate if Fe(III) in common iron silicate minerals in Olkiluoto rock types can serve as electron acceptors for iron reducing bacteria (IRB). The minerals chlorite, garnet, and biotite were used in this study, because they represent the major iron phases with a possible content of Fe(III) in Olkiluoto bedrock (Kärki and Paulamäki 2006).

¹ This section distinguishes between iron in solid phases and in the dissolved phase. Ferrous and ferric iron in solid phases, such as minerals or precipitates, are denoted Fe(II) and Fe(III), respectively. Dissolved iron in solution is denoted Fe²⁺. Fe³⁺ only occurs in solution as an ion at pH below ~3 and is, therefore, not relevant for the purpose and results of the presented work.

2.5.1 Performance

The investigation was executed in four steps. The first step comprised laboratory investigations with enrichment cultures in laboratory bottles inoculated with groundwater from boreholes in the ONKALO tunnel. The second and third steps included pressure cells where minerals were exposed to bacteria from ONKALO groundwater for attachment and growth. The final step investigated the effect of dissolved sulfide on iron release from the minerals in the laboratory.

High quality biotite, garnet and chlorite concentrates were prepared from samples collected in ONKALO to be used in the experiments. The mineralogical composition and liberation of the concentrates were studied by FE-SEM-EDS. The Fe(II)/Fe(III) ratios of the concentrates were measured by Mössbauer spectrometry and by chemical titration according to Pratt's method. The Mössbauer measurements showed that the ferrous iron component in garnet was 100 %, but by titration it was less than 20 %. Since natural garnet is rich in ferrous iron, it is most probable that the sample has been oxidised during titration. Mössbauer measurements on biotite and chlorite gave 85.5 % for the ferrous component. The value is in accordance with the literature. Titration, again, showed much lower values for the biotite concentrate, probably due to oxidation. The chlorite concentrate was not analysed by the titration method. Due to this, only the Mössbauer results were found feasible.

Step 1: The aim of the laboratory bottle batch experiment was to study the effect, on Fe^{2+} release from iron in the minerals, from arrays of electron donors and sources of microorganisms. The bottles were loaded with the minerals garnet or biotite. A cultivation medium was added with various electron donors and then they were inoculated with groundwater collected from 5 different boreholes in ONKALO representing different groundwater compositions (Figure 2-12). Several bottles were also prepared with ferrihydrite (FeOOH) which has been used previously for the cultivation of IRB from Olkiluoto samples for other purposes. The amounts of dissolved Fe^{2+} were analysed after 28 and 56 days. It was not in the initial plan to analyse sulfide, but a smell of sulfide was noticed at the first sampling occasion (after 28 days of cultivation). Therefore, sulfide was analysed in all bottles at the last sampling occasion (after 56 days).

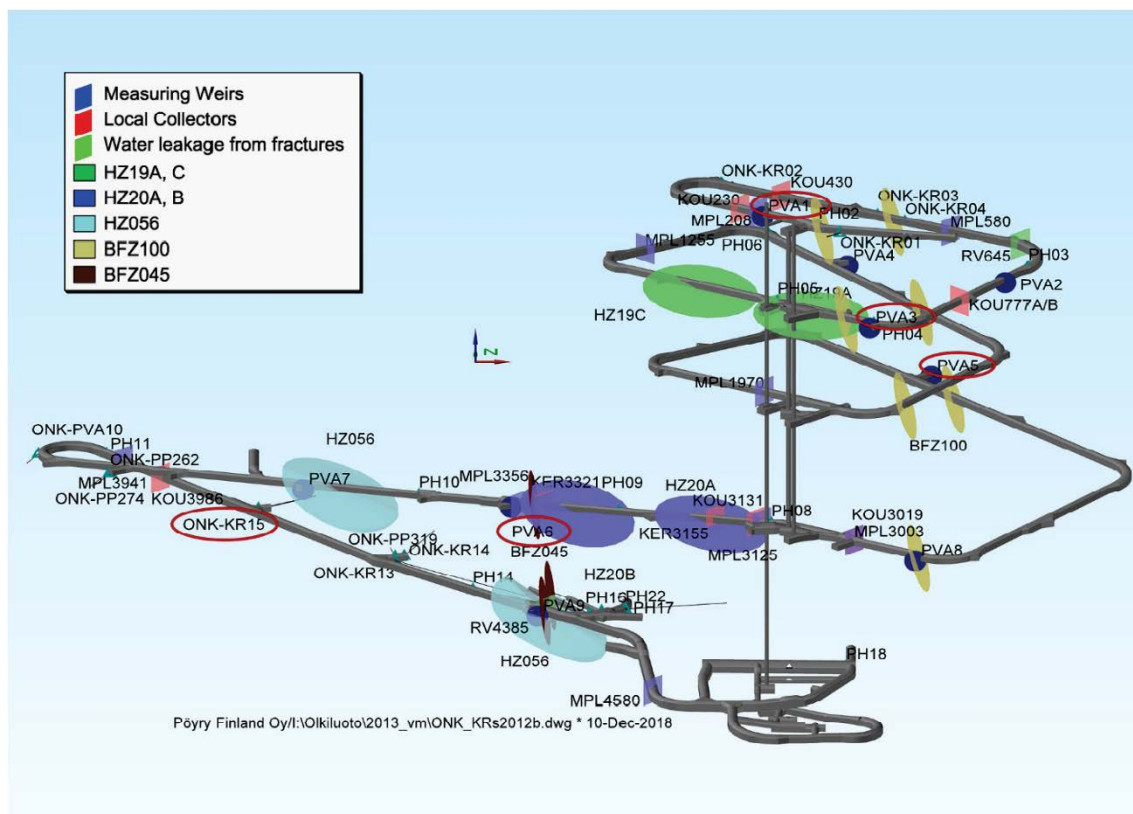


Figure 2-12. Groundwater sampling locations in ONKALO. The disks represent different hydrological water conductive fracture zones (HZ and BFZ). The sampling locations used in the experiments are marked with red ellipses (Johansson et al. 2019).

The different electron donors added to the bottles and their concentrations were as follows: Acetate, 12.2 mM (0.72 g L⁻¹); Lactate, 27.9 mM (2.52 g L⁻¹); D-glucose, 19.4 mM (3.5 g L⁻¹); Mix of 3.7 mM acetate (0.22 g L⁻¹), 5.8 mM D-glucose (1.05 g L⁻¹) and 11.2 mM lactate (1.01 g L⁻¹) to a final carbon source concentration of 20.7 mM; Acetate, 12.2 mM (0.72 g L⁻¹) + 100 kPa H₂. The medium was distributed in 50 mL portions under O₂-free conditions in the 120 mL serum bottles. A small amount of MgSO₄ (405 μM) was added to all the bottles to serve as a source of sulfur for growing bacteria. A total of 205 bottles were prepared: three parallel bottles for biotite and garnet samples, a single bottle for FeOOH, and positive and negative medium control bottles (Figure 2-13).



Figure 2-13. Bottle set-up for the laboratory bottle experiment (Johansson et al. 2019).

Step 2 and 3: The next steps included experiments to test if bacteria in ONK-PVA6 or ONK-KR15 groundwater can release Fe(III) from rock minerals and reduce it to Fe²⁺. Pressure cells were loaded with garnet, biotite, or chlorite. Groundwater (Figure 2-14) from isolated borehole sections were then circulated through the cells to allow bacteria to attach and form micro colonies on the minerals before electron donors were added in the laboratory, see below. Sulfate-rich ONK-PVA6 groundwater was used in a first test and sulfate-poor ONK-KR15 groundwater was used in a second test.

The additions of electron donors to the pressure cells with ONK-PVA6 and ONK-KR15 groundwaters were done after eight and four weeks, respectively. Different electron donors were added to the pressure cells at oxygen-free condition. Groundwater was then added to the pressure cells and the pressure increased to 25 bars. The concentrations of electron donors were as follows: Acetate, 12.2 mM (0.72 g L⁻¹); CH₄, 1.1 mM (1 mL at 25 bars); H₂, 0.5 mM (0.5 mL at 25 bars); N₂, 0.5 mM (0.5 mL at 25 bars). There were two parallel pressure cells for each mineral and electron donor. All pressure cells were incubated at 20 °C. The ONK-PVA6 pressure cells were sampled after 53 to 61 days of incubation in the laboratory and the ONK-KR15 were sampled after 42 to 45 days.

Step 4: The final step was to investigate the effect of dissolved sulfide on iron release in the laboratory without microbes. This additional experiment was carried out by exposing the same minerals to sulfide under bacteria-free laboratory conditions and by studying the release of Fe²⁺, the loss of free sulfide and the formation of elemental sulfur.

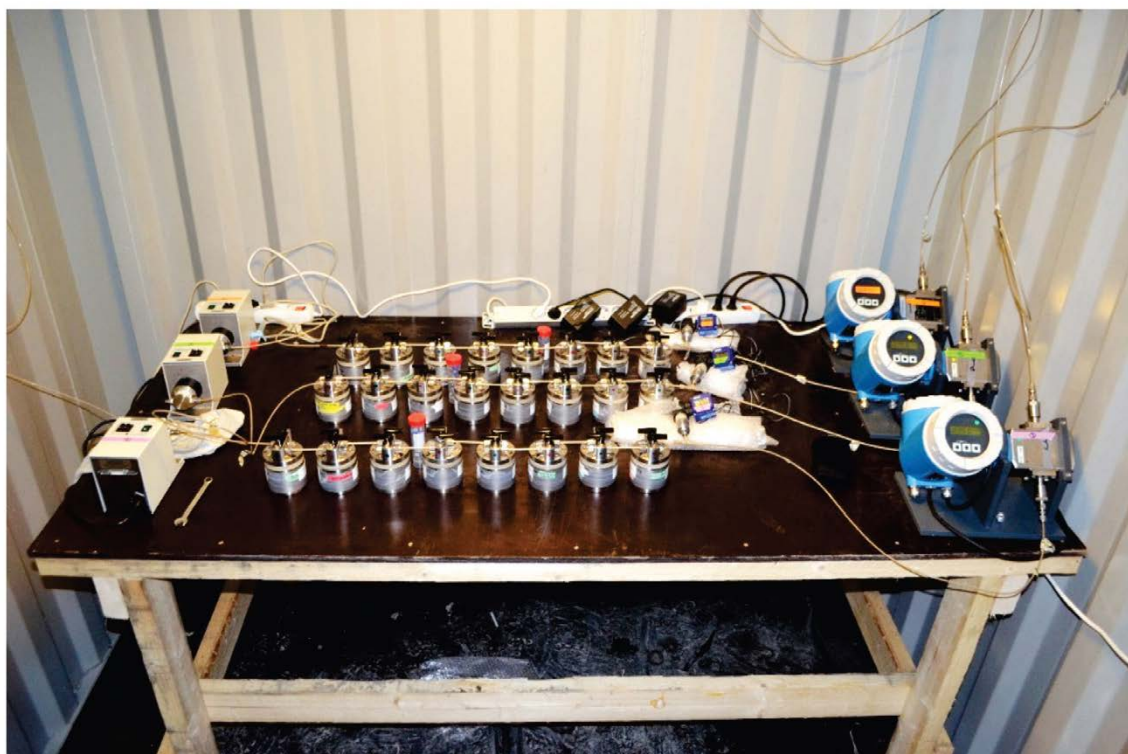


Figure 2-14. Pressure cells set-up with different minerals and groundwater circulation (Johansson et al. 2019).

2.5.2 Results

The compositions of the minerals are shown in Table 2-7. The grain sizes of the concentrates used in the mineral characterization were: 0.5–1.0 mm for biotite, 0.25–2.0 mm for garnet and 0.063–2.0 mm for chlorite.

Table 2-7. The mineral contents of the biotite (Bt1), chlorite (Chl1) and garnet (Alm1 and Alm2) concentrates.

Biotite (Bt1)		Chlorite (Chl1)		Garnet (Alm1)		Garnet (Alm2)	
Phase	Mass %	Phase	Mass %	Phase	Mass %	Phase	Mass %
Biotite	82.3	Chlorite	48.5	Almandine	89.7	Almandine	95.5
Albite	4.9	Muscovite	10.3	Pyrrhotite	4.3	Pyrrhotite	0.2
Quartz	3.2	Cassiterite	20.6	Biotite	1.5	Biotite	0.3
Muscovite	3.2	Quartz	6.2	Quartz	0.8	Quartz	0.2
Kaolinite	1.6	Biotite	3.6	Pyrite	1.2	Muscovite	0.1
Chlorite	0.6	Albite	1	Albite	0.3	Cassiterite	0.1
Al-silicate	0.6	K-feldspar	0.7	Muscovite	0.2	Unclassified	3.4
K-feldspar	0.4	Pyrite	1.3	Xenotime	0.1		
Pyrrhotite	0.2	Ti-Fe-min alt	0.6	Fe-oxide	0.2		
Unclassified	2.5	Calcite	0.2	Unclassified	1.1		
		Kaolinite	0.1				
		Sphalerite	0.1				
		Unclassified	6.4				

The following mineral concentrate batches were used for further experimental work:

- Bt1 and Alm1 in laboratory bottle experiment.
- Bt2, Alm2, and Chl1 in pressure cell experiment with ONK-PVA6 groundwater.
- Bt2, Alm2 and Chl2 in pressure cell experiment with ONK-KR15 groundwater.
- Bt1, Alm1, Bt2, Alm2, Chl1, and Chl2 in mineral control experiment using filtrated ONK-PVA6 groundwater.
- Bt2, Alm2 and Chl2 in laboratory mineral experiment.

Step 1: Five different electron donors were tested in the laboratory bottle experiments. Fe²⁺ release and sulfide production occurred in all the tests with different electron donors. The Fe²⁺ concentrations were the highest in the bottles with glucose, lactate, acetate + H₂ and in bottle with the mix of acetate, lactate, and glucose. Generally, the released Fe²⁺ amounts were larger after 56 days compared to after 28 days. When the different minerals were compared, there was a Fe²⁺ release for all minerals and sulfide was produced in the biotite and garnet bottles, but not in the FeOOH bottles. The largest amounts of Fe²⁺ per gram of mineral were found in the garnet bottles. There were also Fe²⁺ release in the biotite bottles; but in the acetate and acetate + H₂ bottles, Fe²⁺ was found only in slightly higher amounts than in the negative medium control bottles. The negative medium control bottles generally showed some Fe²⁺, but in most cases, much less than what was found in inoculated bottles. Probably, some inorganic leaching of Fe²⁺ occurred in the negative controls as indicated by the negative control experiment. Alternatively, there may have been bacteria present on the minerals that did exert some ferric iron reduction. Nevertheless, the Fe²⁺ release was significantly larger in bottles inoculated with ONKALO groundwater.

Sulfide production occurred in some of the biotite and garnet bottles but was not detected in the FeOOH bottles and the largest amount of sulfide was found in the garnet bottles. It is likely that sulfide was produced in the FeOOH bottles as well, but since those samples were not shaken before analysis, any sulfide produced may have been present in the precipitate, probably as FeS, and the precipitate was not analysed.

Step 2: The pressure cell experiments with ONK-PVA6 water (SO₄-rich water) show Fe²⁺ release and sulfide production/release from all minerals with acetate. The largest amounts of dissolved Fe²⁺ and sulfide were found in the pressure cells with garnets (Figure 2-15 and Figure 2-16). Dissolved ferrous iron was found in pressure cells with additions of acetate, CH₄, or N₂. The largest amount of dissolved ferrous iron was observed in pressure cells with added acetate. The production of dissolved sulfide occurred only in pressure cells with additions of H₂ and no dissolved ferrous iron was observed. The elevated sulfide concentration probably precipitated all the dissolved iron in these cells.

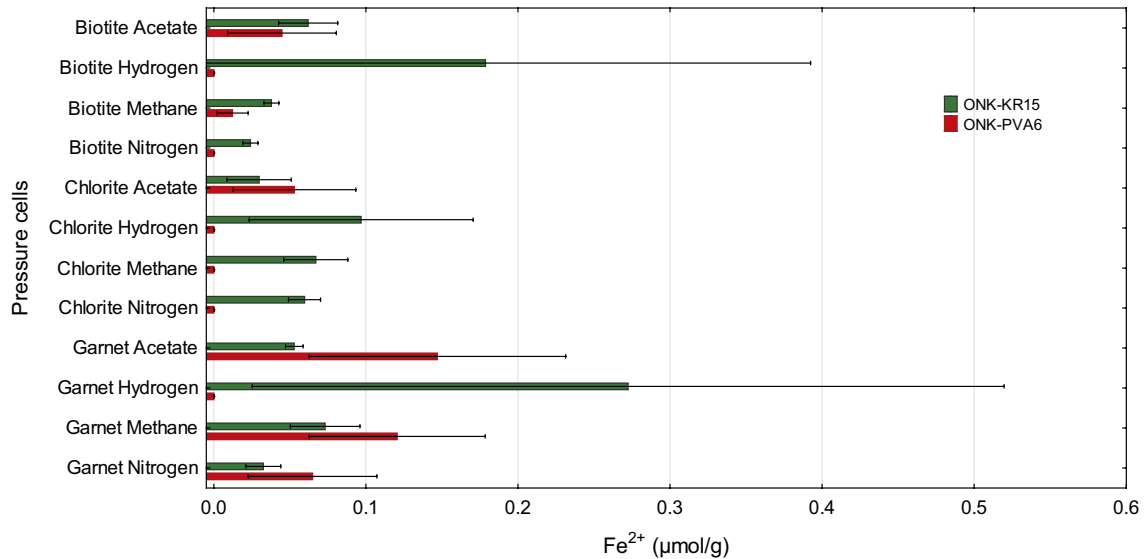


Figure 2-15. Dissolved Fe²⁺ per g mineral (average values from two samples) for pressure cells with ONK-PVA6 and ONK-KR15 groundwater. The standard deviation is indicated by the bars (Johansson et al. 2019).

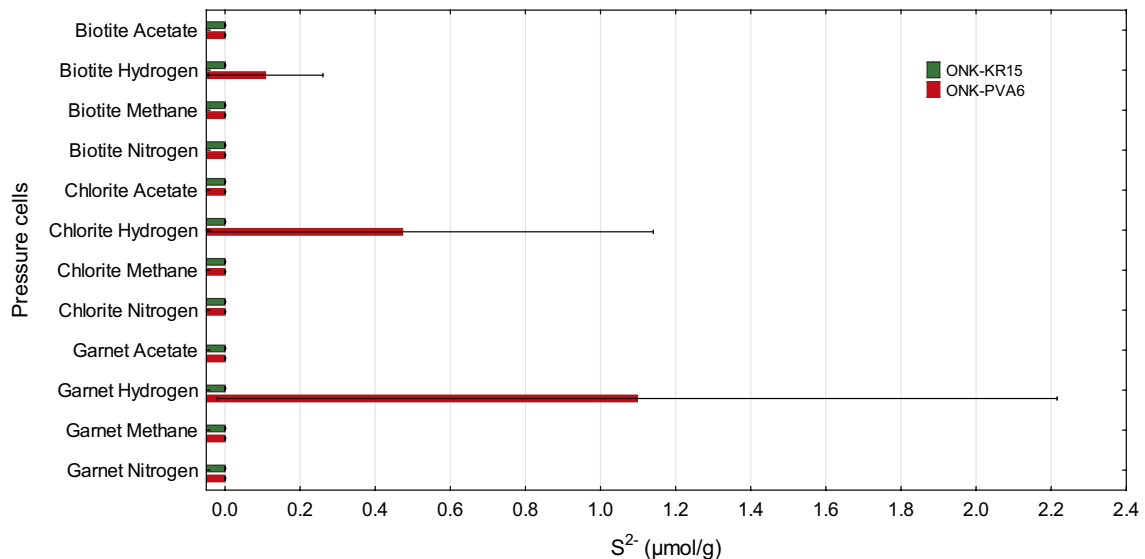


Figure 2-16. Dissolved sulfide per g mineral (average values from two samples) for pressure cells with ONK-PVA6 and ONK-KR15 groundwater. The standard deviation is indicated by the bars (Johansson et al. 2019).

Step 3: In the pressure cell experiments with ONK-KR15 water, the ATP analysis indicated a significant microbial presence in all pressure cells. In most cases the amounts were like those observed with ONK-PVA6 groundwater. Since the sulfate concentration was generally below the detection limit ($< 20 \mu\text{M}$), sulfide production could not occur, and sulfide was consequently not observed (Figure 2-16). All tested cells showed some Fe^{2+} in solution. High concentrations of acetate and methane indicate that there were no active IRB in the pressure cells with acetate or methane added. Consequently, the observed Fe^{2+} was mainly due to a background inorganic release from the minerals. One uncertainty is that ONK-KR15 groundwater contains about $140\text{--}150 \text{ mL L}^{-1}$ methane (observed in 2012). This was not considered in the analytical programme for pressure cells. Therefore, some IRB may have already been activated during the cultivation in ONKALO and used the residual methane in the groundwater from the pressure cells after the transfer of the cells to the laboratory. This may have resulted in some dissolved Fe^{2+} formed via bacterial metabolism. However, the pressure cells with H_2 showed a larger Fe^{2+} release than any other pressure cell (Figure 2-16). The standard deviation was large, but the data correlated with the amount of remaining H_2 for biotite and garnet. The pressure cell with a large release of Fe^{2+} were void of H_2 while there was hydrogen remaining in the gas phase in the replicate test cell with less released Fe^{2+} . This suggests that H_2 was oxidised by IRB with mineral Fe(III) .

Step 4: In the final step it was investigated if sulfide *per se* releases iron from minerals. This was studied by adding Na_2S to solutions with garnet, biotite, and garnet, respectively. The tested minerals released less amounts of volatile H_2S than the added amounts. The calculated difference between added sulfide (including the H_2S in biotite) and measured sulfide in the solution is assigned to immobilised H_2S and is shown in Figure 2-17. The amount of immobilised H_2S corresponds to 5–40 % of the added Na_2S . Also, elemental sulfur was detected in the mineral suspensions with Na_2S additions. However, biotite contained detectable S^0 without the addition of sulfide. The amounts of S^0 correlated with the increase of the Na_2S concentration for all minerals, though less sulfur was detected compared to the immobilised H_2S .

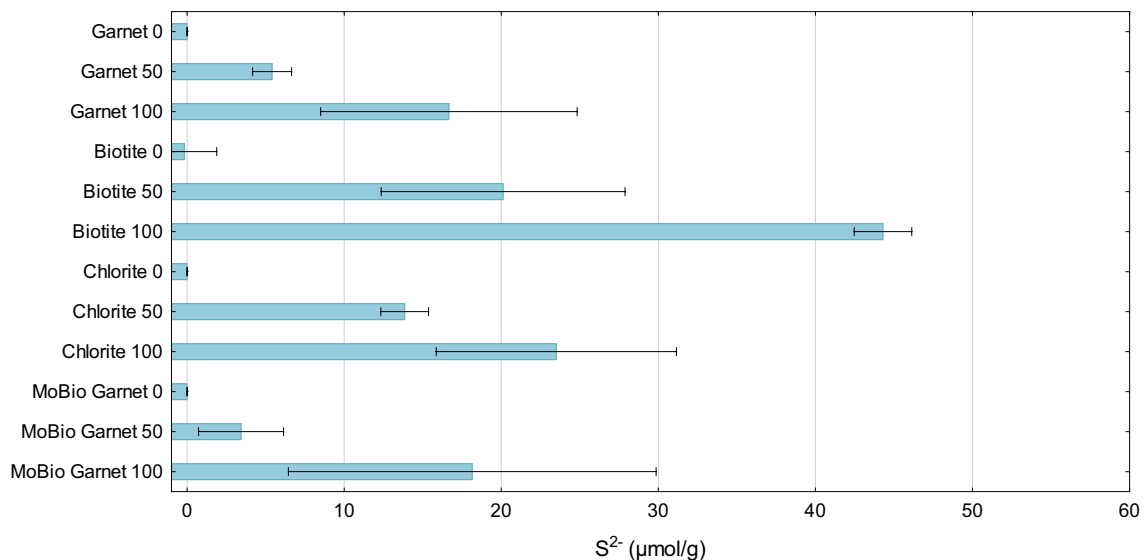
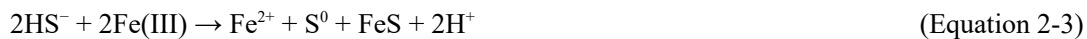
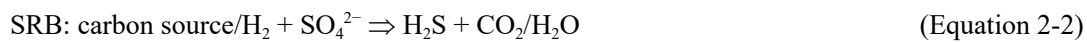
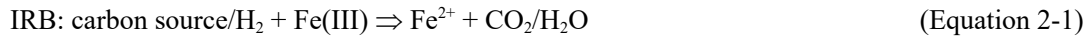


Figure 2-17. Immobilised, non-volatile, acid-extractable H_2S for four different minerals and two different amounts of added Na_2S . The numbers after the respective mineral show the amount of added sulfide ($\mu\text{mol g}^{-1}$). The bars indicate the standard deviation of three parallel samples (Johansson et al. 2019).

2.5.3 Conclusions

The objective of this study was to investigate if potential Fe(III) in iron silicates that occur in Olkiluoto rock types can serve as electron acceptors for IRB (Equation 2-1). The experiments were planned to enable investigation and evaluation of the effect of different minerals, electron donors and sources of microorganisms on the release of Fe²⁺. During the course of these experiments, it became obvious that dissolved sulfide, *per se*, can generate a release of Fe²⁺ without the involvement of bacteria, except for the microbial production of sulfide by SRB (Equation 2-2 and Equation 2-3). Therefore, experiments were also performed to investigate the effect of dissolved sulfide on the release of Fe²⁺. Garnet, chlorite, and biotite, and FeOOH were studied. Garnet contains only Fe(II), while the tested biotite and chlorite contained 319 and 343 µmol Fe(III) per gram mineral, and FeOOH should contain 11 mmol Fe(III) per gram oxide. However, at least the garnet concentrate used in this study contained Fe(III) oxide.



The minerals biotite and chlorite showed a release of Fe²⁺ amounting to maximum 20 % of the available Fe(III) but in most cases the release was only a few percent. The case with 20 % release was obtained for garnets in the laboratory experiments and may be due to oxidation. Although it is relevant to assume that only Fe(III) on the surface of the minerals was available for iron reduction, it cannot be excluded that the bacteria may have had means to extract Fe(III) from depth in the mineral grains (Brookshaw et al. 2014). Consequently, there should have been an excess of Fe(III) available for iron reduction in the experiments.

When the Fe²⁺ release from the negative controls are compared with the Fe²⁺ release from the pressure cells with groundwater (i.e. with bacteria), there is generally no significant difference. The exceptions are pressure cells with H₂ addition and some of the pressure cells with garnet. However, it may be assumed that releasable Fe²⁺ without the action of bacteria was removed during the incubation in ONKALO. If so, all observed Fe²⁺ release in the pressure cells at the laboratory, were due to microbial activity. In other words, at least the H₂ pressure cells showed bacterial iron reduction. It is also possible that some bacterial iron reduction together with methane oxidation occurred in the case of ONK-KR15 groundwater. In addition to the production of dissolved Fe²⁺ which can react with sulfide and form FeS, sulfide in Olkiluoto groundwater can also be immobilised by direct reaction with Fe(III)-bearing minerals (Equation 2-3).

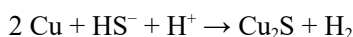
3 WP2 – Sulfide processes in the buffer and backfill

Detailed information concerning the work described in Sections 3.2 and 3.3 are given in Svensson et al. (2017), Bengtsson et al. (2015, 2017a, b), Haynes et al. (2019) and Maanoja et al. (2020a, b).

3.1 Background

When the repository is closed there will be remaining air in the void and unsaturated parts of the buffer and backfill. There will also be dissolved air in the saturated part of the bentonite barriers. Oxygen in air, both as gaseous and dissolved specie will react with minerals, metals (including the canister) and organic material, mainly through microbial reaction, in the repository. The consumption of oxygen is expected to be relatively fast.

After all the oxygen has been consumed, sulfide will be the remaining corroding agent present in the repository. The possible sources of sulfide will be 1) dissolution of sulfide minerals in the buffer and backfill, 2) sulfide formed by microbial sulfate reduction in the buffer and backfill and 3) dissolved sulfide in the groundwater (either from dissolution of sulfide minerals in the rock or as a result of microbial reduction of sulfates in the groundwater-rock system). The corrosion of copper by sulfide will proceed with formation of copper sulfide (for simplicity written as Cu_2S even though other non-stoichiometric forms are possible) and molecular hydrogen.



Corrosion due to sulfide from the pyrite initially present in the buffer can be bounded by a simple mass balance estimate. The assessment in SR-Site (SKB 2011) used a mass balance and assumed that all initially present pyrite in the buffer sections surrounding the canister side attacks the canister side as sulfide. This resulted in a corrosion of 0.1 mm and 0.9 mm copper for MX-80 and Ibeco-RWC bentonite, respectively. The corresponding values on the top of the canister, based on the assumption that most of the oxygen comes from the tunnel, i.e. on the canister lid were 0.4 and 2.9 mm, respectively. A less pessimistic estimate of corrosion should include the dissolution of pyrite and the diffusion transport of the sulfide from the pyrite. The time required for complete depletion of this sulfide from the pyrite can be estimated with a simple transport expression involving the diffusivity and the concentration limit of sulfide in the buffer. Both the diffusivity and the sulfide solubility are uncertain. Assuming very pessimistically a diffusivity of $1.2 \times 10^{-10} \text{ m}^2 \text{ s}^{-1}$ (corresponding to neutral H_2S , diffusing as HTO, tritium labelled water) and a solubility of $3.84 \times 10^{-9} \text{ mol dm}^{-3}$ (assuming a very low iron content in the bentonite, $1 \times 10^{-10} \text{ moles dm}^{-3}$) the bentonite at the side of the canister would be depleted of pyrite. The pyrite in the bentonite on top of the canister would not be depleted in one million years as the depletion front reaches at a maximum 40 cm, and thus not allowing time for any pyrite in the backfill to reach the canister.

If sulfide minerals from the tunnel backfill are also included, the mass balance approach will not be useful since the mass is so large. The dissolution-diffusion still gives the same corrosion depth in a million years since the depletion front remains in the buffer. Since the diffusivity can be easily bounded, the key factor in this assessment is the maximum concentration of dissolved sulfide in the porewater of the buffer. Assuming pyrite as the solubility limiting phase will give a low value even with a pessimistic assumption of porewater composition. Pyrite is a reasonable selection since it is the most stable phase and the one that can be found in commercial bentonites. Despite this, another solubility limiting phase cannot be entirely ruled out. The objective of the study presented here was to directly measure sulfide concentrations in water in “equilibrium” with bentonite to check whether the concentration used in the corrosion assessment is reasonable.

Microbial activity in the buffer can produce chemical species that may accelerate the corrosion of copper. The most important types of microbes are sulfate-reducing bacteria, which produce sulfide. The prerequisites for significant viability of microbes are sufficient availability of free water, nutrients, and space for living cells to grow. Mechanical forces, low water activity and pore size will therefore affect the microbial activity in the buffer. The presence of sulfate reducing bacteria in commercial

bentonite and their potential to be active after exposure to elevated temperature and salinity has been shown in Masurat et al. (2010) and Svensson et al. (2011). A safety function for the buffer was defined in the Safety assessment SR-Site (SKB 2011) which involves the limitation of microbial activity. The safety function indicator was defined as high swelling pressure due to the uncertainties associated with the mechanism. In Posiva SKB (2017), the question was discussed further, and it was established that the conclusions regarding swelling pressure/dry density and potential other factors that limit microbial activity are somewhat incomplete. The lower limit of bentonite density and thereby the swelling pressure for which the microbial sulfate reduction can be considered to be insignificant have been studied in this project. In addition, the potential of organic matter dissolving from bentonite in sustaining activity of SRB was studied in the experiments of Posiva's FaTSu project.

3.2 Solubility of sulfide minerals originally present in the buffer

3.2.1 Description

Experiments were performed with Ibeco backfill (Milos, Greece) and MX-80 (Wyoming, USA) bentonite and in selected cases sulfide solutions (Svensson et al. 2017). The main target was to determine the solubility of the sulfides in the bentonites and their equilibrium concentrations.

Methylene Blue (MB) method for sulfide

After stabilisation, the sulfide content was analysed according to the SKB MD 452.011 SULFID method (based on SIS 028115). To the sample 2 ml amine sulfuric acid was added, followed by 0.5 ml iron(III)chloride solution and the solution was mixed thoroughly, and placed dark for 1 h. In the next step 3 ml diammonium-hydrogen-phosphate solution was added and the solution was mixed and placed dark for 15 minutes. The evaluation was done by measuring the absorbance at 665 nm with UV/Vis spectrometer (this corresponds to absorbance by methylene blue which is proportional to the sulfide concentration). The method was calibrated by analysing the stock solution with an independent silver electrode.

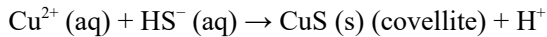
Several experiments were performed, and the experimental setup was refined with time (Table 3-1). Each type of setup is denominated by MB-*n*, where *n* is I to VI (I the first and VI the last type of experimental setup used).

Table 3-1. Overview of the MB experimental types and evolution with time. Ibeco BF is the Milos bentonite (Greece), and MX-80 is the Wyoming bentonite (USA) (Svensson et al. 2017).

Experiment type	Time	Materials	Comments
MB-I	2013	Ibeco BF	
MB-II	2014	Ibeco BF, Na ₂ S	
MB-III	2015	Ibeco BF, MX-80, Na ₂ S	Air removed. Bentonite not separated from the liquid (artefact).
MB-IV	2015	Ibeco BF, Na ₂ S	Air removed. No complete separation of montmorillonite from solution (artefact).
MB-V	2016	Ibeco BF, Ca-Ibeco BF, Na ₂ S, CaCl ₂	Complete montmorillonite separation. Air removed.
MB-VI	2016	Ca-MX-80, CaCl ₂ , Na ₂ S	Complete separation. Anaerobic box (< 1 ppm O ₂) used. Still sulfide loss.

Copper Sulfate (CS) method for sulfide

The following reaction was used as an independent alternative method for sulfide detection:



This reaction can be used to determine sulfide content in water (e.g. Cord-Ruwisch 1985). The $\text{Cu}^{2+}(\text{aq})$ ion has a blue colour, while the covellite is brown or black, and hence the reaction with HS^{-} decreases the blue colour of the solution and forms initially a brown dark colloid and later after aggregation a more solid black precipitate (Figure 3-1). Evaluation can be done visually with documentation by photography, or by spectrophotometric measurement of the absorption of the $\text{Cu}^{2+}(\text{aq})$ (the blue colour).

The experiments were performed in a glove box similar to MB-V, including the addition of CaCl_2 to reach a final concentration of 0.1 M CaCl_2 . To minimize effects from oxidation, higher concentrations of sulfide were used in the CS-I and CS-II compared to the MB-experiments. A summary of the experiments can be seen in Table 3-2.

Table 3-2. Overview of the CS experimental types with details (Svensson et al. 2017).

Type	Time	Materials
CS-I	2016	Ca-bentonite, Kaolinite, Blank Blank 30 ml water + 3.5 ml 1 M CaCl_2 + 1 ml 700 mg/L sulfide solution Ca-bentonit 1 g diluted with water until 30 ml. 3.5 ml 1 M CaCl_2 + 1 ml 700 mg/L sulfide solution Kaolin 1 g diluted with water until 30 ml. 3.5 ml 1 M CaCl_2 + 1 ml 700 mg/L sulfide solution
CS-II	2016	MX-80 bentonite different masses Blank-0, Blank-0 30 ml water + 3.5 ml 1 M CaCl_2 + 1 ml 1000 mg/L sulfide solution (c = 29 mg/L) Bentonite-10, Bentonite-50, Bentonite-100, Bentonite-500 (10 to 500 mg of MX-80 bentonite was added)

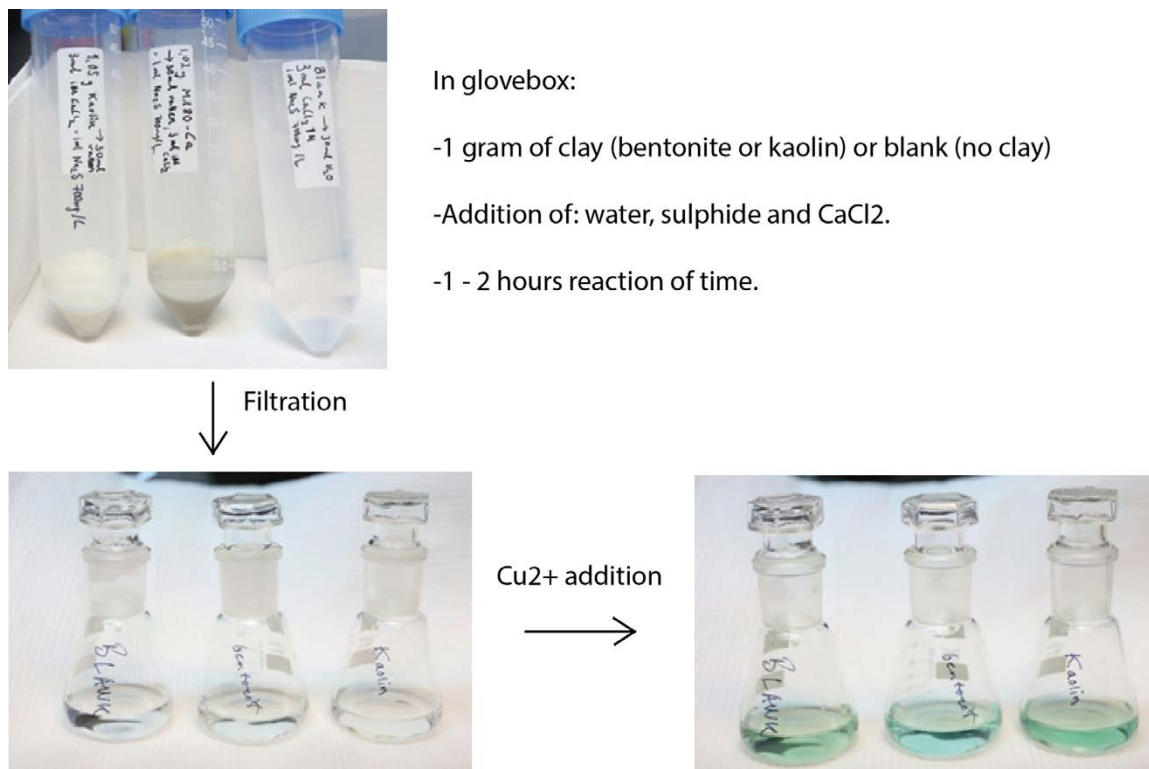


Figure 3-1. CS-I: Experiment with clay, water, sulfide and CaCl_2 , illustrating the steps of filtration and Cu^{2+} addition. Overview of how the CS-experiments were performed (Svensson et al. 2017).

3.2.2 Results

Methylene Blue (MB) method for sulfide

The first four series of Methylene Blue experiments had some artefacts in them due to the interaction between methylene blue and montmorillonite.

In the MB-V experiment there was no problem with bentonite in the solution during the addition of the reagents, however, there were still some problems with sulfide escape/oxidation as the total values were much lower than expected.

Although some oxidation occurred, the MB-V experiment was free from artefacts and hence it provided some interesting data. In the experiment with no added sulfide, different amounts of bentonite were added to the water. Both raw bentonite and Ca-exchanged bentonite was used, and no sulfide was detected in any of the cases (Figure 3-2). However, this behaviour could still have been due to oxidation or H₂S escape.

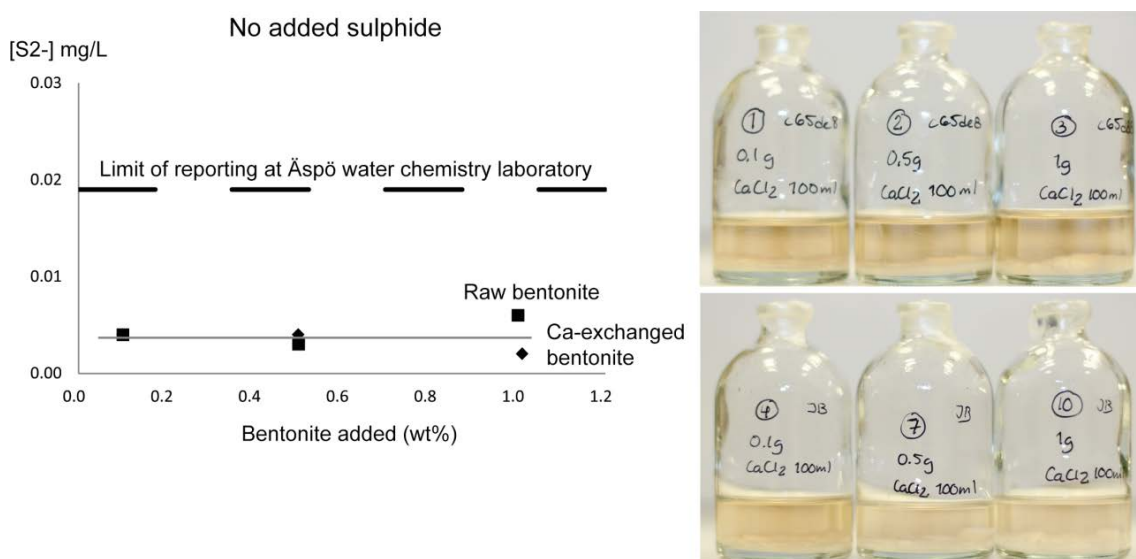


Figure 3-2. MB-V: The measured sulfide content in the solution after the addition of different amounts of Ibeco BF bentonite. All the points are below the limit of quantification (LOQ) 0.019 mg L⁻¹. The limit of detection is 0.006 mg L⁻¹. The uncertainty in the measurements is approximately ± 32 %. The lines are given as guides for the eyes (Svensson et al. 2017).

More interesting are the two series of samples that were spiked with a lower (0.9 mg L^{-1} ; Figure 3-3) and higher (1.6 mg L^{-1} ; Figure 3-4) level of sulfide. In both series a clear trend could be seen showing that the added bentonite lowered the amount of sulfide in the solution by absorption or some kind of chemical reaction. One possibility is that the bentonite porosity contained some air (oxygen) and the more bentonite that was added; the more oxygen was introduced into the system and this oxygen could have reacted with the added H_2S .

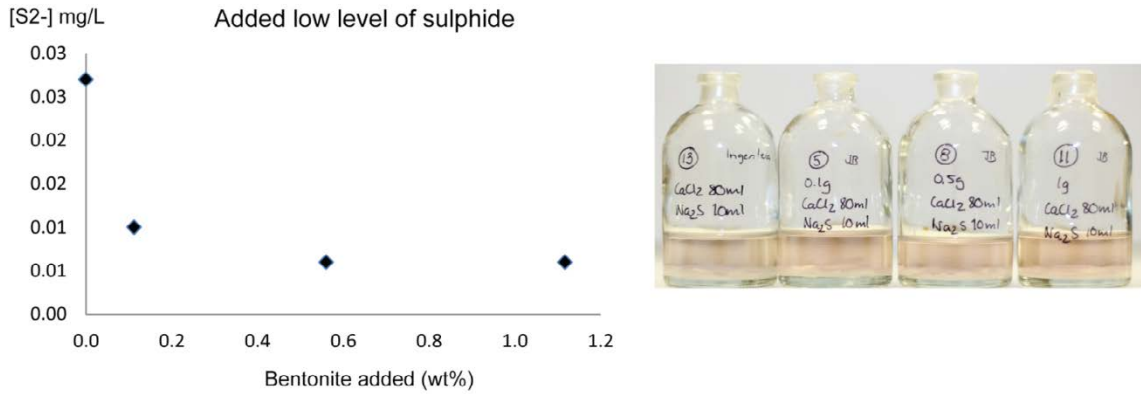


Figure 3-3. MB-V: Constant sulfide addition ($c = 0.9 \text{ mg L}^{-1}$) with different amounts of Ibeco BF bentonite (wt%). The limit of quantification (LOQ) is 0.019 mg L^{-1} and the limit of detection is 0.006 mg L^{-1} (Svensson et al. 2017).

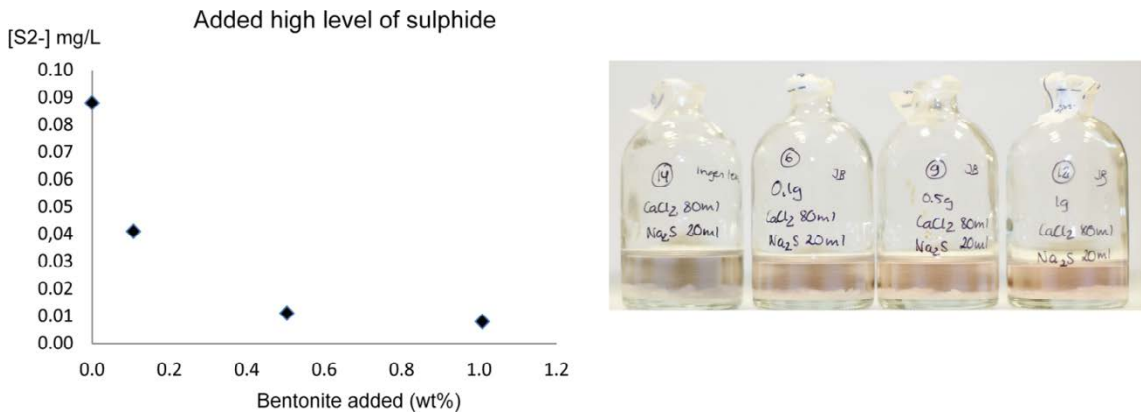


Figure 3-4. MB-V: Constant sulfide addition ($c = 1.6 \text{ mg L}^{-1}$) with different amounts of Ibeco BF bentonite (wt%). The limit of quantification (LOQ) is 0.019 mg L^{-1} and the limit of detection is 0.006 mg L^{-1} (Svensson et al. 2017).

To fully exclude the effect from oxidation by air, the MB-VI experiment was done inside an anaerobic box (< 0.1 ppm O_2). In MB-VI all solutions and reagents were prepared inside the box, using oxygen free water that had been standing to equilibrate in the box for about 2 months. As previous data indicated that bentonite reduced the sulfide concentrations, more sulfide was added to the samples with bentonite in order to ensure detectable sulfide concentrations at the end of the experiment. Hence, the proportions of sulfide and bentonite that could give measurable and comparable data were estimated. It was clear from the results that the addition of bentonite lowered the sulfide content (Figure 3-5), however, for some reason a large part of the sulfide still seemed to be lost during the steps (artefact). In this case, no oxygen is present in the bentonite, and the unintentional oxidation should be equal for all samples and also the H_2S escape (which should be even lower in samples with bentonite due to the higher pH). It is clear that the bentonite lowers the sulfide content, but to what extent is still unknown due to the impact from oxidation/ H_2S escape and as the investigated interval of samples with and without bentonite was fairly large.

Copper Sulfate (CS) method for sulfide

In the CS-I experiment a fixed amount of sulfide was added to test tubes with 1) no clay, 2) bentonite and 3) kaolin clay (field sample collected at Rokle mine, Czech Republic). In the case of no bentonite and/or kaolin, sulfide could be detected while with bentonite (MX-80) no visible signs of sulfide could be seen. Hence, the CS-I experiment confirms the sulfide loss behaviour observed in the MB-experiments. In the next experiment, CS-II, only bentonite was used. A series of bentonite aliquots (0, 0, 10, 50, 100 and 500 mg of bentonite) was added to samples with a fixed sulfide concentration (initial value = 29 mg L^{-1}) (Figure 3-6).

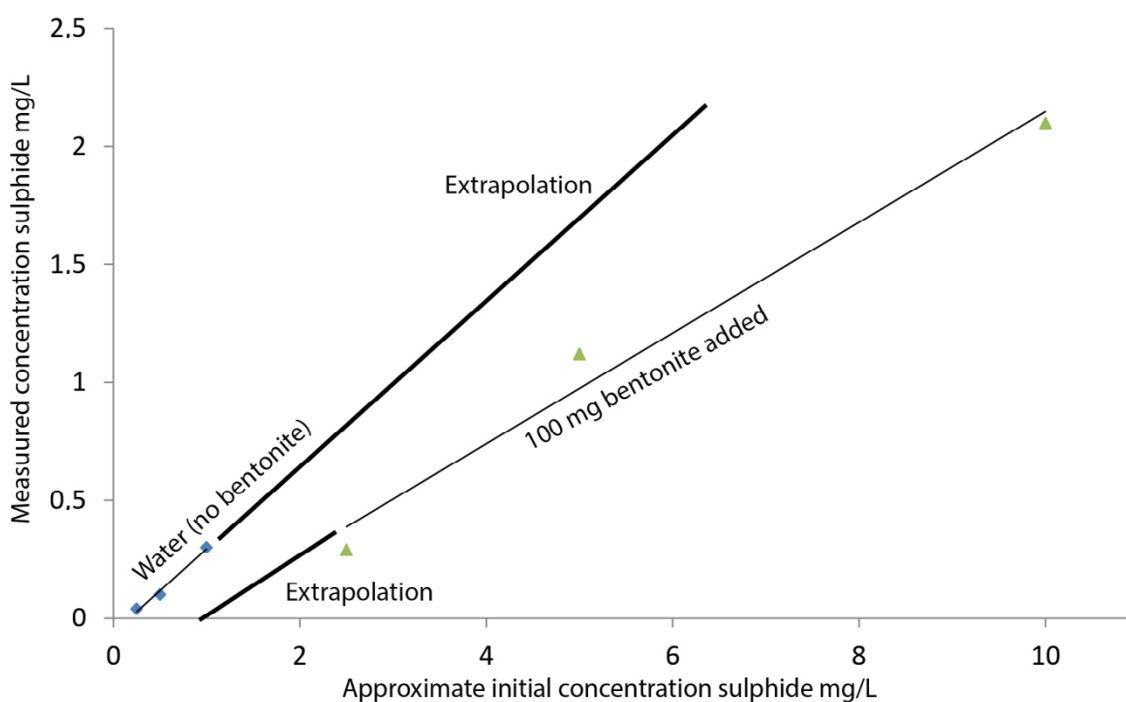


Figure 3-5. MB-VI: Measured sulfide concentrations as a function of the theoretical value in pure water and in water-bentonite mixtures (100 mg MX-80 bentonite). The lines are given as guides for the eyes. The triangles mark samples with bentonite. The squares show samples without bentonite. The limit of quantification (LOQ) is 0.019 mg L^{-1} and the limit of detection is 0.006 mg L^{-1} (Svensson et al. 2017).

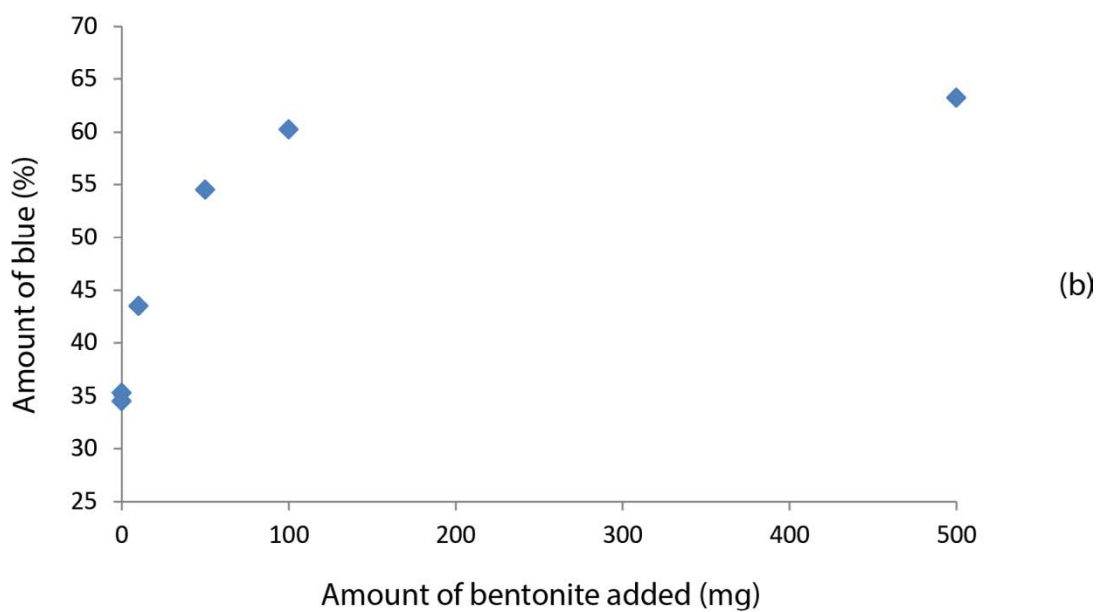
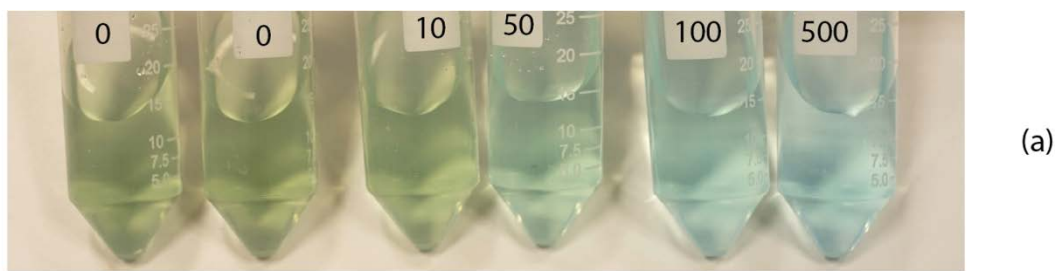


Figure 3-6. CS-II: Five test tubes with constant sulfide concentration (29 mg L^{-1} in 33 ml) and different additions of bentonite (0–500 mg). In the photo (a) the filtered supernatant is shown after Cu^{2+} addition (1 ml 1 M/tube). From left: 0, 0, 10, 50, 100 and 500 mg. The blue colour indicates Cu^{2+} . In the diagram (b) the results from colour measurements (the amount of blue) are given versus the amount of added bentonite. The blue colour in the samples is proportional to Cu^{2+} and inversely proportional to S^{2-} (Svensson et al. 2017).

3.2.3 Conclusions

The concentration of sulfide in the water after contact with bentonite was below the limit of quantification when no additional sulfide was added. Moreover, the concentration was below the limit of quantification (Figure 3-2) also after minor additions of extra sulfide to the bentonite. This may be regarded as evidence or at least strong indications that bentonite lowers the sulfide concentration in solution (Figure 3-3, Figure 3-4 and Figure 3-5) which supports the suggestion that the equilibrium concentration of sulfide in a solution in contact with bentonite is very low. There were no indications of high sulfide concentrations in the bentonite porewater in any of the experiments. The low values for the sulfide concentration used in previous corrosion calculations are therefore supported by this work.

The exact amount of sulfide that is lost by the bentonite cannot be precisely determined from these measurements due to the uncertainties.

The expected mechanism for the sulfide removal is that trivalent iron in montmorillonite is oxidising sulfide to elemental sulfur. The reduction of trivalent iron in clays using sulfide is previously known (Bergaya et al. 2006, Chapter 13). Independently on the mechanism it is possible to roughly estimate the magnitude of the sulfide removal. This is important for the interpretation of various experiments and possibly for the long term safety function. It is however possible to do rough estimations based on the results obtained to make an estimate of the magnitude.

Based on (Figure 3-5), about 66 % of the added sulfide is lost (when 1 mg L⁻¹ was added 0.4 mg L⁻¹ was detected, when no bentonite was added). The initial sulfide concentration in the CS-II experiment was 29 mg L⁻¹ (very high). The volume was 34.5 ml. Based on (Figure 3-6) 100 mg bentonite approximately removed the added amount of sulfide. The added amount $(34.5 \text{ ml} \times 29 \text{ mg L}^{-1}) \times (1/3) = 0.33 \text{ mg}$. $0.33 \text{ mg}/100 \text{ mg bentonite} = 0.3 \text{ wt}\%$. Hence, based on the experiments done, a very rough estimation indicates a sulfide loss in the order of 0.3 wt% of the bentonite, or 1 000 kg bentonite would remove about 3 kg of sulfide (a better estimate is perhaps 1–10 kg sulfide/1 000 kg bentonite).

3.3 Threshold buffer density

3.3.1 Description

Bengtsson et al. (2017a) investigated three different bentonite clays for microbial sulfide producing activity as a function of total density at full water saturation. The clays were Wyoming MX-80, Asha and Calcigel, under saturated densities in a range from 1 500 to 2 000 kg m⁻³.

To further study the effects on bacterial sulfide production in different bentonites, the series described above continued with two additional materials and three densities for each material (Bengtsson et al. 2017b). This study included an iron-rich bentonite clay (Rokle) and a bentonite clay with a low content of iron (Gaomiaozhi, GMZ).

A weakness in the studies reported in Bengtsson et al. (2017a, b) is that they have been carried out by the same personnel in the same laboratory and that there were no independent verifications of the results. To remedy this, Haynes et al. (2019) repeated a small part of the tests from Bengtsson et al. (2017a). Two saturated densities of Calcigel were studied: 1 750 kg m⁻³ as a positive control where sulfide production was expected, and 1 900 kg m⁻³ where no activity was expected.

All the tests were performed with a type of equipment described by Bengtsson et al. (2017a). The test cell consisted of a titanium cylinder with top and bottom lid attached by six Allen screws for each lid. A piston operated inside the cylinder (Figure 3-7). When the piston was at its most extended position, a 35 × 20 mm confined cavity was produced inside the cylinder (Figure 3-8). This cavity was filled with MX-80, Asha or Calcigel bentonite powder. By using spacers on the screws running through the top lid the volume inside the test cell was kept constant. The pressure created by the swelling bentonite pushed the piston upwards and by doing so a force transducer mounted between the piston and top lid was compressed. The amount of compression, which stood in direct correlation to the bentonite swelling pressure, was recorded by a data collection system connected to a computer. During the water saturation phase of each experiment a water saturation (WS) bottom lid and piston were used. The lid had a 2 mm inlet hole which allowed water to enter the test cell and reach the bentonite. In addition, the piston had a longitudinal inside hole to get water inflow from both top and bottom. To stop the bentonite from swelling into the inlet holes, and to get an evenly distributed inlet flow, a 40 µm pore size titanium filter was mounted with two Phillips screws on the inside of the saturation lid and piston. After the saturation phase the bottom lid and piston were replaced with a lid and a piston without inlet. The new piston was equipped with a removable ventilation plug to not trap gas inside of the test cell upon insertion of the piston. The titanium filter on the saturation bottom lid was replaced with a copper disc.

Three different species of SRB were used in the experiment. *Desulfovibrio aespoeensis* (DSM 10631), *Desulfotomaculum nigrificans* (DSM 574) and *Desulfosporosinus orientis* (DSM 765). *D. aespoeensis* was isolated from deep groundwater (Motamedi and Pedersen 1998), *D. nigrificans* is a thermophilic, spore-forming sulfide-producing bacterium and *D. orientis* is a spore-forming sulfide-producing bacterium with the ability to grow with H₂ as the source of energy. The three different bacterial cultures were mixed into one cocktail and poured or sprayed carefully out on a bed of bentonite powder in a large glass Petri dish for each of the bentonite types. This created small lumps of bentonite with cocktail. The whole content of the Petri dish was then passed through a mesh where the lumps were pulverised with sterile spoons. This created batches of bacteria doped bentonite with a bacterial content of approximately $1 \times 10^7 \text{ SRB g}^{-1}$. Each test cell was assembled with bottom lid and a titanium filter and placed on an analytical scale where the calculated amounts of bentonite powder with or without added SRB, was weighed in. A water saturation piston was inserted in each test cell cylinder and in those cases where the bentonite powder volume was larger than the test cell volume the bentonite powder was compacted with a workshop press. After compaction of the bentonite the test cells were assembled and

mounted on a custom-built water saturation system. The pressures created by the swelling bentonites were monitored and the test cells were kept unaltered until stable swelling pressures were obtained. Water could move freely in and out of the bentonite during the water saturation phase. In the second phase of the experiment where the two titanium filters were replaced with a copper disc and a 2 mm taller piston, respectively; water was not in contact with the clay. By using an identical confined space before and after contact with water, the swelling pressures were approximately reproduced. All the work performed including additions of $^{35}\text{SO}_4^{2-}$ and lactate as well as the cleaning and insertion of the copper discs were carried out in the anaerobic box. Batches of $\text{Na}_2^{35}\text{SO}_4$ were distributed over the test cells by a pipette to final calculated concentrations.



Figure 3-7. All the parts included in a test cell. The parts in contact with the bentonites were made of titanium. See text for details. WS = water saturation (Bengtsson et al. 2017a).

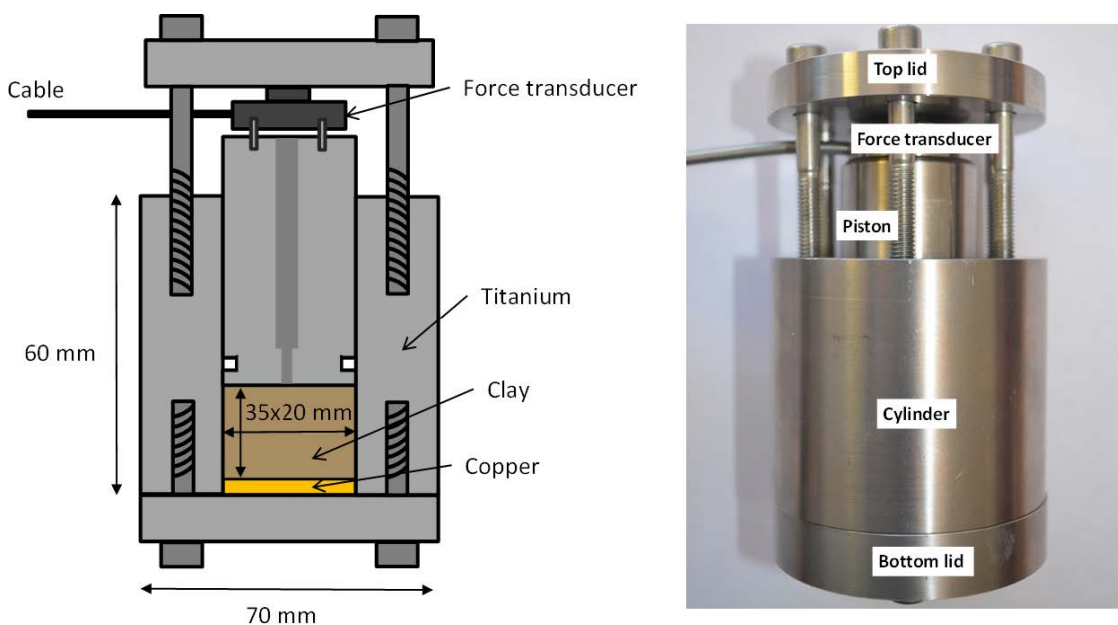


Figure 3-8. Left: A schematic cross section of a test cell. Right: An assembled test cell, spacers are not mounted (Bengtsson et al. 2017a).

At the sampling day, the pressure logging in the force transducer software was stopped and the force transducer was removed together with the top lid and screws. The top lid was then attached again, however with shorter screws to be able to push the piston all the way to the bottom. The test cells were moved to a fume hood and the bottom plates were carefully removed. The piston was then pressed up by turning the screws so that the edge of the copper disc became visible. The copper discs were removed with sterile tweezers and put in sterile Petri dishes and then immediately transferred to the anaerobic box where the Petri dishes were filled with anaerobic sterile AGW to completely cover the discs in order to remove bentonite residues and $^{35}\text{SO}_4^{2-}$. When dried, the radioactivity of the Cu_x^{35}S that had formed on the copper discs was located and quantified using a Packard Instant Imager electronic autoradiography system. The distribution of ^{35}S and sulfate were analysed from six different layers in the bentonite. The layers were: the first millimetre of bentonite closest to the copper surface (0–1 mm), the next four millimetres (1–5 mm), the next five millimetres (5–10 mm), the next five millimetres (10–15 mm), the next two and a half millimetres (15–17.5 mm) and the last two and a half millimetres (17.5–20 mm).

3.3.2 Results

MX-80, Bengtsson et al. (2017a)

For MX-80, the $1\,750\text{ kg m}^{-3}$ and the $2\,000\text{ kg m}^{-3}$ saturated densities were reported in Bengtsson et al. (2015) and are included in this report for comparison with the results from the $1\,900\text{ kg m}^{-3}$ test cells. Immediately when the test cells were opened an obvious difference between the $1\,750\text{ kg m}^{-3}$, $1\,900\text{ kg m}^{-3}$ and the $2\,000\text{ kg m}^{-3}$ copper discs were observed. All the $1\,750\text{ kg m}^{-3}$ discs had black precipitates of iron sulfide on the surface while the $1\,900$ and $2\,000\text{ kg m}^{-3}$ discs were free from precipitates. When analysed in the Instant Imager autoradiograph, on average, a 10 000 times higher surface radioactivity was measured on the (+) $1\,750\text{ kg m}^{-3}$ discs compared to the (+) $2\,000$ and (+) $1\,900\text{ kg m}^{-3}$ discs Table 3-3).

Heat treatment of the bentonite did not have any significant sterilization effect in the (–) $1\,750\text{ kg m}^{-3}$ cells that showed similar levels of radioactivity on the discs compared to the discs in (+) $1\,750\text{ kg m}^{-3}$ cells with added SRB.

Table 3-3. MX-80 reproduced swelling pressures deduced from data obtained with force transducers for each test cell, radioactivity detected on the copper discs recalculated for half-life of the isotope and the total amount of copper sulfide on the discs calculated from the surface activity and the isotope dilutions ($[\text{SO}_4^{2-}]/[^{35}\text{SO}_4^{2-}]$) (Bengtsson et al. 2017a).

Test cell code	Mean reproduced swelling pressure (kPa)	Surface activity (kBq)	Total amount of Cu_xS (nmole)
MX-80			
T3 1750 (+) 47d.	600	1600	21600
T4 1750 (+) 77d.	600	1600	21400
T5 1750 (+) 123d.	600	528	7130
T1 1750 (–) 123d.	600	593	7630
T2 1750 (–) 123d.	600	1130	14500
TC12 1900 (+) 35d.	1000	0.05	1.17
TC13 1900 (+) 84d.	800	0.04	1.07
TC11 1900 (–) 84d.	800	0.03	0.675
T8 2000 (+) 47d.	5000	0.2	3.99
T9 2000 (+) 77d.	5000	0.1	1.47
T10 2000 (+) 123d.	5000	0.6	13.7
T6 2000 (–) 123d.	5000	0.0001	0.002
T7 2000 (–) 123d.	5000	0.0001	0.002

Asha (Bengtsson et al. 2017a)

In the experiments described in this section, copper discs with bevelled edges were used. This eliminated the density issue with the bentonite in the narrow boundary space between the test cell inner wall and the edge of the copper disc. With bevelled edge, the bentonite could swell properly around the edges of the titanium filters. Table 3-4 shows data from three different experiments performed at three different date intervals, however with the same experimental setup. The tested saturated densities for the first experiment with Asha ranged from 1 850 to 2 000 kg m⁻³. However, no substantial surface radioactivity was found on any of the copper discs in that experiment. Therefore, two new experiments with densities that ranged from 1 500 to 1 850 kg m⁻³ were performed. When evaluating all experiments together, a considerable surface radioactivity was found on the 1 500 to 1 700 kg m⁻³ discs. The measured radioactivity on the discs for all other densities was close to or at the detection limit (Table 3-4).

Table 3-4. Asha reproduced swelling pressures deduced from data obtained with force transducers. The radioactivity detected on the copper discs is recalculated considering the half-life of the isotope and the total amount of copper sulfide on the discs is calculated from the surface activity and the isotope dilutions ($[\text{SO}_4^{2-}]/[^{35}\text{SO}_4^{2-}]$) (Bengtsson et al. 2017a).

Test cell code Asha	Mean reproduced swelling pressure (kPa)	Surface activity (kBq)	Total amount of Cu _x S (nmole)
TC29 1500 (+) 43d.	90	1070	12000
TC32 1500 (+) 88d.	90	1340	15200
TC27 1500 (-) 88d.	90	311	3380
TC37 1600 (+) 33d.	40	309	4590
TC38 1600 (+) 78d.	55	736	10900
TC35 1600 (-) 78d.	30	866	13100
TC39 1700 (+) 33d.	110	807	13200
TC40 1700 (+) 78d.	190	4	62.0
TC36 1700 (-) 78d.	130	0.99	16.4
TC30 1750 (+) 43d.	380	11.0	254
TC33 1750 (+) 88d.	380	191	4450
TC3 1850 (+) 35d.	500	0.001	0.028
TC31 1850 (+) 43d.	900	0.01	0.162
TC7 1850 (+) 84d.	500	0.09	3.10
TC1 1850 (-) 84d.	500	0.001	0.021
TC34 1850 (+) 88d.	900	0.2	4.69
TC28 1850 (-) 88d.	900	0.03	0.774
TC4 1900 (+) 35d.	1200	0.01	0.191
TC8 1900 (+) 84d.	800	0.01	0.413
TC5 1950 (+) 35d.	1400	0.03	1.42
TC9 1950 (+) 84d.	1400	0.0003	0.015
TC6 2000 (+) 35d.	3000	0.002	0.106
TC10 2000 (+) 84d.	2500	0.02	0.794
TC2 2000 (-) 84d.	3800	0.0001	0.002

Calcigel (Bengtsson et al. 2017a)

A clear difference in the measured surface radioactivity was found between the densities 1 850 and 1 900 kg m⁻³ in the Calcigel experiment (Table 3-5). The 1 850 kg m⁻³ case was the heaviest density where considerable microbial sulfide-producing activity could be observed for the three tested bentonite types. The Calcigel bentonite had a very low natural sulfate content but still harboured inherent SRB in numbers well above the detection limit (Svensson et al. 2011). In the Calcigel experiment we added 1 mM sulfate to the saturation salt solution which evidently was enough to activate the SRB present in this commercial bentonite since also the control test cell (TC14 1850 (-) 99d.) without any addition of SRB produced detectable amounts of radioactive ³⁵S²⁻ on the copper disc.

Table 3-5. Calcigel reproduced swelling pressures deduced from data obtained with force transducers. The radioactivity detected on the copper discs is recalculated considering the half-life of the isotope and the total amount of copper sulfide on the discs is calculated from the surface activity and the isotope dilutions ($[\text{SO}_4^{2-}]/[^{35}\text{SO}_4^{2-}]$) (Bengtsson et al. 2017a).

Test cell code	Mean reproduced swelling pressure (kPa)	Surface activity (kBq)	Total amount of Cu_2S (nmole)
Calcigel			
TC16 1850 (+) 56d.	400	1 110	332
TC19 1850 (+) 99d.	400	1 580	484
TC14 1850 (-) 99d.	400	123	31
TC17 1900 (+) 56d.	750	9	3
TC20 1900 (+) 99d.	750	23	8
TC18 1950 (+) 56d.	1 500	43	16
TC21 1950 (+) 99d.	1 500	12	4
TC15 1950 (-) 99d.	1 600	0.03	0.01

Rokle and GMZ (Bengtsson et al. 2017b)

For the Rokle bentonite, only TC44, which had a low density ($1\,750\text{ kg m}^{-3}$) and the longest incubation time (78 days), had a substantial accumulation of surface radioactivity on the copper disc (Table 3-6).

In the GMZ case, the accumulation of Cu_2^{35}S was almost as high for the low density as the high-density copper surfaces ($1\,750$ and $2\,000\text{ kg m}^{-3}$) (Table 3-1). The intermediate density with $1\,850\text{ kg m}^{-3}$ clay had more than ten times less surface radioactivity than some of the test cells with lower or higher density (Table 3-1). Similar results as in Bengtsson et al. (2017a), have been reported previously for other bentonite clays in the experiments series, with no clear understanding on why high densities occasionally have more accumulation of surface radioactivity than lower densities. The recorded swelling pressures for GMZ was lower than for Rokle at the same densities. However, the swelling pressure for GMZ at a saturated density of $1\,950\text{ kg m}^{-3}$, where sulfide production was detected, was still higher than for Rokle at $1\,850\text{ kg m}^{-3}$, where no sulfide production was found.



Table 3-6. Rokle and GMZ analysed saturated densities. The radioactivity detected on the copper discs is recalculated considering the half-life of the isotope and the total amount of copper sulfide on the discs is calculated from the surface activity and the isotope dilutions ($[\text{SO}_4^{2-}]/[^{35}\text{SO}_4^{2-}]$) (Bengtsson et al. 2017b).

Test cell code	Analysed saturated density (kg m^{-3})	Surface activity (kBq)	Total amount of Cu_2S (nmole)
Rokle			
TC41 1750 (-) 78d.	1 676	0.41	0.14
TC43 1750 (+) 33d.	1 692	0.05	0.02
TC44 1750 (+) 78d.	1 670	577	180
TC45 1850 (+) 33d.	1 838	0.06	0.02
TC46 1850 (+) 78d.	1 830	0.09	0.03
TC42 1950 (-) 78d.	1 924	0.15	0.05
TC47 1950 (+) 33d.	1 932	0.02	0.01
TC48 1950 (+) 78d.	1 940	0.02	0.01
GMZ			
TC51 1750 (-) 77d.	1 692	1 570	1 690
TC53 1750 (+) 33d.	1 715	243	247
TC54 1750 (+) 77d.	1 716	425	436
TC55 1850 (+) 33d.	1 832	34.2	38.2
TC56 1850 (+) 77d.	1 824	20.5	21.7
TC52 1950 (-) 77d.	1 910	54.2	64.6
TC57 1950 (+) 33d.	1 945	151	167
TC58 1950 (+) 77d.	1 929	1 110	1 170

Haynes et al. (2019)

Accumulation of the copper sulfide corrosion product on the copper discs was identified by exposing a phosphor image plate to the corroded copper surface, and therefore radioactive S-35 was introduced to the bentonite after the saturation stage. The saturated density of Calcigel of 1 750 kg m⁻³ tested positive for S-35 accumulation accounting for 99.96 % of the illumination (Table 3-7). The saturated density 1 900 kg m⁻³ produced a negative result (0 %), lower than the background signal of the phosphor image plate (0.04 %) (Table 3-7). The copper discs were also inspected using a beta radiation dose rate monitor which detected 120 cps (counts per second) on the 1 750 kg m⁻³ copper disc, and 9 cps on the 1 900 kg m⁻³ copper disc (Table 3-7). The background count for the room was 9 cps.

Table 3-7. Images of the copper discs after the removal from the pressure cells, along with the counts per second (cps) using a beta radiation dose monitor, and the fluorescence intensity of the discs when placed on the phosphor plate (Haynes et al. 2019).

	Background	1 750 kg m ⁻³	1 900 kg m ⁻³
			
Beta radiation count (cps)	9	120	9
Flourescence intensity	0.04 %	99.96 %	0 %

3.3.3 Conclusions

This work demonstrated that there are threshold bentonite saturated densities for MX-80, Asha, Rokle and Calcigel above which microbial sulfide-producing activity was practically inhibited even if all other conditions were favourable for growth of SRB. The cut-off density for GMZ is more uncertain. The sulfide-production results for the three clays (MX-80, Asha, Rokle and Calcigel) indicated a saturated density interval between 1 670–1 880 kg m⁻³ within which sulfide-producing activity dropped from high to very low or below detection.

The observed differences of accumulated Cu₂³⁵S (Figure 3-9) may depend on several different variables. The recorded swelling pressures for the different bentonites were different at similar densities, mainly explained by different smectite contents. This should have some impact on the sulfide production. The swelling pressures for GMZ and Calcigel were however rather similar in the density interval of 1 850–1 950 kg m⁻³, which means that the swelling pressure is not the only explanation. Reactions of sulfide with metals, mostly iron, in the clays may have decreased the amount of sulfide that reached the copper discs compared to what was produced in the test cells. Finally, increasing saturated densities generally had a mitigating effect on the sulfide production. There was, consequently, an increased stress on the SRB by increasing the saturated density that resulted in a loss of high sulfide production at discrete saturated density intervals that differed from clay to clay.

By using the methods previously described in Bengtsson et al. (2015, 2017a), Haynes et al. (2019) were able to confirm that microbial sulfide-production in Calcigel bentonite would be prevented if the saturated density of the bentonite was maintained at 1 900 kg m⁻³ or greater. Proving that sulfide-producing activity can be prevented at a target bentonite density is critical in proving that such activity cannot occur in a bentonite buffer.

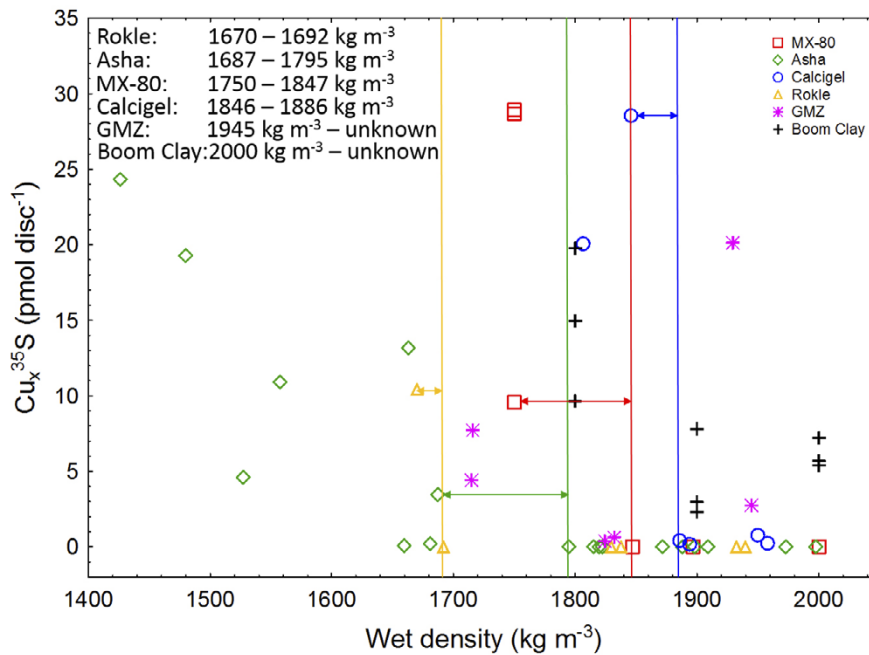


Figure 3-9. Accumulated Cu_x^{35}S on copper discs (pmol) over saturated density. The respective intervals where sulfide-production shifts from high to low are indicated with arrows. The corresponding analysed saturated density intervals are inserted, and for GMZ all tested saturated densities show high sulfide production. Data for Asha, MX-80 and Calcigel from Bengtsson et al. (2017a) and for GMZ and Rokle from Bengtsson et al. (2017b).

3.4 FaTSu – Microbial utilization of bentonite organic matter

The experimental work and the obtained results are summarized below, while the detailed description is provided in Maanoja et al. (2020a, b).

3.4.1 Description

The main target of the experiment was to study whether organic matter can dissolve from compacted bentonite and sustain biological sulfate reduction. The experiment was performed with Wyoming, Greece, India and Bulgaria compacted at a dry density of 1 314–1 369 kg m⁻³. That corresponded to a saturated density of 1 792–1 894 kg m⁻³, which was assumed to inhibit activity of microbes in the bentonites (Figure 3-10).

The experiment was carried out in anaerobic cell systems, where compacted saturated unsterile bentonite was separated from a loosely packed saturated sand layer with a porous sinter. Two cells were prepared for each bentonite and the sand layer of the first cell was inoculated with SRB and Olkiluoto groundwater microbes, while the sand layer of the other cell was not inoculated. The dissolution of bentonite constituents in the sand layer solution and activity of microbes was monitored by measuring the concentrations of DOC and CH₄, sulfate, sulfide and total iron and the redox potential (Eh) of the sand layer solution among other parameters. Duration of the experiment was 265–454 days depending on the cell.

3.4.2 Results

In all the cells, the concentration in the sand layer solution of DOC was 2–23 mg L⁻¹ on average throughout the experiment apart from the uninoculated cell of the Greek bentonite, where the concentration was higher than in the other cells for unknown reason (75 mg L⁻¹; Figure 3-11). When these concentrations were compared to the TOC contents of the bentonites (1 100–1 500 mg kg⁻¹), it could be concluded that only a small part of the bentonite organic matter (0.01 %–0.22 % TOC w/w) was readily soluble to the water phase of the sand layer.

Microbial activity in the cells can be inferred from evolution of several parameters. The concentrations of DOC and sulfate were lower in the sand layers of the inoculated than in the uninoculated cells following from microbial consumption of DOC and reduction of sulfate in the inoculated cells. In the uninoculated cells, the highest dissolved sulfate concentrations observed were 11, 3.2, 2.1 and 0.245 g L⁻¹ for cells containing the Greek, Wyoming, Indian and Bulgarian bentonites, respectively (Figure 3-10). Concentration of dissolved sulfide was below limit of detection of the analytical method (< 4 mg L⁻¹) throughout the experiment, but the observed decrease in concentration of total iron and identification of iron sulfide precipitates from the sand of the inoculated cells suggested that the formed sulfide had precipitated with iron dissolving from the bentonites. Dissolved methane was detected from all eight cells (on average 10–650 µg L⁻¹), which indicated activation of methanogens both in the inoculated and uninoculated cells.

The redox potential decreased to –150 mV (versus standard hydrogen electrode) on average in all the inoculated cells apart from the inoculated cell of the Indian bentonite, where it remained > 200 mV throughout the experiment. As the SRB require reduced conditions for growth (below –50 mV; Frindt et al. 2015), the growth of SRB was highly unlikely in the sand layers of the cells with Indian bentonite and, consequently, they were presumably growing within the bentonite. The growth of microbes within the bentonite of other cells could not be excluded either based on the data measured.

3.4.3 Conclusions

The results showed that organic matter, sulfate, and iron, among other compounds, dissolved from the compacted bentonites into the sand layer solution, but the bentonites differed in the quantity of the ions leached to the solution. The Greek bentonite released the highest concentration of organic matter in the sand solution of all bentonites, while the presence of microcrystalline Fe(III)-oxide phases in the Indian bentonite resulted in high redox potential of the sand layer solution, which, in turn, could suppress the activity of SRB.

Microbial activity was detected from all eight experimental cells, both inoculated and uninoculated, which indicated that the organic matter in all bentonites could sustain activity of added and bentonite borne SRB and other microbes (e.g. methanogens). The exact location of active microbes in sand layers or bentonites could not be confirmed based on the measured data, but it is likely that some of the microbial activity occurred within the bentonites as the saturated densities determined post-experiment (data not shown) were below the suggested threshold densities (Section 3.3.3; Figure 3-9). The findings also showed that the bentonites were able to immobilize the formed sulfide through precipitation with iron; clay mineralogy seemed to play a role in the extent of sulfate reduction and immobilization in the studied density range.

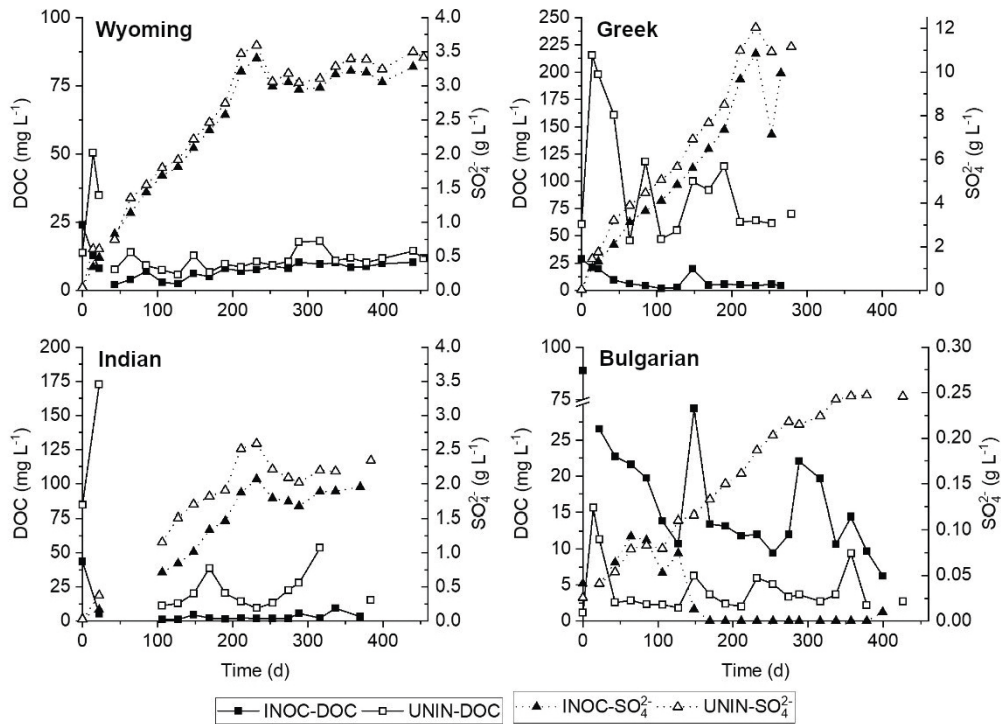


Figure 3-10. Dissolved organic carbon (DOC) and sulfate in the solution of sand layers (inoculated [INOC] or uninoculated [UNIN] with microbes) of the experimental cells with different bentonites. Note the different scales on the y-axes (Maanoja et al. 2020a, b).

4 WP3 – Integration for the safety case – modelling

The modelling work in WP3 is described in Pękala et al. (2019), Idiart et al. (2019) and King and Kolář (2019).

4.1 Background

The aim of WP3 was to further *develop reactive transport modelling tools* that are able to describe and simulate the sulfide fluxes and evolution (sources and sinks) in the different parts of the near field of a KBS-3 repository (canister, buffer, backfill, rock-backfill interface and rock bolts), see Figure 4-1.

It must be stressed here that it was *not* the objective of this task to provide safety assessment results for any repository. Furthermore, the purpose of WP3 was *neither* to provide a correct generic conceptual model *nor* a thorough analysis of the processes or fluxes of sulfide in the near field of a spent nuclear fuel repository.

It was decided at the start of the project, by the funding organisations, to include the following teams in WP3:

- Institute of Geological Sciences, University of Bern, Switzerland. This team will be referred as “UniBern” team.
- Amphos 21 Consulting S. L. (Barcelona, Spain), together with Clay Technology AB (Lund, Sweden). This team will be referred to as “Amphos/CT” team.
- Integrity Corrosion Consulting Ltd., together with LS Computing Ltd., both based in British Columbia, Canada. This team will be referred as the “ICC” team.

Initial planning discussions lead to the definition of a Base Case that would be used in a modelling tool inter-comparison and partial verification (Appendix A1). Furthermore, a series of Variant Cases were defined to test the capabilities of the different modelling strategies implemented in the modelling tools being developed (Appendix A2), as well as give some indication of the sensitivity to different parameters.

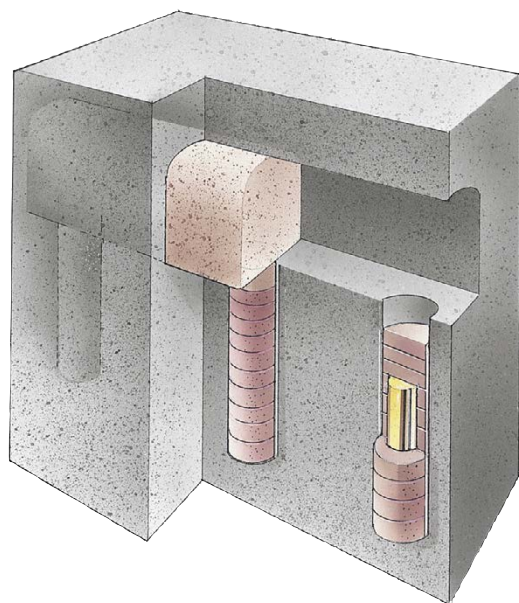
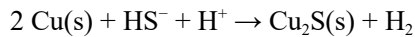


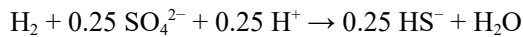
Figure 4-1. The KBS-3 system with canisters deposited one by one in vertical holes.

4.2 The conceptual model

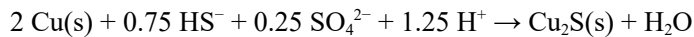
The copper sulfide corrosion reaction may be described as:



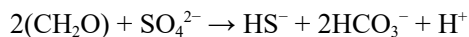
In these and following reactions, species without the “(s)” solid phase designator indicate species in the aqueous solution. The molecular hydrogen generated by the corrosion process may be used in bacterial sulfate reduction:



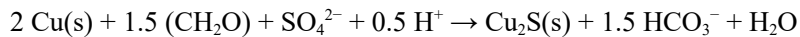
The overall corrosion reaction is then:



For the WP3 Base Case, sulfate reduction takes place only in the rock-bentonite interfaces through bacterial activity. These interfaces are conceived as a relatively thin layer of rock assumed to have a higher fracture frequency due to excavation damages. The microbial process may be driven by organic matter, initially present in the bentonite, or by molecular hydrogen (H₂) generated by corrosion processes, either by structural steel (rock bolts or stretch metal) or by the copper canister as mentioned above. The organic matter is assumed in the WP3 to have the stoichiometry of formaldehyde (CH₂O), for example acetic acid (CH₃COOH). The overall organic matter reduction of sulfate is described within the WP3 as follows



The overall stoichiometry of the organic matter driven copper corrosion is then



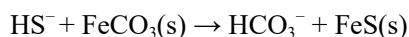
Rates of microbial sulfate reduction were defined in the Base Case from literature studies. Dimensions and properties for the backfill and buffer were chosen in the Base Case to be among those reported in previous safety assessments by Posiva and SKB. The amount of organic carbon, for example, corresponds to 0.1 weight % of clay. The amounts of calcium sulfate, organic carbon and iron in the backfill are reported in Table 4-1.

Table 4-1. Base Case amounts of calcium sulfate, available organic carbon and iron(II) in the backfill and buffer.

	Backfill [mol per m ³ of bulk bentonite]	Buffer [mol per m ³ of bulk bentonite]
CaSO ₄ (gypsum)	190	37
Available organic carbon (of assumed stoichiometry CH ₂ O)	140	113
Fe(II) (for simplicity the iron(II) was assumed to be present as siderite, FeCO ₃ (s))	163	0

Because two carbon atoms (in the assumed carbohydrate stoichiometry) are needed to reduce one sulfate molecule according to the stoichiometry in the reactions above, the amount of organic carbon is limiting in the backfill.

In the Base Case, SO₄²⁻ and organic matter are transported through diffusion towards the rock-bentonite interfaces, where they are consumed by sulfate reducing bacteria. The sulfide thus produced then diffuses into the rock (small quantities) and towards the canister, where copper corrosion occurs. However, in the backfill the sulfide reacts with iron(II) and is precipitated



According to the amounts established for the Base Case, Fe(II) is in excess. Note however that the amount of iron reported in accessory minerals in the bentonite could perhaps be goethite or some other Fe(III) oxyhydroxide, rather than Fe(II) in FeCO₃. The reduction of Fe(III) to Fe(II) by sulfide is possible, but it has not been modelled within the WP3.

For the buffer, the situation is similar to that of the backfill. The amounts of calcium sulfate, organic carbon and iron in the buffer are reported in Table 4-1.

In this case all sulfate may be exhausted by bacterial activity. As there is no Fe(II) in the buffer, all sulfide generated at the rock-bentonite interface (except for a negligible amount that diffuses into the rock matrix) will be transported by diffusion to the canister surface, where corrosion will occur.

4.3 The models used by the teams

It was apparent, from the start of the WP3, that some of the modelling tools to be developed would have the capability of simulating the repository near field in three dimensions (3D models), while other modelling tools would only have the capability of one-dimensional modelling (1D models). Furthermore, the 1D models could be set either on a vertical direction (from the rock above the deposition tunnel to the lid of the canister, through the backfill and the buffer on top of the canister) or they could describe a horizontal system, from the rock in the deposition hole to the canister, through the buffer. Figures 4-2 to 4-4 give schematic views of the models from the three modelling teams. The UniBern team used both 1D (vertical) and 3D models, the Amphos/CT team used a vertical 1D model, and the ICC team had a vertical 1D model and the same model where the backfill layer was excluded, to simulate a horizontal 1D model (see Figure 4-4).

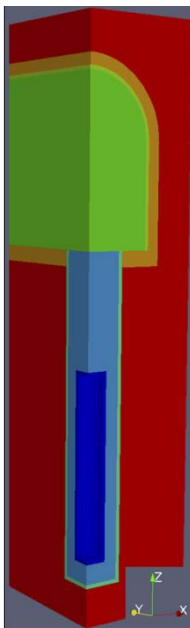


Figure 4-2. The 3D model described in Peřkala et al. (2019): the model geometry was reduced to one quarter of the system containing a deposition hole.

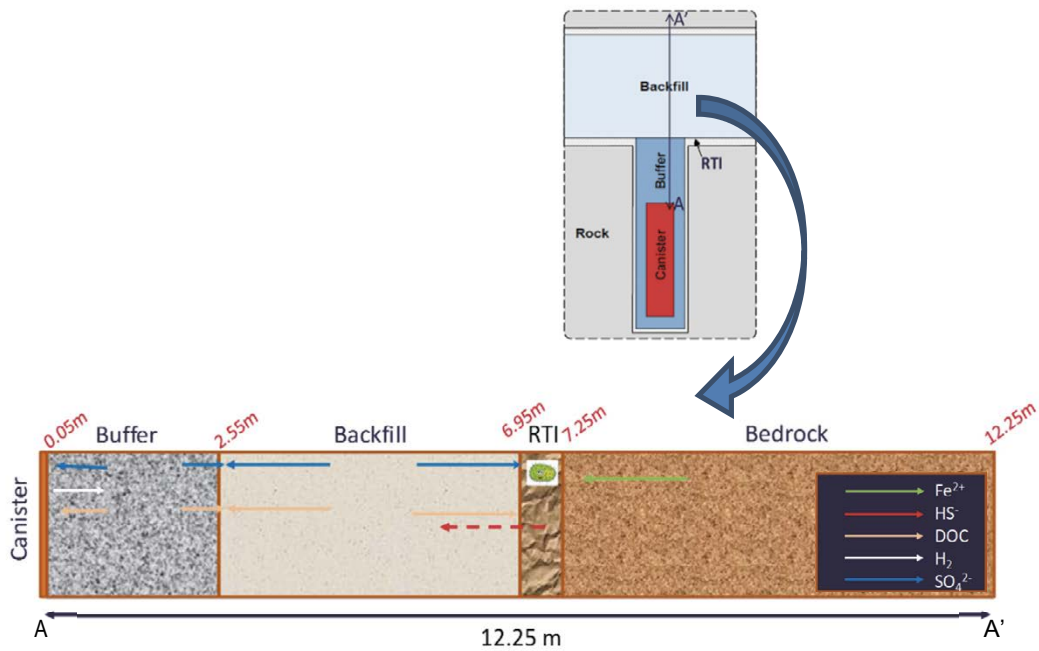


Figure 4-3. The 1D model used in Idiart et al. (2019): a vertical profile (A-A') from the canister top lid to the rock, with arrows showing the sulfate/sulfide pathways along the five domains considered in this model.

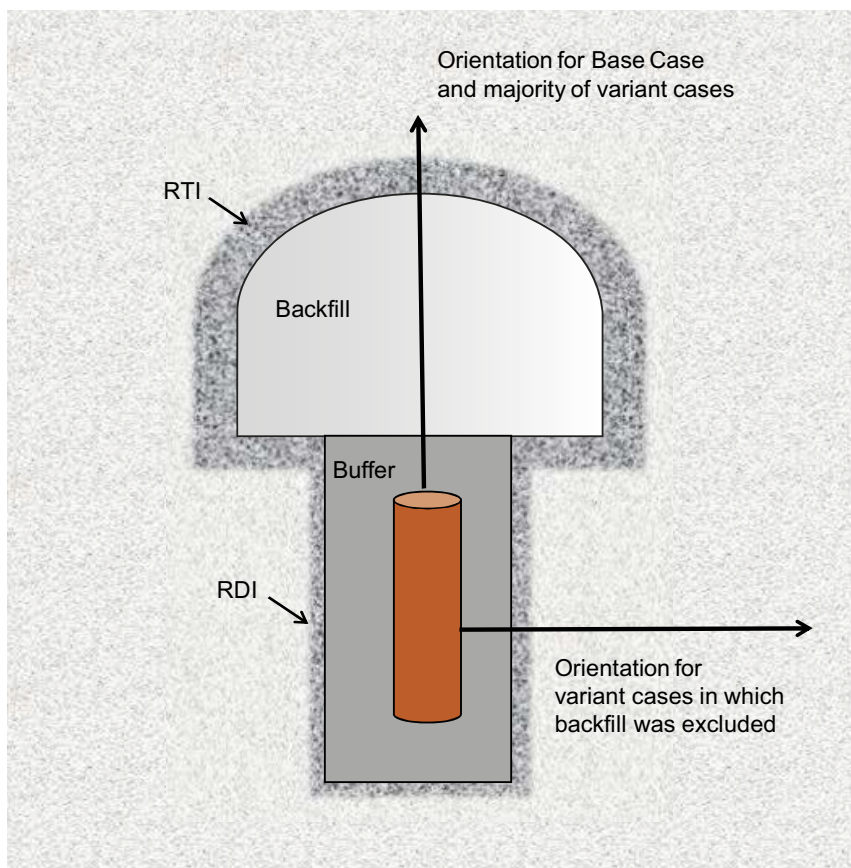


Figure 4-4. The 1D model used in King and Kolář (2019): the figure shows the orientations assumed for the Base Case simulations and the majority of variant cases, and the alternative orientation for the variant cases in which the backfill was excluded. In the vertical orientation, the buffer and backfill volumes to canister surface area ratios are used to obtain equivalent layer thicknesses: 0.831, 5.98, 0.3 and 5 m for the buffer, bentonite, rock-tunnel interface and intact rock layers, respectively. For the horizontal orientation, the backfill layer is absent, that is, the model is not axisymmetric.

Because the clay particles in the backfill and in the compacted bentonite buffer have a permanent negative charge, special models have been developed to describe the concentration and diffusion of anions or cations in the porewaters, also called “interlayer” water because clay particles are idealized as a set of thin planes lying parallel to each other. These models of compacted bentonite assume a Donnan equilibrium between the internal (interlayer) solution, and an external solution. The nomenclature used by the different WP3 teams is not entirely consistent, reflecting the different ways of describing these models in the scientific literature:

- The UniBern team describes the use of a *single* porosity model, which does not include Donnan equilibrium, and a Donnan *dual* porosity model. A porosity fraction describes the volume affected by the electrical potential at the clay surfaces (they use the term Donnan porosity), while the remaining porosity contains charge-balanced porewater, unaffected by the surface charges, and denoted as “free” porosity.
- The Amphos/CT team uses the term “hybrid model” for their compacted bentonite model. Two types of porosity are considered: interlayer water, and “bulk” water. Donnan equilibrium is maintained between the two solutions, and ion diffusion takes place only in the interlayer water. As an alternative to the hybrid model, this team uses a “traditional” reactive transport model, with a single “bulk” porosity.
- The ICC team uses the term “alternative bentonite model”. This model is described as a single interlayer porosity model. No simulations using this alternative model were performed within the WP3.

A further difference between the models is the detailed treatment of the corrosion reactions. The UniBern team and the Amphos/CT team assume an instant reaction when the sulfide reaches the copper surface, and the corrosion model could be said to be the stoichiometry (one mol sulfide corrodes two mol copper). On the other hand, the ICC team has separately anodic and cathodic reactions at the copper surface, and thus includes a more detailed electrochemical model for the corrosion reactions.

4.4 Results

4.4.1 Progress in development

The main result from the WP3 is that several modelling tools were successfully developed and tested.

The UniBern team used a modified version of the PFLOTRAN code (Hammond et al. 2014) in all their simulations for the 3D single porosity model and for the 1D dual porosity (Donnan) model (Peřkala et al. 2019).

The Amphos/CT team developed a 1D hybrid (Donnan) model using iCP (Nardi et al. 2014), an interface between Comsol multiphysics (www.comsol.com) and PhreeqC (Charlton and Parkhurst 2011, Parkhurst and Appelo 2013). A traditional (cation exchange) 1D model was also implemented using iCP. However, 3D models were not developed due to long execution times (Idiart et al. 2019).

The ICC team further developed their Copper Sulfide Model (CSM) entirely based on kinetic (rate) equations (King 2008). Chemical equilibrium was simulated with forward and backward rate equations. The CSM is exclusively a 1D model. No simulations using the “alternative” (Donnan) bentonite model were performed within the WP3 (King and Kolář 2019).

4.4.2 Inter-model comparison for the Base Case

Sulfide sinks

The sulfide reaching the canister surface causes corrosion, and thus the fate of the sulfide (sources, sinks and transport) is an important feature in the modelling. The 3D simulations by the UniBern team show that practically all sulfide generated at the rock-backfill interface precipitates as FeS(s) very close to the rock interface, and that FeS(s) also precipitates at the interface between the backfill and the buffer, above the canister lid (Peřkala et al. 2019, Figure 29). This is confirmed by the 1D simulations by the same team (Peřkala et al. 2019, Figure 42), by the ICC team (King and Kolář 2019, Figure 5-11) and by the Amphos/CT team (Idiart et al. 2019, Figure 6-4). The distribution of sulfide at different times is illustrated in Figure 4-5, from the 3D simulations (Peřkala et al. 2019, Figure 28).

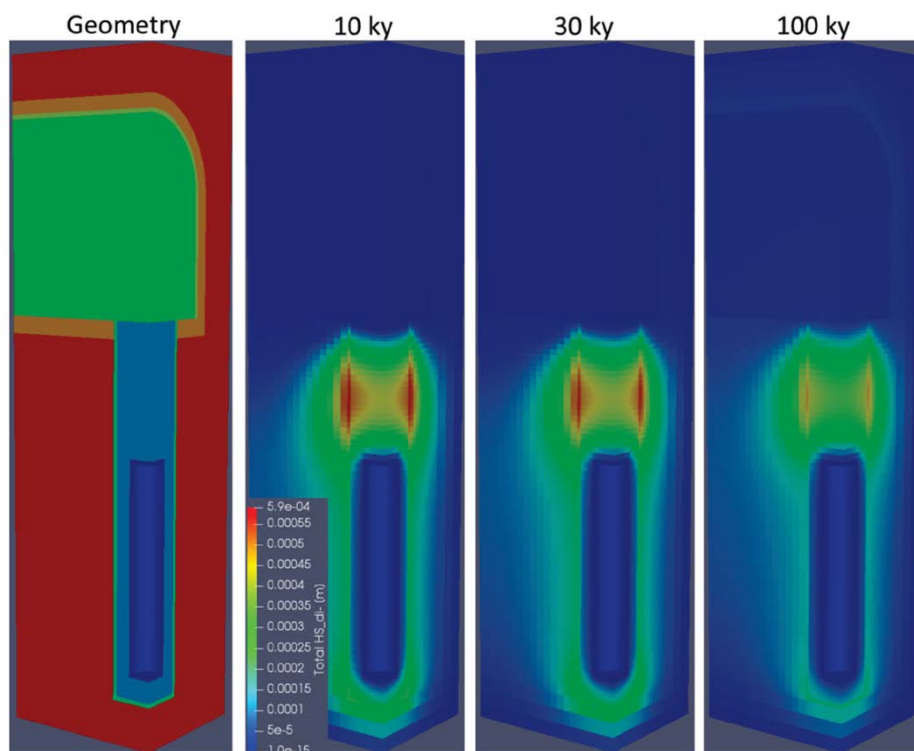


Figure 4-5. Model geometry (left, for orientation) and total dissolved sulfide (m is molality, [mol/kg of water]) at selected times predicted by the model for the Base Case. ky – thousand years (Pekala et al. 2019, Figure 28).

Corrosion depths – 1D models

The calculated corrosion depths at 100 000 years are summarised in Table 4-2.

It should be noted that the 1D models implemented by the different teams are not strictly equivalent. For the ICC team the dimensions were adjusted to preserve a correct buffer/backfill volume to canister surface area ratio, so that the buffer layer was 0.83 m and the backfill was ~6 m for the vertical 1D model. For the horizontal 1D model, the ICC team just removed the backfill layer. The UniBern and Amphos/CT teams used a vertical 1D model with a 2.5 m buffer layer (between the canister lid and the bottom of the backfill), and a 4.4 m backfill layer.

- The ICC team reports a corrosion depth of 0.75 μm after 100 000 years for the vertical 1D model (King and Kolář 2019, Table 5-4). For the horizontal 1D model (without backfill) the calculated corrosion depth is ~0.2 mm. No simulations using the “alternative” (Donnan) bentonite model were performed by the ICC team within the WP3.
- The UniBern team reports a corrosion depth of ~0.4 μm for the dual porosity (Donnan) model and ~0.25 μm for the single porosity “ion exchange” model (Pekala et al. 2019, Figure 51). These results correspond to a vertical 1D model.
- The Amphos/CT team reports 1.2 μm for the hybrid (Donnan) model and ~0.68 μm for the traditional “ion exchange” model (Idiart et al. 2019, Table 8-1). These results correspond to a vertical 1D model.

3D models

Base Case 3D model simulations were performed by the UniBern team, and the average canister corrosion depth at 100 000 years was found to be ~0.5 mm (over the whole, or “full”, canister), with a maximum corrosion depth of 2.7 mm (for any of the cells in the numerical mesh covering the canister surface), while when a “fast” bacterial sulfate reduction rate was used, the corresponding values were ~0.8 mm and 5.6 mm, respectively (Pękala et al. 2019, Table 12). The rationale behind choosing “fast” and reduced bacterial sulfate reduction rates in the 3D simulations is discussed in Pękala et al. (2019, Chapter 6).

4.4.3 Results for the Variant Cases

The calculated corrosion depths at 100 000 years are summarised in Table 4-2 for the Variant Cases as well. An inter-model comparison is not possible between the results from the three modelling teams for most of the variant cases, as (due to time and budget constraints) not all cases were modelled by more than one team.

The results reported in Table 4-2 represent an overview of the capabilities of the modelling tools developed within the WP3, and they are *not* to be considered a sensitivity analysis of the expected corrosion depths in a KBS-3 repository. It is recalled that the purpose of WP3 was *neither* to provide a correct generic conceptual model *nor* a thorough analysis of the processes or fluxes of sulfide in the near field of a spent nuclear fuel repository. The case BACKFILL DENSITY & Fe(II) MINERALS assumed that sulfate reduction by SRB could take place in the whole backfill volume, and that the bentonite material did not contain reactive iron minerals (in the model assumed to be Fe(II) carbonate, siderite). This case resulted in the highest canister corrosion. The case where bacterial activity was postulated in the backfill, with unchanged iron content (BACKFILL DENSITY in Table 4-2), resulted in a calculated canister corrosion increased by less than 10 % as compared with the 3D base case, but increased by a factor of ≈ 60 for the vertical 1D model. The case where it was postulated that SRB activity was not possible in neither the backfill nor the buffer, but with no Fe(II) minerals (Fe(II) MINERALS in Table 4-2), resulted in a calculated canister corrosion increased by a factor larger than 150 as compared with base case for the vertical 1D model.

However, from the modelling exercise it can be seen that generally important parameters are the location of possible microbial activity (in interfaces between rock and clay, or also in the backfill), as well as the presence of Fe(II) as siderite. Other factors seem to have less influence, such as the diffusivities in the interfaces, the amount of organic matter in the clay, or the groundwater composition. Because the purpose of the WP3 was to develop modelling tools, the question of adequate conditions for SRB activity was not addressed, for example, it was taken for granted that sulfate reduction may take place at rock interfaces with postulated increased of fracture intensity. A case with SRB activity exclusively at the intact rock surface, next to the backfill (or buffer) was not included in the WP3, and it is not certain that such a case could have been numerically implemented in the models, see the discussion in Chapter 6 of Pękala et al. (2019).

Table 4-2. Overview of corrosion depths (μm at 100 000 years) calculated for the Base and Variant Cases modelled by each WP3 team. Two model types were used: “ion exchange” (IE) and Donnan model. The 1D models are vertical unless otherwise stated. For the 3D model of the UniBern team this table lists the average corrosion depth over the whole canister for simulations using SRB rates decreased 1000 times, see discussion in Peřkala et al. (2019, Chapter 6). The corrosion depths corresponding to the agreed Base Case SRB rates are reported to be larger (70 % larger for the Base Case).

Simulation Name	Description	Type of model	Model dimension	Corrosion depth (μm at 100 000 years) reported by each WP3 Team		
				Uni. Bern	Amphos /CT	ICC
BASE CASE		IE	1D	~0.25	~0.68	0.75 197 †
		Donnan	1D	~0.4	~1.2	
		IE	3D	464		
BUFFER DENSITY	Buffer: localized loss of density so that SRB are active in the buffer.	IE IE	1D 3D	629		237 †
BACKFILL DENSITY	SRB activity in the entire backfill	IE Donnan IE	1D 1D 3D	499	250 218	46
Fe(II) MINERALS	FeCO ₃ increased to 0.5 wt% in buffer and 2.2 wt % in backfill	IE Donnan	1D 1D		~0.7 ~1.2	0.58
	No FeCO ₃ and no Fe(II) in cation exchangers	IE	1D		43	126
BACKFILL DENSITY and Fe(II) MINERALS	SRB activity in the entire backfill and no FeCO ₃	IE	3D	3500		
ORGANIC MATTER	Effect of decreasing TOC (total organic carbon) content in buffer and backfill (10 times decrease)	IE	1D	81		0.75
		IE	3D			
	Effect of increasing DOC (dissolved organic carbon) content in buffer and backfill (10 times increase)	IE	1D	818		0.75
		IE	3D			
INTERFACE METALS	Metal corrosion: effect of rock bolts and stretch metal producing H ₂ and magnetite	IE Donnan IE	1D 1D 3D	~500	~0.03 0.12	
SPATIAL GRID	Check numerical accuracy by increased discretization	IE		†		No effect
INTERFACE De	100 times higher effective diffusivities in both interfaces	IE	1D	724		No effect
		IE	3D			
THERMAL EFFECTS	Maximum canister temperature 75 °C	IE	1D			0.37
GROUNDWATER COMPOSITION	Groundwater in the intact rock: include sulfate and/or sulfide and/or DOC (when specific fractures are not modelled)	IE	1D			No effect
FRACTURE	A fracture intersecting the deposition hole, acting as source/sink of sulfide, sulfate and DOC. Three different groundwater flows modelled	IE	3D	~480		
KINETIC RATES	Effect of slower/faster SRB kinetics in the interfaces	IE	1D			No effect

†: The numerical issues related to special grid resolution are reported in Chapter 6 of Peřkala et al. (2019).

‡: Results for 1D-horizontal simulation (without backfill layer).

4.5 WP3 – Achievements and implications for the KBS-3 safety case

Reliability of models

The three WP3 teams successfully developed reactive transport modelling tools that are able to describe and simulate the sulfide evolution (sources and sinks) and fluxes in the different parts of the near field of a KBS-3 repository (canister, buffer, backfill, rock-backfill interface, rock bolts).

The agreement between the results from the three WP3 teams shown in Table 4-2 is reasonable when considering the profound differences between the modelling tools. This gives confidence in the reliability of the modelling tools.

One of the outcomes of the inter-model comparison is the importance to check that the spatial discretisation of the calculation grid is small enough to capture the diffusion effects in the different media, that is, bentonite versus rock interfaces versus intact rock.

Donnan versus “ion-exchange” models

The results reported in Table 4-2 show that the Donnan models may result in a somewhat larger corrosion depth (a factor of approximately two), apparently caused by the increased diffusion of the FeHS^+ complex ion, as compared to the diffusion of sulfide ($\text{H}_2\text{S}(\text{aq})$ and HS^-). However, this effect is reversed in some simulation cases. In conclusion: it is not clear that Donnan equilibrium models would affect substantially the calculated corrosion depths.

1D versus 3D models

The inter-model comparison shows that vertical 1D models are not able to capture the main features of sulfide generation and transport in 3D. The horizontal 1D model developed by the ICC team results in a reasonable agreement of the calculated corrosion depth (~ 0.2 mm) with that obtained with the 3D model (0.5 mm). This difference is explained by the difference in the diffusion distances (buffer thickness): 0.83 m in the 1D model implemented by the ICC team and 0.35 m in the 3D model developed by the UniBern team.

Implications for the performance of the KBS-3 system

Although the aim of the WP3 was not to provide conclusions about the KBS-3 system, the results of the inter-model comparison indicate clearly that without an iron source in the backfill, and if the backfill is not able to suppress the activity of SRB, then the corrosion could be extensive. The assumption made in WP3 concerning the siderite (FeCO_3) contents of bentonite was based on Table 7-11 of Hellä et al. (2014), similar data is found for example in Table 5-10 of SKB (2011), and in Arcos et al. (2003). If the iron in the backfill is instead present as an Fe(III) oxide, its reduction by sulfide is also a possible process, but this was not included in the WP3 modelling.

5 Overall conclusions

The reported collaboration project includes studies of different character and complexity from laboratory and field experiments to modelling tasks. A short summary of the most important findings and conclusion from each study are given in the bullet list below.

Leaching experiments

- Metallic and organic materials in the borehole equipment can provide electron donors to stimulate sulfide production by SRB.
- Sulfide production favoured by these and similar materials may cause high concentrations of sulfide during the construction of the repository. For these reasons, the choice of materials in boreholes and possibly also in some parts of tunnel installations needs to be reconsidered.

Development of gas sampling equipment and sampling methods

- The dissolved gas concentrations in groundwater are influenced by the sampling conditions in the borehole i.e. flushed volume before sampling, pressure drop during sampling, possible corrosion of metal parts in the borehole equipment etc.
- Regular routine sampling of groundwater for determinations of dissolved gas require manageable equipment, and repeatable conditions and procedure. It is recommendable with as small pressure drop as possible although it may be impossible to prevent loss of H₂ gas.

GAME

- Matrix pore water acts as a storage for gases and when intact bedrock is disturbed by drilling or excavation the gas will be released. The increase in H₂ may cause increased SRB activity and consequently elevated sulfide concentrations. However, after the rapid release of matrix porewater gases into groundwater after disturbance, the transport of gases is probably limited by diffusion rates in the rock matrix, and the dissolved concentrations in groundwater reach certain gas-specific levels depending on the prevailing conditions, e.g., hydrostatic pressure and salinity as well as the availability/consumption of electron donors/acceptors for microbial metabolism. Thus, probably also sulfide concentrations will reduce with time.

FRED

- Microbial reduction of Fe³⁺ was observed in the pressure cells that were supplemented with iron silicates from Olkiluoto rocks.
- Dissolved sulfide can generate a release of Fe²⁺ without the involvement of bacteria (i.e. initial microbial production of sulfide by SRB is disregarded).

Sulfur minerals in the bentonite

- There is no dissolution of sulfur containing minerals in the clay.
- Bentonite seems to lower the sulfide concentration in solution. This supports the suggestion that the equilibrium concentration of sulfide in a solution in contact with bentonite is low.

Threshold buffer densities

- There are threshold densities above which microbial sulfide producing activity is suppressed. This density varies between different clays.
- The threshold buffer densities will have impacts on the repository design as well as on the choice of clay material.

FaTSu

- Organic matter, sulfate, and iron, among others can be dissolved from the compacted bentonites into sand layer solutions.
- Organic matter in bentonites can sustain activity of added as well as bentonite borne SRB and other microbes (e.g. methanogens). The bentonites can immobilize the formed sulfide through precipitation with iron.

Integrations for the safety case

- Reactive transport modelling tools that are able to describe and simulate the sulfide evolution (sources and sinks) and fluxes in the different parts of the near field of a KBS-3 repository were developed.
- The inter-model comparison revealed that vertical 1D models are not always able to capture the main features of sulfide generation and transport in 3D. It was noted that the spatial discretisation of the calculation grid must be small enough to capture the diffusion effects in the different media. No clear conclusion could be drawn on that Donnan equilibrium models would affect substantially the calculated corrosion depths.
- Although the aim of the WP3 was not to provide conclusions about the KBS-3 system, the results of the inter-model comparison clearly indicate that the assumptions on SRB activity and contents of Fe(II) in the clay material are important for the formation and transport of sulfides, and thus the resulting corrosion depth.

The Integrated Sulfide Project has thus pointed to the difference in different clays to encompass microbial activity, as well as the need for a more thorough understanding of the form and role of iron in the bentonite. In addition, monitoring of the gas inventory in the rock matrix is important as available gases may provide electron donors for sulfate reduction.

References

SKB's (Svensk Kärnbränslehantering AB) publications can be found at www.skb.com/publications.
Posiva's publications can be found at <http://posiva.fi/en/databank>.

- Arcos D, Bruno J, Karnland O, 2003.** Geochemical model of the granite–bentonite–groundwater interaction at Äspö HRL (LOT experiment). *Applied Clay Science* 23, 219–228.
- Bell E, Lamminmäki T, Pitkänen P, Bernier-Latmani R, 2020.** Microbial metabolism resulting from the mixing of sulfate-rich and methane-rich deep Olkiluoto groundwaters in drillholes OL-KR11, OL-KR13 and OL-KR46. Posiva Working Report 2020-2, Posiva Oy.
- Bengtsson A, Edlund J, Hallbeck B, Heed C, Pedersen K, 2015.** Microbial sulfide-producing activity in MX-80 bentonite at 1 750 and 2 000 kg m⁻³ wet density. SKB R-15-05, Svensk Kärnbränslehantering AB.
- Bengtsson A, Blom A, Hallbeck B, Heed C, Johansson L, Ståhlén J, Pedersen K, 2017a.** Microbial sulfide-producing activity in water saturated MX-80, Asha and Calcigel bentonite at wet densities from 1 500 to 2 000 kg m⁻³. SKB TR-16-09, Svensk Kärnbränslehantering AB.
- Bengtsson A, Blom A, Johansson L, Taborowski T, Eriksson L, Pedersen K, 2017b.** Bacterial sulfide-producing activity in water saturated iron-rich Rokle and iron-poor Gaomiaozi bentonite at wet densities from 1 750 to 1 950 kg m⁻³. SKB TR-17-05, Svensk Kärnbränslehantering AB.
- Bengtsson A, Blom A, Hallbeck B, Taborowski T, Johansson L, Morsing J, Chukharkina A, Pedersen K, 2019.** The effects of biofilm formation on deep groundwater chemistry and microbial sulfide production. Summary report. SKB R-19-19, Svensk Kärnbränslehantering AB.
- Bergaya F, Theng B K G, Lagaly G (eds), 2006.** Handbook of clay science. Amsterdam: Elsevier.
- Brookshaw D R, Lloyd J R, Vaughan D J, Patrick R A D, 2014.** Bioreduction of biotite and chlorite by a *Shewanella* species. *American Mineralogist* 99, 1746–1754.
- Byegård J, Selnert E, Tullborg E-L, 2008.** Bedrock transport properties. Data evaluation and retardation model. Site descriptive modelling SDM-Site Forsmark. SKB R-08-98, Svensk Kärnbränslehantering AB.
- Charlton S R, Parkhurst D L, 2011.** Modules based on the geochemical model PHREEQC for use in scripting and programming languages. *Computers & Geosciences* 37, 1653–1663.
- Chukharkina A, Blom A, Pedersen K, 2016.** Release of H₂ and organic compounds from metallic and polymeric materials used to construct stationary borehole equipment. SKB R-16-01, Svensk Kärnbränslehantering AB.
- Chukharkina A, Blom A, Pedersen K, 2017.** Microbial sulfide production during consumption of H₂ and organic compounds released from stationary borehole equipment. SKB R-16-17, Svensk Kärnbränslehantering AB.
- Cord-Ruwisch R, 1985.** A quick method for the determination of dissolved and precipitated sulfides in cultures of sulfate-reducing bacteria. *Journal of Microbiological Methods* 4, 33–36.
- Drake H, Hallbeck L, Pedersen K, Rosdahl A, Tullborg E-L, Wallin B, Sandberg B, Blomfeldt T, 2014.** Investigation of sulfide production in core-drilled boreholes in Äspö Hard Rock Laboratory. Boreholes KA3110A, KA3385A and KA3105A. SKB TR-13-12, Svensk Kärnbränslehantering AB.
- Edlund J, Rabe L, Bengtsson A, Hallbeck B, Eriksson L, Johansson J, Johansson L, Pedersen K, 2016.** Understanding microbial production of sulfide in deep Olkiluoto groundwater compilation and evaluation of three consecutive Sulfate Reduction Experiments (SURE) performed in 2010–2014. Posiva Working Report 2016-48, Posiva Oy.
- Eichinger F, Hämmerli J, Waber H N, Diamond L W, Smellie J A T, 2013.** Chemistry and dissolved gases of matrix pore water and fluid inclusions in Olkiluoto bedrock from drillhole ONK-PH9. Posiva Working Report 2011-63, Posiva Oy.

- Eichinger F, Rufer D, Waber H N, 2018.** Matrix porewater and gases in porewater in Olkiluoto bedrock from drilling OL-KR56. Posiva Working Report 2018-07, Posiva Oy.
- Frindte K, Allgaier M, Grossart H, Eckert W, 2015.** Microbial responses to experimentally controlled redox transitions at the sediment water interface. PLoS ONE 10. doi:10.1371/journal.pone.0143428
- Gimeno M J, Auqué L F, Gómez J B, Acero P, 2008.** Water–rock interaction modelling and uncertainties of mixing modelling. SDM-Site Forsmark. SKB R-08-86, Svensk Kärnbränslehantering AB.
- Hallbeck L, Pedersen K, 2008a.** Explorative analysis of microbes, colloids and gases. SDM-Site Forsmark. SKB R-08-85, Svensk Kärnbränslehantering AB.
- Hallbeck L, Pedersen K, 2008b.** Characterization of microbial processes in deep aquifers of the Fennoscandian Shield. Applied Geochemistry 23, 1796–1819.
- Hammond G, Lichtner P, Mills R, 2014.** Evaluating the performance of parallel subsurface simulators: An illustrative example with PFLOTRAN. Water Resources Research, 50, 208–228.
- Hartley L, Hoek J, Swan D, Appleyard P, Baxter S, Roberts D, Simpson T, 2013.** Hydrogeological modelling for assessment of radionuclide release scenarios for the repository system 2012. Posiva Working Report 2012-42, Posiva Oy.
- Haynes H M, Nixon S, Lloyd J R, Birgersson M, 2019.** Verification of microbial sulfide-producing activity in Calcigel bentonite at saturated densities of 1 750 and 1 900 kg m⁻³. SKB P-19-07, Svensk Kärnbränslehantering AB.
- Hellä P, Pitkänen P, Löfman J, Partamies S, Vuorinen U, Wersin P, 2014.** Safety case for the disposal of spent nuclear fuel at Olkiluoto. Definition of reference and bounding groundwaters, buffer and backfill porewaters. Posiva 2014-04, Posiva Oy.
- Idiart A, Coene E, Bagaria F, Román-Ross G, Birgersson M, 2019.** Reactive transport modelling considering transport in interlayer water. New model, sensitivity analyses and results from the Integrated Sulfide Project inter-model comparison exercise. SKB TR-18-07, Svensk Kärnbränslehantering AB.
- Jin Q, Roden E E, Giska J R, 2013.** Geomicrobial kinetics: Extrapolating laboratory studies to natural environments. Geomicrobiology Journal 30, 173–185.
- Johansson L, Stahlén J, Taborowski T, Pedersen K, Lukkari S, Marmo J, 2019.** Microbial release of iron from Olkiluoto rock minerals. Posiva Working Report 2018-30, Posiva Oy.
- Kietäväinen R, Ahonen L, Pedersen K, 2017.** Interim report on deep gases and sulphur compounds as biogeochemical energy sources in crystalline rock. Deliverable D2.3. MIND. Euratom research and training programme 2014–2018 under grant agreement No. 661880.
- King, 2008.** Mixed-potential modelling of the corrosion of copper in the presence of sulfide. Posiva Working Report 2007-63, Posiva Oy.
- King F, Kolář M, 2019.** Copper Sulfide Model (CSM). Model improvements, sensitivity analyses, and results from the Integrated Sulfide Project inter-model comparison exercise. SKB TR-18-08, Svensk Kärnbränslehantering AB.
- Kristjansson J K, Schönheit P, Thauer R K, 1982.** Different K_s values for hydrogen of methanogenic bacteria and sulfate reducing bacteria: Explanation for the apparent inhibition of methanogenesis by sulfate. Archives of Microbiology 131, 278–282.
- Kärki A, Paulamäki S, 2006.** Petrology of Olkiluoto. Posiva 2006-02, Posiva Oy.
- Lamminmäki T, Eichinger F, Sunberg J, Stoor J, Hansson K, Svensson T, Vainikka P, 2021.** The Gas Monitoring Experiment in Olkiluoto underground drillhole ONK-KR17: Extracting gases from crystalline rock matrix. Posiva Working Report 2021-01, Posiva Oy.
- Maanoja S, Lakaniemi A, Lehtinen L, Salminen L, Auvinen H, Kokko M, Palmroth M, Muuri E, Rintala J, 2020a.** Compacted bentonite as a source of substrates for sulfate-reducing microorganisms in a simulated excavation-damaged zone of a spent nuclear fuel repository. Applied Clay Science 196. doi:10.1016/j.clay.2020.105746

- Maanoja S, Lehtinen L, Salminen L, Lakaniemi A, Auvinen H, Kokko M, Palmroth M, Rintala J, 2020b.** Simulating the dissolution of organic compounds and sulfate from compacted clay and growth of sulfate-reducing bacteria in an excavation-damaged zone (FaTSu theme 3). Internal memorandum POS-029982, Posiva Oy.
- Maia F, Puigdomenech I, Molinero J, 2016.** Modelling rates of bacterial sulfide production using lactate and hydrogen as energy sources. SKB TR-16-05, Svensk Kärnbränslehantering AB.
- Masurat P, Eriksson S, Pedersen K, 2010.** Microbial sulfide production in compacted Wyoming bentonite MX-80 under *in situ* conditions relevant to repository for high-level radioactive waste. Applied Clay Science 47, 58–64.
- Mayhew L E, Ellison E T, McCollom T M, Trainor T P, Templeton A S, 2013.** Hydrogen generation from low-temperature water-rock reactions. Nature Geoscience 6, 478–484.
- Motamedi M, Pedersen K, 1998.** *Desulfovibrio aespoensis* sp. nov., a mesophilic sulfate-reducing bacterium from deep groundwater at Aspö hard rock laboratory, Sweden. International Journal of Systematic Bacteriology 48, 311–315.
- Nardi A, Idiart A, Trincherio P, de Vries L. M, Molinero J, 2014.** Interface COMSOL–PHREEQC (iCP), an efficient numerical framework for the solution of coupled multiphysics and geochemistry. Computers & Geosciences 69, 10–21.
- Nethe-Jaenchen R, Thauer R K, 1984.** Growth yields and saturation constant of *Desulfovibrio vulgaris* in chemostat culture. Archives of Microbiology 137, 236–240.
- Nilsson A-C, Pedersen K, Hallbeck B, Johansson J, Tullborg E-L, 2017.** Development and testing of gas samplers in tunnel environments. SKB R-16-16, Svensk Kärnbränslehantering AB.
- Parkhurst D L, Appelo C A J, 2013.** Description of input and examples for PHREEQC Version 3 – A computer program for speciation, batch-reaction, one-dimensional transport, and inverse geochemical calculations. Techniques and Methods 6–A43, U.S. Geological Survey, U.S. Geological Survey, Denver, Colorado.
- Pedersen K, 2012a.** Subterranean microbial populations metabolize hydrogen and acetate under *in situ* conditions in granitic groundwater at 450 m depth in the Äspö Hard Rock Laboratory, Sweden. FEMS Microbiology Ecology 81, 217–229.
- Pedersen K, 2012b.** Influence of H₂ and O₂ on sulfate-reducing activity of a subterranean community and the coupled response in redox potential. FEMS Microbiology Ecology 82, 653–665.
- Pedersen K, Bengtsson A, Blom A, Johansson L, Taborowski T, 2017.** Mobility and reactivity of sulfide in bentonite clays – Implications for engineered bentonite barriers in geological repositories for radioactive wastes. Applied Clay Science 146, 495–502.
- Pekala M, Alt-Epping P, Wersin P, 2019.** 3D and 1D dual-porosity reactive transport simulations – Model improvements, sensitivity analyses, and results from the integrated sulfide project inter-model comparison exercise. Posiva Working Report 2018-31, Posiva Oy.
- Penttinen T, Wichmann A, Ripatti K, Nummela J, Yli-Rantala E, Wendling L, Partamies S, Lamminmäki T, Pitkänen P, Vuorio M, Ylöstalo R, 2019.** Results of monitoring at Olkiluoto in 2018, Hydrogeochemistry. Posiva Working Report 2019-44, Posiva Oy.
- Pitkänen P, Partamies S, 2007.** Origin and implications of dissolved gases in groundwater at Olkiluoto. Posiva 2007-04, Posiva Oy.
- Posiva 2012a.** Olkiluoto site description 2011. Posiva 2011-02, Posiva Oy.
- Posiva, 2012b.** Safety case for the disposal of spent nuclear fuel at Olkiluoto – Description of the disposal system 2012. Posiva 2012-05, Posiva Oy.
- Posiva, 2013a.** Safety case for the disposal of spent nuclear fuel at Olkiluoto – Performance assessment 2012. Posiva 2012-04, Posiva Oy.
- Posiva, 2013b.** Safety case for the disposal of spent nuclear fuel at Olkiluoto – Models and data for the repository system 2012. Posiva Report 2013-01, Posiva Oy.

Posiva SKB, 2017. Safety functions, performance targets and technical design requirements for a KBS-3V repository. Conclusions and recommendations from a joint SKB and Posiva working group. Posiva SKB Report 01, Posiva Oy, Svensk Kärnbränslehantering AB.

Rosdahl A, Pedersen K, Hallbeck L, Wallin B, 2011. Investigation of sulfide in core drilled boreholes KLX06, KAS03 and KAS09 at Laxemar and Äspö. Chemical-, microbiological- and dissolved gas data from groundwater in four borehole sections SKB P-10-18, Svensk Kärnbränslehantering AB.

Saario T, Ikonen A, Keto P, Kirkkomäki T, Kukkola T, Nieminen J, Raiko H, 2013. Design of the disposal facility 2012. Posiva Working Report 2013-17, Posiva Oy.

Seitsamo-Ryynänen M, Karhu J, 2020. Investigations of low temperature mineral precipitates at Kyläniemi KYL-KR1, KYL-KR2 and Olkiluoto OL-KR46, OL-KR58. Posiva Working Report 2020-16, Posiva Oy.

SKB, 2011. Long-term safety for the final repository for spent nuclear fuel at Forsmark. Main report of the SR-Site project. SKB TR-11-01, Svensk Kärnbränslehantering AB.

Stams A J M, Oude Elferink S J W H, Westerman P, 2003. Metabolic interaction between methanogenic consortia and anaerobic respiring bacteria. In Ahring B K (ed). Biomethanation I. Berlin: Springer.

Svensson D, Dueck A, Nilsson U, Olsson S, Sandén T, Lydmark S, Jägerwall S, Pedersen K, Hansen S, 2011. Alternative buffer material. Status of the ongoing laboratory investigation of reference materials and test package 1. SKB TR-11-06, Svensk Kärnbränslehantering AB.

Svensson D, Lundgren C, Wikberg P, 2017. Experiments with bentonite and sulfide – results from experiments 2013–2016. SKB P-16-31, Svensk Kärnbränslehantering AB.

Tullborg E-L, Smellie J, Nilsson A-C, Gimeno M J, Auqué L F, Brüchert V, Molinero J, 2010. SR-Site – Sulfide content in the groundwater at Forsmark. SKB TR-10-39, Svensk Kärnbränslehantering AB.

Tuomi P, Lamminmäki T, Pedersen K, Miettinen H, Bomberg M, Bell E, Bernier-Latmani R, Pitkänen P, 2020. Conceptual model of microbial effects on hydrogeochemical conditions at the Olkiluoto site. Posiva 2020-03, Posiva Oy.

Vaittinen T, Hurmerinta E, Nummela J, Pentti E, Tammisto E, Turku J, Karvonen T, 2019. results of monitoring at olkiluoto in 2018 – Hydrology and hydrogeology. Posiva Working Report 2019-43, Posiva Oy.

Wersin P, Alt-Epping P, Pitkänen P, Román-Ross G, Trincherro P, Molinero J, Smith P, Snellman M, Filby A, Kiczka M, 2014. Sulfide fluxes and concentrations in the spent nuclear fuel repository at Olkiluoto. Posiva 2014-01, Posiva Oy.

Simulation cases for WP3

This appendix describes the Base Case and the variant cases agreed by the WP3 managers and modeling teams. It is therefore similar to Appendix D in King and Kolář (2019).

The following conditions were applied to the WP3 simulations:

- Models may use a subset of the reactions in version 9b of Thermochemie database (www.thermochemie-tdb.com).
- Chemical equilibria may be represented by equivalent kinetically-controlled forward and backward reaction.
- Because pyrite (FeS_2) is known to form irreversibly, chemical equilibrium with pyrite will be *excluded* from the calculations. An additional reason for this is that dissolution-precipitation reactions involving Fe(II)-monosulfides result in higher sulfide equilibrium concentrations, which in turn will result in pessimistic sulfide corrosion consequences.
- Mackinawite (rather than amorphous iron(II) monosulfide) will be used to control the solubility of sulfide and Fe(II).
- Redox disequilibrium: to simulate microbial sulfate reduction, redox equilibrium between SO_4^{2-} and HS^- must be disabled. To simulate H_2 utilisation by SRB, redox equilibrium involving H_2 must also be disabled.
- Diffusion coefficients in aqueous solution and effective diffusion coefficients for anion and neutral species or cations will be defined, if needed tortuosities should be derived from these. If temperature effects are to be considered, then activation energies for the diffusion coefficients will also be defined. For models that cannot use species-specific diffusion coefficients average values should be used.
- Threshold relative humidity expressions for interfacial electrochemical reactions will be used only if saturation effects are to be included in any variant case.
- Temperature coefficients will be used if temperature changes are included in a given variant case.

A1 Base Case

The Base Case includes the most important sulfide-related processes that are to be handled by each of the models developed within WP3. There are, however, differences in the way these processes are implemented in the models because of conceptual differences in the models (for example Donnan equilibrium).

The initial conditions for the Base Case are a *hypothetical state*: fully saturated repository, no remaining O_2 , thermally equilibrated to 25 °C. In the Base Case the temperature in all parts of the system was 25 °C.

The simulation time for the Base Case is 100 000 years. The rationale behind this choice was that it was expected that the initial transient conditions caused by the presence of bentonite accessory minerals (such as gypsum and sulfides) will stabilise in time periods shorter than 100 000 years.

Geometry

The geometry of a typical KBS-3 repository is shown in Figure A-1, see also (Hellä et al. 2014, Posiva 2013b, Saanio et al. 2013). The size of the intact rock domain was chosen to be large enough to act as a diffusion sink, around three or more times the thickness of the rock-backfill interface, for example 5 m. The minimum spacing between deposition holes is 7.5 m, and therefore a 3D model should include 7.5 m of backfilled tunnel.

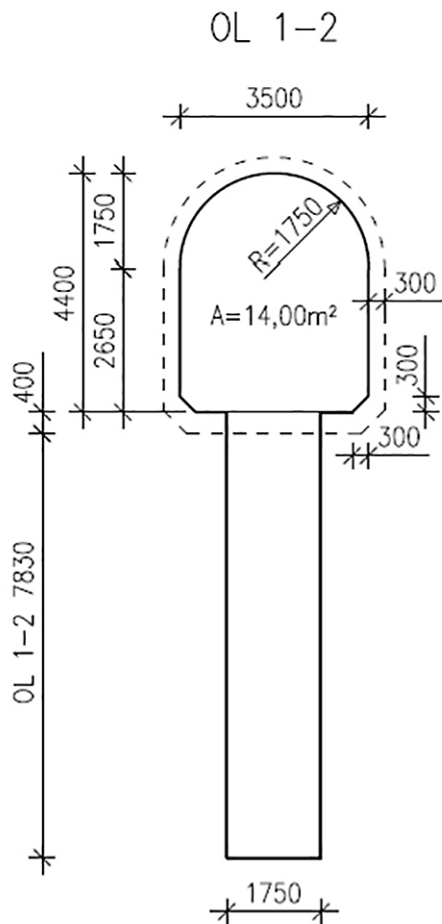


Figure A-1. Dimensions of the near-field for the Base Case (Saanio et al. 2013, Figure 3-5). The canister (not shown in this figure) in the Base Case is 1.05 m in diameter and 4.8 m high, and the bottom of the canister is at 0.5 m from the bottom of the deposition hole.

Intact rock

In the Base Case intact rock is included as an ECPM (Equivalent Continuous Porous Medium) representation of the rock matrix and fractures. The porosity should correspond to a fractured rock, i.e., it must include the fracture porosity, see table below. Transport of substances between the intact rock and the backfill/buffer/rock-backfill interface is by diffusion. In a variant case fractures are considered explicitly.

- Groundwater. The sulfate-rich brackish water defined in Hellä et al. (2014) is the reference groundwater. To simplify matters sulfur concentrations are set to zero at the start of the simulations. The concentration of sodium or calcium might have to be adjusted in some models to achieve electrical neutrality.
- SO_4 concentration in groundwater is initially zero. This is a simplification for the Base Case. The sulfate concentration in the rock groundwater will vary with time because of diffusion from the backfill or buffer into the rock.
- Sulfide concentration in groundwater is initially zero. This is a simplification for the Base Case. The sulfide concentration in the rock groundwater will vary with time because of diffusion from the backfill into the rock. Equilibrium precipitation of iron(II) sulfide in the rock matrix assuming $\text{pH} = 7.6$ and $[\text{Fe(II)}]_{\text{TOT}} = 5.7 \times 10^{-6} \text{ M}$. These values correspond to the sulfate-rich brackish water in Table 6-3 in Hellä et al. (2014).

- The concentration of reductants (H₂, hydrocarbons, other organic matter) in the groundwater was set initially to zero in the Base Case. The concentration of organic matter and other components in the intact rock will vary with time because of diffusion from the backfill or buffer into the rock.
- Initial concentration of Fe(II) = 5.7 × 10⁻⁶ M assumed in the groundwater in the intact rock. This Fe(II) may diffuse into the rock-backfill interface, into the backfill and into the buffer. This value is kept constant at the outer rock boundaries.
- Initial O₂ concentration in the groundwater set to zero.
- Initial concentration of Cl⁻ = 0.1131 M (4010 mg L⁻¹) assumed in the groundwater in the intact rock. The value corresponds to the sulfate-rich brackish water in Table 6-3 in Hellä et al. (2014). This chloride may diffuse into the rock-backfill interface, into the backfill and into the buffer. This value is kept constant at the outer rock boundaries.
- The initial amount of sulfide minerals in the rock matrix (for example pyrite) is simplified to be zero.
- No groundwater flow around the modelled system (deposition tunnel etc).
- Diffusion coefficients: see Table A-1 (Posiva 2013b).
- Constant boundary properties (fixed groundwater concentrations) are assumed at a distance of 5 m from the backfill/buffer interfaces.
- No SRB activity in the intact rock.
- No sorption processes considered in the intact rock.

Table A-1. Porosity and diffusion parameters for the intact rock.

Geosphere data (Posiva 2013b): Other flow-related parameters.		
Total porosity (θ)	0.515 %	Matrix porosity and interconnected porosity to be used in an ECPM representation of the rock (matrix and fractures) From the rock matrix porosity (0.5 %) and a kinematic porosity of 0.15 % on p 22, Table 2-5 and p 57, Table 4-2 of Hartley et al. (2013)
Diffusion accessible porosity (Rock matrix porosity)	0.5 %	Groundwater flow modelling in Hartley et al. (2013); cited in Posiva (2013b, Section 6.1, Section 7.8, Table 7-13)
Molecular diffusion coefficient in water (D _w)	1.0 × 10 ⁻⁹ m ² /s	Posiva (2013b, Table I-1)
Effective diffusion coefficient (D _e) for intact rock matrix	6 × 10 ⁻¹⁴ m ² /s	Posiva (2013b, Table I-1)
Effective diffusion coefficient (D _e) for fractured rock	2 × 10 ⁻¹³ m ² /s	Estimated in this project to provide diffusion in a ECPM representation of the intact rock (rock matrix and fractures)

Rock-backfill interface and rock-buffer interface (thermally spalled rock volume)

The rock-tunnel interface (**RTI**), and the rock-deposition hole interface (**RDI**) are represented as volumes of ECPM (Equivalent Continuous Porous Medium). The RTI and the RDI are arbitrarily represented by a porosity that is about 4 times higher than the porosity of the intact rock, see Table A-2. The thickness of the RDI is 0.1 m around deposition holes and for the RTI it is 0.4 m below the tunnel floor and 0.3 m on other parts of the tunnel perimeter. When considering 7.5 m of backfilled tunnel, the area of the RTI in contact with the tunnel is 110.1 m², and its volume is 35.4 m³, for the RDI the area in contact with the deposition hole is 45.3 m² and the volume is 2.45 m³.

Table A-2. Parameters for the rock-backfill and rock-buffer interfaces.

UNDERGROUND OPENINGS DATA (Posiva 2013)		
Rock-backfill interface (RTI)		
Thickness, except below tunnel floor	0.3 m	Agreed in this project
Thickness below tunnel floor	0.4 m	Section 5.1.5 and Table E-1 in Hartley et al. (2013)
Hydraulic conductivity	2.5×10^{-8} m/s	p 91 and p 234 in Hartley et al. (2013)
Porosity	1 %	Table E-1 in Hartley et al. (2013)
Effective diffusion coefficient (D_e) for fractured rock	5×10^{-13} m ² /s	Estimated as $D_e = D_w F_f$ with the formation factor estimated using an Archie's law: $F_f = 0.71 \theta^{1.58}$ (see Figure 3-5 in Byegård et al. 2008) and $\theta = 0.01$
Damaged rock around deposition holes (RDI)		
Thickness of affected area	0.1 m	p 74 and Table E-1 in Hartley et al. (2013)
Hydraulic conductivity	2.5×10^{-8} m/s	p 234 in Hartley et al. (2013)
Porosity of affected area	2 %	Table E-1 in Hartley et al. (2013)
Effective diffusion coefficient (D_e) for fractured rock	1.5×10^{-12} m ² /s	Estimated as $D_e = D_w F_f$ with the formation factor estimated using an Archie's law: $F_f = 0.71 \theta^{1.58}$ (see Figure 3-5 in Byegård et al. 2008) and $\theta = 0.02$

- The same groundwater as for the intact rock is initially present in the fragmented rock. The sulfate-rich brackish water defined in Table 6-3 in Hellä et al. (2014) is the reference water. To simplify matters sulfur concentrations are set to zero initially.
- No metals such as rock bolts and stretch metal are present in the Base Case. Metal corrosion is a source of H₂, which will be used by SRB, and Fe(II), which could remove sulfide through precipitation.
- Initially there are no reductants in these interface volumes (DOC, H₂, etc). Out- and in-diffusion of substances (SO₄, organic carbon, H₂, etc) from/to the backfill or buffer and to the intact rock.
- Sulfate and organic matter is provided by diffusion from the backfill (dissolution of gypsum). Hydrogen (H₂), originating from the sulfide corrosion of the canister, reaches these repository volumes by diffusion through the backfill and/or the buffer.
- Solid sulfide (pyrite and mackinawite) initial concentration assumed to be zero.
- FeS (mackinawite) precipitation included either as an equilibrium or kinetic process, where Fe(II) diffuses from/to the intact rock.
- Diffusion coefficients set to those of the intact rock.
- No sorption processes considered in the fragmented rock.
- SRB activity is expected to be possible in these repository volumes.
 - **Biomass:**
 - Fraction of SRB – the proportion between the total number of microorganisms and SRB is quite uncertain; in Table 6 of Hallbeck and Pedersen (2008b) 35 % of the bacteria are SRB in borehole KJ0052F01, while Figures 1 and 2 in Pedersen (2012a) indicate 20 % of SRB, but the data in Table 1 of Pedersen (2012b) suggest 50 % SRB. For WP3 simulations a value of 20 % may be used.

- Attached cells on fracture surfaces – at Äspö, $\approx 10^{5.6}$ cells/cm² were found on glass surfaces (Pedersen 2012a). One can assume the same cell density on fracture surfaces. For the RTI with 1 % porosity, the volume occupied by “fractures” is 5 L, and if the average “fracture” aperture is 0.1 mm, then the area of the fractures should be at least 100 m² per m³ of ECPM, resulting in 8.0×10^{10} attached SRB cells per m³ of ECPM. For the RDI (2 % porosity) the fracture surface is at least 300 m² per m³ of ECPM, resulting in 2.4×10^{11} attached SRB cells per m³ of ECPM.
- Suspended cells in groundwater – the number microorganisms is based on a TNC of 10^5 cells/mL, see Figure 2(b) in Pedersen (2012b). For the RTI with 1 % porosity, the volume occupied by “fractures” is 5 L, resulting in 1×10^8 suspended SRB cells per m³ of ECPM. For the RDI (2 % porosity) the fracture volume is 15 L per m³ of ECPM, resulting in 3×10^8 suspended SRB cells per m³ of ECPM.
- Biomass composition – to transform cells to mg of biomass, an average cell dry mass of 5×10^{-13} g will be used in the Base Case, and an average formula of C₅H₇O₂N (113.115 g/mol).
- Total biomass – from the data above, the biomass concentration (in moles) for the RTI is calculated to be 3.54×10^{-4} mol m⁻³ of ECPM (3.54×10^{-5} mol L⁻¹_w), and for the RDI it is 1.06×10^{-3} mol m⁻³ of ECPM (5.31×10^{-5} mol L⁻¹_w).

The corresponding biomass concentrations (in mass) for the RTI is 4.01×10^{-3} g L⁻¹_w and for the RDI it is 6.01×10^{-3} g L⁻¹_w. The biomass is kept constant as a function of time.

- **Rate:** Monod kinetics may be written as

$$\frac{d[\text{SO}_4^{2-}]}{dt} = -\frac{d[\text{HS}^-]}{dt} = -[X] \cdot k_{max} \frac{[\text{H}_2]}{K_{\text{H}_2} + [\text{H}_2]} \frac{[\text{SO}_4^{2-}]_{Tot}}{K_{\text{SO}_4} + [\text{SO}_4^{2-}]_{Tot}}$$

where $[X]$ is the biomass concentration given above. If the process involves organic matter, then $[org]$ and K_{org} should be used instead of $[\text{H}_2]$ and K_{H_2} . To calculate the concentration of organic matter, $[org]$, a stoichiometric composition equivalent to that of acetate (C₂H₄O₂) may be used. If needed, first order kinetics (on biomass) for SO₄ reduction may be assumed. Monod kinetics gives a slower reduction rate at low concentrations of substrates, and therefore, a first order kinetics should be pessimistic.

The Monod rate equation from Jin et al. (2013) for SO₄ reduction using organic matter (acetate) will be used in the Base Case, although the composition of the organic matter is not specified in the Base Case. Their Table 3 gives $k_{max} = 1.3 \times 10^{-6}$ mol (g biomass)⁻¹ s⁻¹ (equivalent to $k_{max} = 1.5 \times 10^{-4}$ mol SO₄ (mol biomass)⁻¹ s⁻¹). For SO₄ reduction using H₂ as electron donor, the rate constants in the literature from laboratory studies are in the range $(1.6 \text{ to } 6.4) \times 10^{-5}$ mol SO₄ (mol biomass)⁻¹ s⁻¹ (Maia et al. 2016). In the Base Case the fastest rate will be used, $k_{max} = 6.4 \times 10^{-5}$ mol SO₄ (mol biomass)⁻¹ s⁻¹.

The maximum rates for organotrophic sulfate reduction are thus 5.2×10^{-9} mol SO₄/(L_w s) for the RTI and 7.8×10^{-9} mol SO₄/(L_w s) for the RDI. For the chemotrophic (H₂) sulfate reduction, the maximum rates are 2.3×10^{-9} mol SO₄/(L_w s) for the RTI and 3.4×10^{-9} mol SO₄/(L_w s) for the RDI.

Half saturation constants: The reported values of K_{H_2} are between 1.3 and 20 μM (Maia et al. 2016) and a value of 4×10^{-6} M will be adopted for the Base Case. The value of $K_{\text{SO}_4} = 1 \times 10^{-5}$ M (Nethe-Jaenchen and Thauer 1984) will be used; note that Jin et al. (2013, Table 3) selected $K_{\text{SO}_4} = 6.8 \times 10^{-5}$ M. For K_{org} the value 5×10^{-6} M will be used, corresponding to that of acetate when used as reductant (Jin et al. 2013, Table 3).

- **Stoichiometry:** The sulfate reduction reaction will have the following overall stoichiometry; $2(\text{CH}_2\text{O}) + \text{SO}_4^{2-} \rightarrow \text{HS}^- + 2\text{HCO}_3^- + \text{H}^+$. Neither biomass growth nor decay will be included in the Base Case.

Backfill

As stated above, a *hypothetical initial state* (i.e., fully saturated backfill, no remaining O₂, thermally equilibrated to 25 °C) will be used. In the Base Case the backfill is modelled as a medium that is initially homogeneous.

- Porosity and diffusion coefficients have been agreed in the project, see Table A-3.
- Dry density defined in Hellä et al. (2014, Table 7-11), i.e. 1 720 kg m⁻³.
- Mineral composition defined as those in Hellä et al. (2014, Table 7-11). Initial amount of gypsum also set to the values reported in Hellä et al. (2014, Table 7-11). Considering the porosity and dry density defined above this gives: 189.8 (mol gypsum) · m⁻³ and 467.2 (mol calcite + dolomite) · m⁻³.
- Availability of iron(II) phases to produce and precipitate sulfide set to Hellä et al. (2014, Table 7-11). Considering the porosity and dry density defined above this gives: 163.3 (mol FeCO₃) · m⁻³. FeS (mackinawite) and FeCO₃ precipitation/dissolution included.
- Porewater composition from Posiva (2013b, Appendix F, Table F-2, column “Reference porewaters – Brackish water”).
- Dimensions of the deposition tunnel: see Section 4-1. The cross-section area is 14 m², with a length of 7.5 m the total volume is 105 m³.
- SRB activity absent in the Base Case.
- For the amount of **organic carbon**, the limit value (1 wt%) reported in Posiva (2012b) will be used, but only 10 % of the organic carbon will be assumed to be mobile (soluble) and degradable by SRB (i.e. 0.1 wt% of carbon). Considering the porosity and dry density defined above this gives: 143.2 (mol organic C) m⁻³. The availability of organic carbon will be varied in a variant case. The concentration of DOC in the porewater will be maintained at 2 (mg of C) L⁻¹, by an equilibrium reaction, until all degradable organic carbon (0.1 % of the backfill in weight) is exhausted. This concentration of DOC is within the values reported by the FaTSu project (see Section 3.4.2). Because in the Base Case SRB activity is absent in the backfill, the DOC may diffuse to the buffer (where SRB activity is also absent), to the RTI and to the RDI (where SRB activity is present).

Table A-3. Backfill porosity and diffusivity.

BACKFILL DATA	
Effective diffusion coefficients and porosity in backfill; values agreed upon by the members of the project. The temperature is 25 °C.	
All neutral species and ions	
Pore diffusivity D _p (m ² /s)	5.00 × 10 ⁻¹¹
ε (physical bulk porosity)	43 %
Effective diffusivity D _e (m ² /s) = (D _p × ε)	2.15 × 10 ⁻¹¹

Buffer

As stated above, a *hypothetical initial state* (i.e., fully saturated buffer, no remaining O₂, thermally equilibrated to 25 °C) will be used. In the Base Case the buffer is modelled as a medium that is initially homogeneous.

- Porosity and diffusion coefficients have been agreed in the project, see Table A-4.
- Dry density defined in Hellä et al. (2014, Table 7-5), i.e. 1 570 kg m⁻³.
- Porewater composition from Posiva (2013b, Appendix E, Table E-2, column “Reference porewaters – Brackish water”).

- Mineral composition defined as those in Hellä et al. (2014, Table 7-5). Initial amount of gypsum set to the values reported in Hellä et al. (2014, Table 7-5). Considering the porosity and dry density defined above this gives: $36.48 \text{ (mol gypsum)} \cdot \text{m}^{-3}$ and $327 \text{ (mol calcite+dolomite)} \cdot \text{m}^{-3}$.
- CEC (cation exchange capacity) from Posiva (2013b, Appendix E, Table E-2), i.e. 2873 meq L^{-1} .
- Siderite is not considered in the initial composition so that the Fe concentration in the porewater ($1.1 \times 10^{-5} \text{ M}$) is not changed. Note that in order to compare single-porosity models with Donnan models, the CEC in the single-porosity model of the buffer must be equilibrated with the initial Fe(II) concentration ($1.1 \times 10^{-5} \text{ M}$). FeS (mackinawite) and FeCO_3 precipitation included.
- SRB activity absent.
- Dimensions: The volume is 14.6 m^3 .
- For the amount of organic carbon, the limit value (1 wt%) reported in Posiva (2012b) will be used, but only 10 % of the organic carbon will be assumed to be mobile (soluble) and degradable by SRB (i.e. 0.1 wt% of C). Considering the porosity and dry density defined above this gives: $130.7 \text{ (mol organic C)} \cdot \text{m}^{-3}$. The availability of organic carbon will be varied in a variant case. The concentration of DOC in the porewater will be maintained at 2 mg L^{-1} (mg of C), by an equilibrium reaction, until all degradable organic carbon (0.1 % of the buffer in weight) is exhausted. Because SRB activity is absent in the buffer, the DOC may diffuse to the backfill (where SRB activity is also absent in the Base Case), to the RTI and to the RDI (where SRB activity is present).

Table A-4. Some physical properties of the buffer.

BUFFER DATA	
Effective diffusion coefficient and porosity in buffer; values agreed upon by the project members. Grain density for the buffer 2760 kg/m^3. The temperature is $25 \text{ }^\circ\text{C}$.	
All neutral species and ions	
Pore diffusivity $D_p \text{ (m}^2\text{/s)}$	5.00×10^{-11}
ϵ (physical bulk porosity)	43 %
Effective diffusivity $D_e \text{ (m}^2\text{/s)} = (D_p \times \epsilon)$	2.15×10^{-11}

Canister

The canister corrosion will be either described fully, or depending on each model's shortcomings it may be treated as an ideal surface where sulfide will be converted according to: $2\text{Cu} + \text{HS}^- + \text{H}^+ \rightarrow \text{Cu}_2\text{S} + \text{H}_2(\text{aq})$. The hydrogen molecules thus formed will diffuse through the bentonite buffer. Assuming a perfect cylinder the surface area of the canister is 17.57 m^2 . The full corrosion model requires:

- Definition of interfacial electrochemical reactions.
- Standard potentials for interfacial electrochemical reactions (and their temperature dependence if temperature changes are considered).
- Interfacial rate constants for electrochemical reactions (and their activation energies if temperature changes are considered).
- Transfer coefficient α for each interfacial reaction from which the Tafel slope can be calculated.
- Number of electrons for each interfacial electrochemical reaction.

Summary of input data

See Table A-5.

Table A-5. Summary of parameters defining the Base Case.

Domain	Groundwater/Porewater	Minerals (equilibrium)		Kinetic reactions	Cation exchange	Transport Properties	Dimensions
		Primary	Secondary				
Intact rock	B-SO ₄ (Table 6-3 in Hellä et al. 2014) SO ₄ ²⁻ and sulfide concs. = 0 Ca or Na: charge balance [Fe(II)] _{TOT} = 5.7 × 10 ⁻⁶ M OM: 0 Anoxic conditions Cl ⁻ : 0.1131 M (4010 mg/L) No SRB activity. No sorption processes	-	calcite, mackinawite	-	-	Porosity = 0.00515 D _{eff} = 2.0 × 10 ⁻¹³ m ² /s	5 m from the interfaces Vol = 2050 m ³
RTI (rock-tunnel interface)	B-SO ₄ (Table 6-3 in Hellä et al. 2014) SO ₄ ²⁻ and sulfide concs. = 0 DOC: Initially set to 0 Charge balance on Na No sorption processes. SRB activity: Yes	-	calcite, mackinawite	Biotic SO ₄ reduction with: C-org: k = 1.5 × 10 ⁻⁴ s ⁻¹ H ₂ (aq): k = 6.4 × 10 ⁻⁵ s ⁻¹ [biomass]: 3.54 × 10 ⁻⁴ mol/m ³ K _{orgC} = 5.0 × 10 ⁻⁶ M; K _{H2} = 4.0 × 10 ⁻⁶ M; K _{SO4} = 1.0 × 10 ⁻⁵ M;	-	Porosity = 0.01 D _{eff} = 5.0 × 10 ⁻¹³ m ² /s	0.3 m, except below tunnel floor, where it is 0.4 m Tunnel contact = 110.1 m ² Vol = 35.4 m ³
RDI (rock- deposition hole interface)	B-SO ₄ (Table 6-3 in Hellä et al. 2014) SO ₄ ²⁻ and sulfide concs. = 0 DOC: Initially set to 0 Charge balance on Na No sorption processes SRB activity: Yes	-	calcite, mackinawite	Biotic SO ₄ reduction with: C-org: k = 1.5 × 10 ⁻⁴ s ⁻¹ H ₂ (aq): k = 6.4 × 10 ⁻⁵ s ⁻¹ [biomass]: 1.06 × 10 ⁻³ mol/m ³ K _{orgC} = 5.0 × 10 ⁻⁶ M; K _{H2} = 4.0 × 10 ⁻⁶ M; K _{SO4} = 1.0 × 10 ⁻⁵ M;	-	Porosity = 0.02 D _{eff} = 1.5 × 10 ⁻¹² m ² /s	0.1 m Contact with deptn. hole = 45.3 m ² Vol = 2.45 m ³
Backfill	Brackish water (Table F-2 in Posiva 2013b) DOC = 2 mg/L of C SOM(s) = 0.1wt% of C (143.2 mol/m ³) SRB activity: No	Gypsum 189.8 mol/m ³ Calcite 467 mol/m ³ Siderite 163.3 mol/m ³ (Table 7-11 in Hellä et al. 2014)	mackinawite	-	CEC = 2 120 meq/L = 0.47 eq/kg (Table F-2 in Posiva 2013b)	Porosity = 0.43 D _{eff} = 2.15 × 10 ⁻¹¹ m ² /s	4 m height, 3.5 m wide, 7.5 m long (distance btwn deptn. holes). Vol = 105 m ² Cross section = 14 m ²
Buffer	Brackish water (Table E-2 in Posiva 2013b) DOC = 2 mg/L of C SOM = 0.1wt% of C (130.7 mol/m ³) SRB activity: No	Gypsum 36.5 mol/m ³ Calcite 327 mol/m ³ (Table 7-5 in Hellä et al. 2014)*	siderite, mackinawite	-	CEC = 2 873 meq/L = 0.79 eq/kg (Table E-2 in Posiva 2013b)	Porosity = 0.43 D _{eff} = 2.15 × 10 ⁻¹¹ m ² /s	7.8 m height, outer diam. 1.75m, inner diam. 1.05m. Vol = 14.6m ³
Canister	-	-	-	-	-	-	4.8 m height, 1.05 m diam, Area = 17.6 m ²
TDB	Thermodynamic database – Thermochemie version 9b: all equilibrium constants; sulfate/sulfide decoupled; hydrogen from corrosion decoupled						

DOC = dissolved organic matter; SOM = solid organic matter.

B-SO₄ = Brackish-sulfate groundwater.

CEC = Cation Exchange Capacity.

SRB = Sulfate Reducing Bacteria.

* No siderite is considered in the buffer initially.

OM = organic matter.

A2 Variant Cases

Fracture

One fracture intersecting the deposition hole is introduced act as a source of sulfide, sulfate and DOC. The fracture will be located midway of the canister height. In this case the groundwater will include concentrations of sulfate, sulfide, and DOC (contrary to the Base Case). The concentration of sulfate and sulfide will be those specified for the brackish sulfate type groundwater (Table 6-3 in Hellä et al. 2014). The concentration of DOC will be 10 mg/L. The matrix rock porosity is then decreased, from the Base Case value to that of intact rock matrix. Three flow rates in the fracture will be modelled: 10^{-4} , 10^{-3} and 10^{-2} m²/y (m³ of flow per m or fracture width per year).

Buffer density

Localized loss of density so that bacterial sulfate reduction is possible. The affected volume in the buffer may defined as a toroid geometry with a rectangular cross-section with a height equal to the width of the buffer around the canister.

This volume will be assumed to have such properties that bacterial sulfate reduction is possible. This eroded volume will be positioned midway in the canister height. Two cases are envisaged.

- In the first case SRB (sulfate reducing bacteria) are assumed to be active in this volume of the buffer but all other parameters are left unchanged. Note that this is an unrealistic case, as the required dry density for SRB activity is lower than in the base case but leaving all other parameters unchanged allows distinct comparisons with the base case. The biomass in the porewater of the buffer is 2×10^8 cells L⁻¹, that is, 8.8×10^{-7} mol L⁻¹ of porewater (using a dry cell mass of 5×10^{-13} g/cell and a molecular weight of 113.115 g mol⁻¹).
- In the second case this buffer volume is considered to be a cavity empty of bentonite (but full of groundwater). Suspended cells in groundwater: The number microorganisms is based on a TNC of 10⁵ cells/mL, see Figure 2(b) in Pedersen (2012b). As in the base case, 20 % of these cells are postulated to be SRB.

Backfill density

Backfill porosity low enough to sustain SRB activity, in the whole of its volume. In order to make an easier comparison with the base case, all other parameters are left unchanged. The biomass in the porewater of the backfill is 2×10^8 cells L⁻¹, that is, 8.8×10^{-7} mol L⁻¹ of porewater (using a dry cell mass of 5×10^{-13} g/cell and a molecular weight of 113.115 g/mol).

Interface diffusivity

Higher effective diffusivities in the rock-backfill and rock-buffer interfaces. The base case diffusivity of RTI is 5×10^{-13} m² s⁻¹ and 1.5×10^{-12} m² s⁻¹ for RDI. At least one order of magnitude higher to be tested in this variant case.

Interface metals

The effect of corroding rock bolts and stretch metal in the backfill next to the rock producing hydrogen (H₂) and magnetite. The metal in the walls and ceiling of the deposition tunnel will be regularly distributed and the amount will be 14 kg per m of tunnel. The corrosion rate of the metal will be 2.8 μm y⁻¹ and the metal will be modelled to be cylindrical in shape with a diameter of 3 mm. The density of steel will be 7800 kg m⁻³. For models that discretize space into finite volumes, the thickness of the backfill compartment containing the steel may be between 5 and 10 cm thick.

Spatial grid

Check the numerical accuracy of the models by increased discretization, especially at the canister surface and at the vicinity of the RTI and RDI.

Organic matter

Increased contents of organic carbon available for sulfate reduction in the buffer and backfill by a factor of ten.

Fe(II) minerals

Different amounts of reactive Fe(II) minerals that may react with sulfide (i.e. carbonates) in the buffer and backfill. Tests will include a total absence of Fe(II).

Groundwater composition

Including sulfate and/or iron(II) and/or DOC in the groundwater in the intact rock (when specific fractures are not modelled). The concentrations of sulfate and Fe(II) in the groundwater will be those for the brackish sulfate type groundwater (Table 6-3 in Hellä et al. 2014). For DOC a value of 10 mg L^{-1} will be used.

Kinetic rates

Faster kinetics for SRB (sulfide reduction) and/or kinetics for organic matter degradation/dissolution in the backfill. A decrease and an increase by a factor of ten will be used.

Thermal effects

Temperature evolution of the canister. This case is modelled by the ICC team which already has a temperature variation as a function of time.

A CO-OPERATION REPORT BETWEEN SVENSK KÄRNBRÄNSLEHANTERING AB AND POSIVA OY

SKB's and Posiva's programmes both aim at the disposal of spent nuclear fuel based on the KBS-3 concept. Formal cooperation between the companies has been in effect since 2001. In 2014 the companies agreed on extended cooperation where SKB and Posiva share the vision "Operating optimised facilities in 2030". To further enhance the cooperation, Posiva and SKB started a series of joint reports in 2016, which includes this report.